

INVESTIGATING MICROBIOME ASSEMBLY AND ITS IMPACT ON THE PHYSIOLOGY
OF *Aedes albopictus* (DIPTERA: CULICIDAE)

A DISSERTATION SUBMITTED TO THE GRADUATE DIVISION OF THE UNIVERSITY OF
HAWAII AT MĀNOA IN PARTIAL FULFILLMENT OF THE REQUIREMENTS FOR THE DEGREE

OF

DOCTOR OF PHILOSOPHY

IN

ZOOLOGY (ECOLOGY, EVOLUTION, AND CONSERVATION BIOLOGY)

AUGUST 2024

BY

CHASEN D. GRIFFIN

DISSERTATION COMMITTEE:

MATTHEW C.I. MEDEIROS (CHAIR)

REBECCA CHONG

ROBERT COWIE

JIA-WEI TAY

MARK WRIGHT

DEDICATION

This dissertation is dedicated to my incredible wife, Remi, our wonderful kids, Nate and Skylar, and to all of my family in Georgia. Without your support, this never would have been possible. I love you all dearly.

ACKNOWLEDGEMENTS

First, I would like to express my immense gratitude to my family. I especially want to thank my amazing wife, Remi, for the love and support throughout this endeavor. Who would have imagined 10 years ago, in those small Georgia towns, that you and I would one day have a life in Hawai‘i? Without you, this would not have been possible. To my sons, Nate and Skylar, thank you for the many nights of laughter over board games; those nights were a wonderful way to decompress from the rigors of pursuing a PhD and I will never forget them. Thank you to my parents and grandparents, who were always there to talk when I missed home, and for sending pecans when it was time for Fall desserts. Thank you to the entire family for the unceasing encouragement for all of these years.

To my advisor, Matt Medeiros, thank you for taking a chance on me and bringing me into the Medeiros Hui. You have been an excellent mentor and taught me so much about the aspects of a career in science including experimental design, biostatistics, mentorship, scientific and grant writing, and of course mosquito microbiomes. Thank you for providing me with the space and tools to explore my interests in the broader scope of mosquito-associated microbes. Combined, those tools and experiences have built a solid foundation for my future career.

I want to thank my committee members: Rebecca Chong, Rob Cowie, Jia-Wei Tay, and Mark Wright for their support and guidance. I owe a special thanks to Rob for supporting me with a research assistantship that introduced me to and allowed me to work with the rat lungworm parasite in the final year of my PhD program. That experience opened new avenues for my future endeavors that I never imagined.

I want to thank my fellow Medeiros Hui graduate students, Mamo Waianuhea, Danya Weber, and Priscilla Seabourn for all of the time spent helping me with my experiments and for

their friendship during these past years. I also want to thank Kacie Kajihara for her help with network analyses and for helping with all of the coding involved. Joshua Schreiber and Abigail Bierwert, two undergraduates who I worked closely with as a mentor, also deserve a special thanks for their contributions to my research and for my personal development as a mentor.

To my long-time mentor, Guy Melvin, thank you for your mentorship and friendship over the last 15 years. This has been a long time coming and it all started on the beaches of the Bahamas collecting and measuring snails. Thank you for the opportunities to develop as a professional scientist and educator and for the many letters of recommendation I have requested over the years.

Lastly, to my friends Randi Rollins and Stevan Stojanović, thank you for the support during some of my most trying times. Whether it was providing a listening ear or taking me surfing, you helped me keep pushing forward. For that, I am truly grateful.

ABSTRACT

Mosquito-borne disease is a major public health burden globally despite decades of efforts towards its eradication. Mosquitoes are difficult to control and many of the most important vectors of human pathogens have developed resistance to conventional insecticides—highlighting the urgency to find novel ways to control mosquito-borne diseases. In recent years, the mosquito microbiome has been the subject of intense study and has revealed interesting insights into its role in mosquito biology. The microbiome is highly influential in shaping many biological processes of mosquitoes including development, fecundity, immunity, metabolism, and nutrient acquisition. Much of a host's microbiome is derived from the environment; thus, the composition of the environmental microbiome is an important driver of host microbiome composition, which could lead to phenotypic heterogeneity between mosquito populations on the landscape—further complicating control efforts. In Hawai'i, the non-native and highly invasive mosquito, *Aedes albopictus*, is well established, but microbiome-driven phenotypic heterogeneity in populations is not well understood. Therefore, I developed three projects to explore how exposure to compositionally manipulated environmental microbiomes impact *A. albopictus* biological and physiological processes.

The first project involved the reintroduction of environmental bacteria to an *A. albopictus* colony that was originally isolated from Mānoa, O'ahu, Hawai'i and had been in the laboratory for 15 generations. To vary the environmental microbial community composition, a series of filters were implemented to manipulate the community by cell size that included: a 10 μm regimen, a 2 μm regimen, a 0.1 μm regimen, and a Millipore filter. Mesocosms were created from the filtrates and *A. albopictus* were reared as larvae into adulthood. Using generalized linear mixed models (GLMM), microbiome α - and β -diversity of the adults from each mesocosm was

investigated. The mesocosm microbiomes were also compared to wild *A. albopictus* pupae that were collected in the environmental water and to wild *A. albopictus* adults collected near the habitats. The results showed that α -diversity did not differ between the filtered mesocosms; however, the microbiomes of mesocosms were significantly different from wild pupae and from wild adults. The β -diversity analysis showed that the microbiomes of the 10 μm and 2 μm mesocosms formed a single group, the 0.1 μm and Millipore mesocosms formed a single group, wild pupae formed a single group, and wild adults formed a single group. Development times were also measured. Pupation occurred 1.59 days earlier in the 10 μm and the 2 μm mesocosms compared to the 0.1 μm and Millipore mesocosms. The ability of adults to survive under starvation was also impacted by the mesocosm from which they emerged. Adults from the 0.1 μm and Millipore mesocosms survived approximately twice as long as those from the 10 μm and 2 μm mesocosms. These findings demonstrate that exposure to compositionally distinct environmental microbiomes impact *i*) the assembly of the host microbiome and *ii*) important biological processes within the host in different ways.

In the second project, a more comprehensive exploration of the *A. albopictus* microbiome was performed. Mosquitoes collected from Makiki, O‘ahu, Hawai‘i and their microbiomes were sequenced using the bacterial 16S rRNA gene and the microbial fungal internal transcribed spacer (ITS) gene. Three networks were generated: a 16S only network, an ITS only network, and a cross-domain network. To test the stability of the networks, attacks on the networks were targeted at the centrality measures of node degree (a measure of how many connections one node makes to another node) and betweenness (the total number of shortest paths from node to node). The cross-domain network showed the highest stability in the face of attacks, remaining more stable as more nodes removed from the network. A keystone species analysis was also performed

using the same centrality measures and of the six highest taxa fungi comprised five of those, further indicating the importance of fungi in the *A. albopictus* microbiome. Using the hypothesis that fungi were influential in the stability of the microbiome, a similar experiment to project one was conducted but added a 30-50 μm filter that allowed for environmental fungi to pass into the filtrate. β -diversity was assessed using GLMMs and the presence of fungi in the filtrate led to different microbial communities structures than when fungi are not present. Those results are interesting not only because they validate and support the theoretical network models that generated the hypothesis but emphasize the necessity of including fungi in *A. albopictus* microbiome studies.

The third project investigated the impacts of developing in compositionally distinct microbial habitats on critical physiological processes in *A. albopictus*. Those processes were development time, development success, fatty acid synthesis, the ability to survive under starvation, and immune function. All physiological processes were impacted by exposure to compositionally distinct environmental microbiomes and varied by filtration level. Furthermore, the ability to withstand starvation and immune expression, both measured in adult mosquitoes, was impacted by the sex of the mosquitoes and also varied by filtration level. Overall, this study highlights the importance of exposure to compositionally distinct environmental microbiomes on *A. albopictus* physiology. Furthermore, these findings emphasize the need to include fungi, which are often omitted, in *A. albopictus* microbiome experiments because of their importance in structuring the microbiome.

TABLE OF CONTENTS

Acknowledgements.....	ii
Abstract.....	iv
List of Tables.....	viii
List of Figures.....	ix
Preface.....	x
Chapter 1.....	1
Chapter 2.....	28
Chapter 3.....	49
Appendix A: Chapter 1 Supplemental Tables.....	50
Appendix B: Chapter 2 Supplemental Tables.....	54
Appendix C: Chapter 2 Supplemental Figures.....	63
Appendix D: Chapter Supplemental Tables.....	92
Literature Cited.....	93

LIST OF TABLES

Table 1.1. The model output for variables included in the full linear model to explain variation in the observed species richness. Observed species richness was used as the response variable in the model.....	21
Table 1.2. The estimates and associated standard errors of the model's fixed effects and the variance and standard deviation of the model's random effects which interrogates the β -diversity of bacteriomes between mesocosm treatments and wild-captured <i>Aedes albopictus</i>	22
Table 2.1. Generalized linear mixed models demonstrating Δ AICc values of distinct models that partitioned variance in the composition of the bacteriome among different hypothetical groupings of the Lyon Arboretum filtration regimens.....	44
Table 2.2. Generalized linear mixed models demonstrating Δ AICc values of distinct models that partitioned variance in the composition of the bacteriome among different hypothetical groupings of the UH-Mānoa filtration regimens.....	45
Table 3.1. Means \pm standard errors of days to pupation and remaining larvae across all treatments.....	83
Table 3.2. Means \pm standard errors of survival times (in days) by sex across all treatments.....	84
Table 3.3. Means \pm standard errors of the DDCt values of CEC-A and LYS-E by sex and treatment and infection status. Values shown are immune gene expression values in infected mosquitoes relative to non-infected mosquitoes. Positive values indicate higher expression of target gene.....	85

LIST OF FIGURES

<p>Figure 1.1. The composition of the bacteriome of <i>A. albopictus</i> among treatments. The top 9 OTUs are represented and comprise 96% of total reads. The wild pupae group were collected in the field during the pupal stage, but bacteriome sequencing was performed on adults after eclosion in the laboratory.....</p>	23
<p>Figure 1.2. Box plots of observed alpha diversity measures and significant results from pairwise comparisons between the filtration treatments and wild-caught mosquito adults and pupae. Observed alpha diversity is presented on a log scale. Significant differences between mesocosms are indicated by letter. Box plots show the median as horizontal lines, and interquartile ranges as boxes with whiskers extending to 1.5 times the interquartile range.....</p>	24
<p>Figure 1.3. Heat maps demonstrating taxonomic abundance across mesocosms using (A) unweighted and (B) weighted unifracs distances.....</p>	25
<p>Figure 1.4. Box plots showing days to pupation by mesocosm. Mosquitoes in mesocosms LF (10 µm filter) and MF (2 µm filter) pupate on average 1.59 days faster than mosquitoes in mesocosms HF (0.2 µm filter) and C (Millipore water). Kruskal-Wallis test was used to identify statistically significant differences in time to pupation ($P < 0.05$). Significant differences between mesocosms are indicated by letter according to Dunn’s post-hoc test. Box plots show the median as horizontal lines, and interquartile ranges as boxes with whiskers extending to 1.5 times the interquartile range.....</p>	26
<p>Figure 1.5. Adult survival in days by (a) diet, (b) by mesocosm on a sterile water diet, (c) by mesocosm on a 10% high-fructose diet, and (d) by mesocosm on a 10% sucrose diet. Cox Hazard regression was used to identify statistically different survival times ($P < 0.05$). Significant differences between mesocosms are indicated by letter. Boxplots show the median as horizontal lines, and interquartile ranges as boxes with whiskers extending to 1.5 times the interquartile range.....</p>	27
<p>Figure 2.1. Robustness curves for all networks by A) betweenness centrality and B) node degree. Each network is expressed as a line on the graph. A more robust network is characterized by having a larger area under the curve.....</p>	46
<p>Figure 2.2. Keystone species analysis. Potential fungal and bacterial keystone ASVs were identified by comparing betweenness centrality and node degree. Nodes with high betweenness centrality represent taxa important to the connectivity of the network. Nodes with high degree represent taxa that are hubs in the network. Taxa are identified at the domain level.....</p>	47
<p>Figure 2.3. Non-metric multidimensional scaling plots demonstrating the composition of the bacteriome that assembled <i>Aedes albopictus</i> mosquitoes by filtration level and mosquito type in the A) Lyon Arboretum treatments and B) UH-Mānoa treatments. Distances are based on the Morisita-Horn index.....</p>	48

Figure 3.1. Bar plot showing the number of days (mean \pm SEM) to reach pupation by each water source and filtration level.....86

Figure 3.2. Bar plot showing the number of larvae remaining (mean \pm SEM) at day 32 of the experiment by each water source and filtration level.....87

Figure 3.3. Bar plot showing the number of days (mean \pm SEM) adult female and male *Aedes albopictus* survived under starvation conditions by each water source and filtration level.....88

Figure 3.4. Bar plot showing the DDcT values (mean \pm SEM) of CEC-A in adult female and male *Aedes albopictus* by treatment. Values shown are immune gene expression values in infected mosquitoes relative to non-infected mosquitoes. Positive values indicate higher expression of target gene.....89

Figure 3.5. Bar plot showing the DDcT values (mean \pm SEM) of LYS-E in adult female and male *Aedes albopictus* by treatment. Values shown are immune gene expression values in infected mosquitoes relative to non-infected mosquitoes. Positive values indicate higher expression of target gene.....90

PREFACE

Emerging and reemerging mosquito-borne diseases are persistent public health and wildlife threats across the world (Chala & Hamde, 2021). Historically, control of mosquito-borne diseases have not directly targeted the pathogens themselves but the mosquitoes that spread them. The middle decades of the 20th century saw some of the most effective mosquito control programs ever conducted and by the 1970's many programs were ended because of their perceived total success (Gubler, 2010). However, in the following decades that success quickly faded as mosquito populations rebounded—with insecticide resistance also appearing in many target species. Aside from the suspension of mosquito control programs and insecticide resistance, many other factors like globalization and urbanization have contributed to the renewed threat of mosquito-borne disease.

Globalization has interconnected the world in unprecedented ways. The process of globalization has been ongoing for approximately five centuries—starting with the age of discovery around the 15th century. However, it was during the 20th century when globalization quickly accelerated. Technological advances have led to the ability to travel the globe in less than a day, bridging geographical regions in a way never experienced in the history of the world. While globalization may be positive for commerce and national economies, it has posed significant challenges for ecosystems and the natural world. One major issue with globalization is the translocation of animals to non-native environments, which is highly problematic when those animals—especially mosquitoes—are vectors of pathogens.

The translocation of mosquitoes has occurred globally for centuries, and Hawai'i is a special case because mosquitoes were not present in the archipelago prior to the 1800's. However, in 1826, *Culex quinquefasciatus* mosquitoes were introduced to Hawai'i (Van Dine,

1904) followed by *Aedes aegypti* around 1890 and *Aedes albopictus* around 1900 (Winchester & Kapan, 2013). Since their introduction, it did not take long for public health challenges to arise. One of the earliest recorded dengue fever epidemics occurred in 1903 and again in 1943-1944 (Winchester & Kapan, 2013); *Aedes aegypti* was the most probable vector during those outbreaks. It was not until the early 21st century when dengue fever was reported again, this time with *A. albopictus* as the primary vector. Several more outbreaks have occurred since, the most recent having occurred in 2015-2016. *Aedes albopictus* was also implicated as the primary vector in that outbreak.

Aedes albopictus is not often the primary vector for dengue virus; thus, its repeated involvement with dengue cases in Hawai‘i served as the impetus for this dissertation. I was particularly interested in how *A. albopictus* responds physiologically to interactions with environmental microorganisms, especially when exposed during the larval phase of its life cycle. It is well known that mosquitoes and microbes form symbiotic partnerships. The microbial community is called a microbiome and it impacts many aspects of mosquito biology. Therefore, I was also interested in linking the community composition of the microbiome to direct physiological outcomes in *A. albopictus*. I found that *A. albopictus* populations respond very differently to compositionally varied environmental microbiomes across a range of important traits that are linked with disease transmission. The end result of this dissertation provides a nuanced, yet complex, view of *A. albopictus* and its relationship to environmental microbiomes in Hawai‘i. These findings fill an important gap in understanding the potential of *A. albopictus* populations to sustain disease transmission in Hawai‘i. These findings also provide the potential for future surveillance strategies that account for the mosquito’s relationship to the environment

by identifying environments where microorganisms influence populations towards a higher capacity to sustain disease transmission.

CHAPTER 1: FILTRATION OF ENVIRONMENTALLY SOURCED AQUATIC MEDIA
IMPACTS LABORATORY-COLONIZED *Aedes albopictus* EARLY DEVELOPMENT
AND ADULT BACTERIOME COMPOSITION

Citation: Griffin, C. D., Weber, D. E., Seabourn, P., Waiyanuhea, L. K., & Medeiros, M. C. I. (2023). Filtration of environmentally sourced aquatic media impacts laboratory-colonised *Aedes albopictus* early development and adult bacteriome composition. *Medical and Veterinary Entomology*, 37(4), 693–704.

Introduction

Mosquito-borne diseases (MBDs) are a persistent problem throughout most of the tropics and subtropics. Millions of people are infected with these diseases annually, resulting in heavy strains on public health resources and reduced economic output in affected regions. For example, dengue virus—responsible for dengue fever and dengue hemorrhagic fever—is estimated to cause 100 million cases a year (Messina et al., 2014); the economic loss associated with dengue is estimated in the billions of dollars (Shepard et al., 2016).

Historically, mosquito-borne diseases have affected the tropics disproportionately, but as regions in higher latitudes warm, the potential threat for these diseases to establish in temperate zones is growing (Garcia-Rejon et al., 2021). One vector of particular concern is *Aedes albopictus*, a known vector of several clinically important arboviruses including dengue virus (DENV) and chikungunya virus (CHKV). Although *A. albopictus* is considered a secondary

vector of DENV, it was solely responsible for recent DENV outbreaks in Hawai'i, Mauritius, China, and Guam (Effler et al., 2005; Johnston et al., 2020; Kern-Allely et al., 2020; Rezza, 2012). Additionally, *A. albopictus* is a highly competent vector for a CHKV strain that emerged from islands in the Indian Ocean called the Indian Ocean lineage (Weaver, 2014) and was indicated as the primary vector in an outbreak occurring on La Reunion Island in 2005-2006 (Vazeille et al., 2007). It is also a competent vector for more than 20 other clinically relevant arboviruses (Gratz, 2004; Moore & Mitchell, 1997; Paupy et al., 2009).

Aedes albopictus is considered among the most invasive mosquito species in the world (Bonizzoni et al., 2013). It has been documented on all continents except for Antarctica (Benedict et al., 2007; Bonizzoni et al., 2013) and is widely distributed throughout the areas it has colonized (Medlock et al., 2012; Rai, 1991). This is likely due to its ability to function and continuously breed at cooler temperatures (Paupy et al., 2009). This mosquito also lays eggs capable of diapause when daily photoperiods are shortened, which is typical of temperate winter months (Lounibos et al., 2003). Furthermore, *A. albopictus* efficiently increases lipid synthesis at lower temperatures, likely providing the energy necessary to survive colder habitats (Briegel & Timmermann, 2001).

The physiology of *A. albopictus* that influences its demography over environmentally-heterogeneous landscapes is modulated by microbes that enter a host symbiosis (Wang et al., 2018). During the larval phase, microbes in the aquatic habitat modulate larval development and growth (Mitraka et al., 2013) by serving as a source of nutrition (Martinson & Strand, 2021) providing amino acids (Yamada et al., 2015) and essential vitamins (Wang et al., 2021). The microbiome also modulates critical biological processes linked to vector competence in adult mosquitoes including immune function (Gabrieli et al., 2021), pathogen extrinsic incubation

period (Ye et al., 2015), and developmental success and reproductive output (Coon et al., 2016a). *A. albopictus* harbors a symbiotic microbiota that is mostly derived from environmental sources such as the aquatic larval habitat and from plant nectar (Mushegian et al., 2019). Geographic location (Tuanudom et al., 2021), environmental gradients (Medeiros et al., 2021), and eukaryotic cosymbionts (Seabourn et al., 2020) are associated with variation in the mosquito microbiome. In addition, mosquito colonization in a laboratory environment is associated with dramatic shifts in the composition and structure of the mosquito microbiome (Boissière et al., 2012; Coon et al., 2016b; Hegde et al., 2015; Osei-Poku et al., 2012; Schrieke et al., 2022) This suggests that phenotypes of lab-reared mosquitoes that are modulated by microbial symbiont partners may diverge from mosquitoes found in natural populations, undermining our capacity to extend knowledge on mosquito biology generated in a lab environment to real-world landscapes where mosquito borne disease transmission actually occurs.

In this study, we investigated the effect of bacteria in the larval habitat on *A. albopictus* development and survival across its life stages. To test this, we designed an experiment using environmentally-exposed artificial container water processed under different filtration regimes to create small, contained larval habitats that varied in microbial compositions—hereafter referred to as mesocosms. We also tested if larval habitat conditions impact adult survival when fed a diet of 10% sucrose (standard lab diet) or when fed a nectar diet containing fructose (Fikrig et al., 2020), a simple carbohydrate common in fruits and plant nectar. In addition to testing the effect of larval habitat manipulation on *A. albopictus* development and survival, we also tested whether larval habitat filtration regimes alter the bacteriome of emerged adults. Lastly, we evaluated how the bacteriome compositions of lab-colonized *A. albopictus* mosquitoes responded when reared in water sourced from environmentally-exposed habitats designed to mimic natural environments

that were subjected to different filtration regimens. We compared the bacteriome compositions of mosquitoes from our filtration habitats to *i*) wild adults that would emerge in our lab from pupae found in the habitat at the time of water collection and *ii*) to those of wild adults captured within a 3 meter radius of the breeding habitats at the time the source water was collected.

Materials and Methods

Habitat preparation and environmental exposure

Three large plastic flowerpots, a preferred habitat for *A. albopictus* oviposition and larval development in anthropogenically modified landscapes (Vezzani, 2007), were filled with one tablespoon of field soil and 1 teaspoon of crushed leaf detritus collected from the University of Hawai'i at Mānoa campus, 600 ml of sterile water and one wooden shim. The flowerpots were placed on the University of Hawai'i at Mānoa campus and were left exposed to the environment for 14 days. The pots were checked every two days and the water level was restored to 600 ml with sterile water when necessary. After 14 days, water from the flowerpots was collected and returned to the laboratory for processing. All *A. albopictus* pupae found in the habitat were collected and returned to the lab, allowed to emerge, and were sacrificed for adult bacteriome analysis.

Inoculum preparation

Three different inoculum preparations were generated from the collected environmental water. Preparations were named Low Filtration (LF), Medium Filtration (MF), and High Filtration (HF) and were created under sterile conditions in a biosafety cabinet. The LF inoculum

was made by filtering 600 ml of environmental water through a sterile syringe and 10 μm filter into a sterile beaker followed by a second filtration using a new 10 μm filter and new sterile beaker. This filter was expected to eliminate most eukaryotes but allow the unicellular eukaryotes such as *Ascogregarina taiwanensis* (9 μm ; Chen et al., 1997) and some small-celled yeasts such as *Saccharomyces spp.* (5-9 μm) to *Cryptococcus spp.* (2-10 μm) flow through. The MF inoculum was made by filtering 600 ml of environmental water through a 10 μm filter into a sterile beaker. The 10 μm filtered water was then filtered using a sterile syringe and 2 μm filter into a new sterile beaker; this step was repeated twice. This would have prevented all eukaryotes and bacteria larger than 2 μm from flowing through. The HF inoculum preparation was produced using 600 ml of environmental water filtered with a sterile syringe and 10 μm filter into a sterile beaker. The 10 μm filtered water was then filtered using a sterile syringe and 2 μm filter into a new sterile beaker. The 2 μm filtered water was then filtered through 0.1 μm vacuum filtration cup into a sterile bottle. The 0.1 μm filtered water was filtered through a 0.1 μm vacuum filtration cup into a new sterile bottle. This process removed bacteria and eukaryotes from the environmentally-exposed water but retained the chemistry of that environment and likely most free-living viruses, including bacteriophages. Lastly, a lab control (C) was included to represent the larval habitat conditions experienced in the typical laboratory environment and consisted of pure water from a Millipore Milli-Q water filtration system (Massachusetts, USA). All mesocosm treatments were treated under the same sanitization protocols as our lab colony (see below), and thus were all also exposed to lab-associated microbes.

Mesocosm design

Mesocosms were divided into four treatment groups: MF, LF, HF, and control (C). Each treatment group contained six replicates for a total of 24 mesocosms. Under sterile conditions, 100 ml of the corresponding treatment inoculum were transferred into a vented-cap T-flask along with 30 non-sanitized *A. albopictus* eggs obtained from our lab colony that originated from wild *A. albopictus* isolated from Mānoa, Oahu, Hawai‘i and were raised in the lab for 15 generations prior to the start of this experiment.

Mosquito rearing and handling

We reared *A. albopictus* with a 12 L:12 D photoperiod. Temperature in the light and dark period was 25°C and 21°C, respectively. Humidity was kept constant at 60% for the entire photoperiod. Larval food consisted of a 1:1 ratio of beef liver powder to dried yeast extract mixed with pure water to a concentration of 18 mg per ml and was autoclaved for 30 minutes to kill viable microorganisms in the food. Larval food water was administered daily at a concentration of 0.6 mg per larvae per mesocosm. Pupae were removed upon pupation using a pipette, washed twice with sterile water, and were housed individually in a 50 ml sterile centrifuge tube. Emerged adults were randomly assigned to either a carbohydrate-diet survival analysis or for bacteriome analysis with 16S amplicon sequencing.

Wild pupae collected from our environmental larval habitats were brought into the lab, washed twice with sterile water, and placed individually into a 50 ml centrifuge containing sterile water. Pupae were allowed to emerge, and adults were collected immediately and stored at -20°C until ready for bacteriome analysis. All bacteriome analyses performed on the wild pupae group were done at the adult stage soon after emergence. We also collected wild adults within a 3 meter

radius of our environmental larval habitats and were returned to the lab and stored at -20°C until ready for bacteriome analysis.

Adult survival on sucrose, high fructose, or sterile water diets

A 10% sucrose solution was prepared by mixing 100 g of sucrose with 1000 ml of pure water. The solution was autoclaved for 30 minutes. A 10% fructose mixture was prepared by mixing fructose and sucrose at a 4:1 ratio. 100 g of the mixture was diluted in 1000 ml and autoclaved for 30 minutes. A sterile water control diet was prepared by autoclaving pure water for 30 minutes. A cotton ball saturated with either sucrose, high-fructose, or sterile water was provided individually to each mosquito. Mosquitoes were allowed to feed *ad libitum* on saturated cotton balls, which were replaced every 24 hours. Adults were housed individually in 50 ml sterile centrifuge tubes for the duration of the survival assay. Mortality was checked daily until all mosquitoes were dead.

DNA extraction, amplification, and sequencing

Prior to DNA extraction all adults that were used for microbiome analysis were subjected to a surface-sterilization protocol adapted from (Poff et al. 2017, Muturi et al. 2018) consisting of one wash in 70% ethanol followed by two rinses in sterile 1X PBS. DNA was extracted and purified on a KingFisher Flex (Thermo Fisher Scientific, Waltham, MA) using a MagAttract PowerSoil DNA KF Kit (Qiagen, Germany) following the manufacturer's protocol. Library preparation was done using a modified version of the Earth Microbiome Project 16S V4 protocol (Caporaso et al. 2011). PCR amplification targeted the V4 region of bacterial 16S rRNA using 515F (5'-GTGCCAGCMGCCGCGGTAA-3') and 806R (5'-GGACTACHVGGGTATCTAAT-

3') primers from the Earth Microbiome Project. Each 20.0 μL PCR reaction contained the following components: 10.0 μL of Platinum II Hot-Start PCR Master Mix (2X), 7.2 μL of nuclease-free water, 0.4 μL of 10 μM barcoded forward primer, 0.4 μL of 10 μM reverse primer, and 2.0 μL of template DNA (approximately 20-80 ng). Two PCR reactions were run as controls per 96-well plate of samples: one no-template reaction using nuclease-free water for a negative control and one PCR reaction containing approximately 5 ng of the ZymoBIOMICS Microbial Community DNA Standard for a positive control. All PCR amplifications were performed with an Applied Biosystems SimpliAmp thermal cycler (Thermo Fisher Scientific, Waltham, MA) using the following cycling conditions: initial denaturation at 94°C for 2 min; 35 cycles of denaturation at 94°C for 15 s, annealing at 54°C for 15 s, extension at 68°C for 7 s; and a final extension step at 68°C for 3 min before an infinite 4°C hold. PCR amplification was confirmed through visualization on a 2% agarose gel. Samples were then purified and normalized to approximately 1.25 – 2.50 ng/ μL using the Just-a-Plate PCR Normalization kit (Charm Biotech, San Diego, CA). A volume of 10 μL from each sample was pooled before being purified and concentrated using a volume of 1.2X of homemade AMPureXP SPRI beads. Final libraries were checked for concentration and purity using a Qubit 1X dsDNA High Sensitivity Kit (Thermo Fisher Scientific, Waltham, MA) and Bioanalyzer (Agilent Technologies, Santa Clara, CA). Sequencing was performed at the Advance Studies in Genomics, Proteomics and Bioinformatics core facility at the University of Hawai'i at Mānoa using a MiSeq Reagent Kit v3 on the Illumina platform.

Estimation of Ascogregarina taiwanensis load

Ascogregarina taiwanensis infection was assessed in each mesocosm and in the wild pupae and wild adults by qPCR using custom-designed primers (AT_SHORT_2_F: 5'-TCGATGAAGGACGCAGCTTA-3', AT_SHORT_2_R: 5'-AGGCACTGAACTGGACATACT-3') derived from an *As. taiwanensis* reference sequence (GenBank [AY326461.1](#)). Each qPCR reaction contained the following components: 5.0 µL of PowerUp SYBR Green Master Mix (Applied Biosystems, Foster City, CA), 3.0 µL of nuclease-free water, 1.0 µL of template DNA (approximately 10–87 ng), 0.5 µL of 10 µM forward primer, and 0.5 µL of 10 µM reverse primer. The reactions were performed using an Applied Biosystems StepOnePlus Real-Time PCR System (Thermo Fisher Scientific, Waltham, MA) using the following conditions: UDG activation at 50°C for 2 min; Dual-Lock DNA polymerase at 95°C for 2 min; and 40 cycles of denaturation at 95°C for 15 s, annealing at 56°C for 15s, and extension at 72°C for 1 min. Fluorescence readings were taken at the 56°C annealing step for each cycle. A melt curve was performed according to PowerUp SYBR protocol to confirm the specificity of amplification. The Cycle threshold (Ct) values were used to measure *A. taiwanensis* infection intensity and were obtained assuming a delta Rn fluorescence threshold of 0.25. Samples were considered negative if *i*) no amplification of the target gene occurred, *ii*) if the cycle threshold (Ct) was greater than 38, and *iii*) if the melt curve did not align with the positive control.

Bioinformatics analysis

Bioinformatics analysis was performed using the MetaFlow|mics pipeline for microbiome marker data (Arisdakessian et al. 2020). The dada2 package in R was used to preprocess raw paired fastq reads. Reads were truncated at position 220 (190 for the reverse read) and were

discarded if they contained at least one base below quality 2 or a number of expected errors above 3. Denoising was performed using the `learnError()` and `dada()` functions with default parameters. Using the `mergePairs()` function, reads were merged if they overlapped by at least 20 bases, and a maximum of one mismatch was allowed. Mothur was used along with the Silva database (version 132) (downloaded from https://mothur.org/wiki/Silva_reference_files) to align and annotate the sequences. Sequences with a start or stop position outside the 5th - 95th percentile range (over all sequences) were discarded. Potential chimeras were removed with `chimera.uchime()` and clustered at 99% similarity thresholds with `chimera.vsearch()`. Taxonomies were assigned using `classify.seqs()` and `classify.otus()`. The `lulu` R package was used to refine operating taxonomic units (OTUs) (Frøslev et al. 2017). Two OTUs were merged if all the three following conditions were satisfied: *i*) they co-occur in every sample, *ii*) one of the two OTUs has a lower relative abundance than the other in every sample, and *iii*) they share a sequence similarity of at least 99%. All singletons (OTUs with reads in only one sample) and OTUs with no annotation at the kingdom level were removed. Further OTU processing was performed by merging the abundance data, taxonomic data, and sample data using the `Phyloseq` package in R.

Statistical Analysis

To compare bacteriomes, we investigated both α - and β -diversity between our mesocosms with different water filtration treatments, wild pupae, and wild adults. To assess α -diversity, a GLM assuming a negative binomial distribution was used to compare the observed species richness (total number of unique OTUs) within each treatment. All candidate models included an offset for sequencing reads per sample and fixed effects for host sex and environment. To assess β -diversity, changes in the composition of the bacteriome in response to

the larval environment (six levels: LF, MF, HF, C, Wild pupae, Wild adult) were tested statistically with a GLMM assuming a negative binomial error distribution. All candidate models included an offset for sequencing reads per sample, fixed effects for host sex and environment, and a random intercept for OTU taxon identity. Among specific models in the candidate set, the responses in relative abundance of every OTU to both host sex and environment were allowed to vary by specifying random interaction effects. In addition, we used a series of similar GLMMs to test several hypotheses on how variation in the composition of the mosquito bacteriome compared among different groupings of the environmental variable. These hypotheses, their model specification, and the distinct hypotheses that motivated them are listed in supplemental table 1. We used Akaike information criterion (AIC) to select the most suitable model among these models included in this candidate set.

Kruskal-Wallis test was used to compare differences in time to pupation among the mesocosms. A post-hoc analysis using Dunn's test was used to compare differences in mosquito pupation times between mesocosms. PERMANOVA was used to analyze pupal duration. Adults were randomly assigned to one of three carbohydrate-diet groups (sterile water, sucrose, or high-fructose) immediately after emergence and survival outcomes were analyzed using a Cox Proportional Hazard regression model. The model included fixed effects for mesocosm, diet treatment, an interaction of mesocosm and diet, and sex. Post-hoc comparisons were performed using a logrank test. All statistical analyses were performed using R Statistical Software (v4.1.1; R Core Team 2021) in RStudio (RStudio Team, 2021).

Results

Bacteriome analysis

A total of 15,743 OTUs were identified. All OTUs that appeared at least once in any sample were included for α -diversity analysis. For β -diversity (i.e. changes in the taxonomic composition of the microbiome among samples), a threshold was set to include OTUs that appeared more than once in greater than 2.5% of total samples; this resulted in 377 OTUs used for downstream analysis. Of these 377 OTUs, 9 bacterial genera accounted for approximately 95% of total reads. These included *Wolbachia_A* (51.6%), *Wolbachia_B* (17.3%), *Entomospira* (17.19%), *Enterobacter* (3.36%), *Sphingobacterium* (1.32%), *Yersinia* (1.18%), *Flectobacillus* (0.92%), *Ralstonia* (0.73%), *Burkholderia* (0.62%), and *Stenotrophomonas* (0.56%) (Figure 1.1). Interestingly, we observed an increase in relative abundance of *Entomospira*, a recently described novel genus in *Aedes* and *Culex* mosquitoes (Graña-Miraglia et al., 2020), in our LF and MF groups compared to the other groups. It comprised 47.57% of the average bacterial abundance in LF, 42.41% in MF, 0.10% in HF, 0.002% in C, 7.81% in wild adults, and 6.36% in wild pupae.

α -diversity. The average number (\pm standard error of the mean) of unique bacterial symbiont taxa identified was 21.67 ± 1.98 in LF (n=18), 17.84 ± 1.34 in MF (n=19), 19.14 ± 1.98 in HF (n=14), 30.30 ± 5.33 in C (n=10), 86.47 ± 25.25 in wild adults (n=49), and 352.27 ± 116.48 in wild pupae (n=22). Species richness of adult mosquitoes varied by mesocosm and wild status ($\chi^2 = 81.13$, df = 5, p = <0.01; Table 1). C (t = -2.62, p = 0.009), HF (t = -3.66, p = <0.001), LF (t = -4.88, p = <0.001), MF (t = -4.62, p = <0.001) all had lower species richness than wild adults. Wild pupae displayed higher species richness than wild adults and all other treatments (t = 3.45, p = <0.001; Figure 1.2). Differences in the species richness of adult mosquitoes did not vary with the sex of the mosquito (t = 0.15, p = 0.88).

β -diversity. We used a GLMM-based approach because it presents distinct advantages over other approaches that rely on distance matrices and multivariate ordinations (Jackson et al., 2012; McMurdie & Holmes, 2014). The GLMM approach, while uncommon, has been used in previous studies of microbiomes (Medeiros et al., 2021; Seabourn et al., 2020). For β -diversity analyses, a threshold was set to include OTUs with more than 1 read in greater than 2.5% of samples, which resulted in a total of 377 OTUs from 26 phyla. *Wolbachia* was also removed since it is a vertically acquired symbiont and would not be part of the environmental source pool we are testing here. To test the hypothesis that larval habitat conditions are a driver of bacteriome assembly, a model including a random interaction between OTU and larval environment treatment—designated full group model (FGM, see supplementary table 1.1)—was compared to a null model that excluded this random interaction. The FGM (AICc weight = 1, Figure 1.3) model based on *a priori* larval environment treatments was a better fit to the data than the reduced model (Δ AICc = 2121.9, AICc weight = \sim 0). To test how similar lab-reared (among the larval environment treatment) and the wild-caught mosquitoes were to each other, a series of *post-hoc* bacteriome groupings were compared. Microbe Filtration Model 3 was best fitted to the data (AICc weight = 1). This model grouped MF with LF, HF with C, wild adults alone and wild pupae alone (Table 1.2). The second-best fitted model (Environmental Exposure Model 3) grouped MF, LF, and HF together, and C, wild adults, and wild pupae as individual groups (Δ AICc = 31.2, AICc weight = \sim 0). All other models (see Supplementary Table 1.2) were very poorly fitted to the data (Δ AICc > 132, AICc weight = \sim 0), including a null model that excluded the fixed effects of larval environment and the random intercept for an interaction between OTU and larval environment (Δ AICc = 2121.9).

Presence of Ascogregarina taiwanensis

Samples from mesocosm LF, MF, HF, control, wild pupae, and wild adults were randomly chosen and tested for *As. taiwanensis*; these sample sizes accounted for 33% of the total samples for each treatment. None of the samples selected from mesocosms LF, MF, HF, or from the control were positive for *As. taiwanensis*. All wild pupae sampled were positive for *As. taiwanensis* infection, confirming that the parasite was present in the larval water before it was filtered since the parasite is acquired during the larval stage from the environment (Stump et al., 2021). All wild adults sampled were also positive for the infection.

Time to pupation

There was a significant difference in days to pupation across mesocosms ($F = 15.6$, $df = 3$, $p < 0.001$). Mean days to pupation in mesocosm LF was 9.68 ± 0.23 days ($n=48$), 9.23 ± 0.12 days in MF ($n=56$), 11.29 ± 0.39 days in HF ($n=34$), and 10.79 ± 0.27 days in C ($n=28$). (Figure 1.4). Dunn's test post-hoc comparisons showed that mosquitoes in the MF mesocosm pupated significantly earlier than those in C ($t = 5.2$, $df = 37$, $p < 0.01$) and HF ($t = 5.1$, $df = 39$, $p < 0.01$). Mosquitoes in the LF mesocosm also pupated significantly earlier than those in C ($t = 3.1$, $df = 61$, $p = 0.02$) and HF ($t = 3.6$, $df = 55$, $p < 0.01$). No significant differences were observed between MF and LF ($t = 1.8$, $df = 71$, $p = 0.3$) or between HF and C ($t = 1.1$, $df = 57$, $p = 0.71$). Days to eclosion did not vary statistically between mesocosm treatment ($R^2 = 0.37$, $df = 3$, $p = 0.09$), though the overall pattern was consistent with the analysis of days to pupation.

Adult survival by diet

Overall, mosquitoes fed 10% high-fructose or 10% sucrose survived longer—2.66 days and 2.22 days respectively—than mosquitoes fed sterile water ($\chi^2 = 19.76$, $df = 2$, $p = <0.01$); mean survival in the 10% high-fructose treatment was 7.68 ± 0.47 days ($n=56$), 8.12 ± 0.48 days in the 10% sucrose treatment ($n=58$), and 5.46 ± 0.39 days in the sterile water treatment ($n=52$). When comparing by diet only, both sucrose-fed and high-fructose-fed adults survived significantly longer than adults fed only sterile water ($z = -3.78$, $HR = 0.48$, $p = <0.01$ and $z = -4.36$, $HR = 0.42$, $p = <0.01$ respectively). There was no statistical difference in survival between sucrose-fed and high-fructose-fed adults ($P = 0.51$; Figure 1.5A).

Within the control sterile water treatment there was a statistically significant difference between mesocosms ($\chi^2 = 25.68$, $df = 3$, $p = <0.01$) with mosquitoes reared in the control and HF treatments surviving 2.32 days longer than those reared in LF and MF. Mean survival on sterile water in mesocosm LF was 4.69 ± 0.46 days ($n=16$), 3.65 ± 0.49 days in MF ($n=17$), 6.80 ± 0.40 days in HF ($n=10$), and 8.78 ± 0.74 days in C ($n=9$). Pairwise comparisons within this group revealed MF did not significantly differ from LF ($z = -1.78$, $HR = 0.53$, $p = 0.08$), but was statistically less than HF ($z = -3.89$, $HR = 0.15$, $p = <0.01$) and C ($z = -4.77$, $HR = 0.06$, $p = <0.01$). LF was statistically lower than HF ($z = -2.82$, $HR = 0.28$, $p = 0.01$) and C ($z = -3.91$, $HR = 0.12$, $p = <0.01$). HF did not differ statistically from C ($z = -1.66$, $HR = 0.42$, $p = 0.1$; Figure 1.5B). When comparing adult survival by mesocosm within the 10% high-fructose treatment, there was no statistically significant difference in mortality between mesocosms ($\chi^2 = 6.23$, $df = 3$, $p = 0.1$; Figure 1.5C). There were also no significant differences in mortality between mesocosms within the 10% sucrose diet treatment ($\chi^2 = 6.23$, $df = 3$, $p = 0.1$; Figure 1.5D).

Discussion

Controlled laboratory conditions are not reflective of the dynamic conditions found in nature and bacteriome dynamics likely reflect this as well. Thus, we explored how the bacteriomes of generationally lab-reared *A. albopictus* would respond when exposed to environmentally sourced aquatic media. If exposure to a similar source pool restricts symbiont colonization of mosquitoes reared in the lab, we anticipated that the bacteriomes of lab-colony mosquitoes reared in the low-filtration regimens would be more similar to wild pupae collected in the field from the same media. However, we observed no similarity in the microbial composition of the mosquitoes reared in the filtration regimens to their wild counterparts. Instead, we saw MF and LF, HF and C, and wild adults and wild pupae form distinct groups based on the composition of their experimental bacteriome. It is unsurprising that MF and LF would be similar, considering that both had access to the same pool of bacteria. However, it suggests that small-bodied yeast and other small eukaryotes did not influence the assembly of the adult mosquito microbiome following emergence through apparent ecological interactions. It is surprising, however, that the compositions of the mosquito associated bacteriomes in MF and LF were very different from those of wild pupae; species richness was approximately 35 times greater in wild pupae than in MF and LF. It is plausible that time was a factor in the assembly of the wild pupae bacteriomes. The species present in the wild pupae that were not seen in LF/MF may have been removed from the habitat via consumption by the wild larvae, thus unavailable to our lab larvae during our experiment. A future study aimed at characterizing this shift in water column composition could potentially resolve this unexpected dynamic. It is also possible that environmental bacteria may be more dependent on exposure to environmental factors and relocation of the water into a laboratory setting may have impacted the survivability of many of the bacteria seen in the wild pupae.

Considering that *As. taiwanensis* was not present in our LF and MF mesocosms, it's likely that many environmental eukaryotes were filtered out of these mesocosms. This could also explain why LF and MF bacteriomes were similar to each other, but significantly different from wild pupae and wild adults. The fungal composition of the mosquito microbiome is diverse with hundreds of species having been described (reviewed in Tawidian et al., 2019) but the role those fungal species play in shaping the microbiome is poorly understood. Interactions between bacteria within the bacteriome network have been shown to modulate the assembly of the bacterial community in mosquitoes (Hegde et al., 2018); the role of fungal networks and their contribution to mosquito microbiome assembly are not well described, however, fungal networks have been shown to have more network connectivity than bacteria in soil (Xiao et al., 2018) and this network connectivity could be an important mechanism that structures mosquito microbiome assembly. A scarcity of fungal symbionts that can colonize mosquito hosts in our LF and MF mesocosms might explain why the bacteriomes of those treatments did not resemble the bacteriomes of wild pupae and wild adults if inter-kingdom interactions contribute to microbiome assembly. A future study aimed at characterizing the role of fungi in mosquito bacteriome assembly could potentially elucidate these mechanisms.

Water chemistry did not appear to impact the bacteriome assembly as evidenced by the similarity of HF and C. These groups were provided the same regional species pool of symbionts (i.e. those bacteria taxa that are dominant in the lab environment colonizing from the egg surface or the filter paper upon which eggs were deposited), but HF was reared in aquatic media likely enriched with compounds from natural organic material and secondary metabolites from the environmental microbiota. Nonetheless, the bacteriomes between HF and C were indistinguishable and assembled similarly in both mesocosm environments. These data suggest

that our lab-based mosquito bacteriome assembly is insensitive to the chemistry of the aquatic environment alone and imply that other factors such as access to the same larval food and access to a similar bacterial symbiont species pool are the driving factors of bacteriome assembly.

There were clear differences in the developmental outcomes depending on the mesocosm in which mosquitoes were reared. Mosquitoes reached the pupal stage on average 38 hours faster in the low and medium filtration mesocosms (MF and LF). Recent work has highlighted that mosquito larval development is likely riboflavin dependent and that gut microbiota are an important source of riboflavin in *Aedes* mosquitoes (Wang et al., 2021). Our lower effectiveness filtration regimes resulted in retaining bacteria capable of synthesizing riboflavin in biologically sufficient amounts in the larval habitat such as *Lactobacillus* spp. Considering that riboflavin decays under most environmental conditions encountered by *Aedes* larvae, our results might imply that the presence of bacteria in the larval habitat, not water chemistry, is a driving factor in early *Aedes* development times. One noticeable taxon, *Entomospira*, was overwhelmingly more abundant in the MF and LF mesocosms and it is possible this organism may have contributed to the noticeably increased developmental rates. For example, the spirochete *Borrelia burgdorferi* has very few metabolic pathways and must obtain its nutrients from its host (Caimano et al., 2016), potentially leading to altered host metabolism and the *Entomospira* spp. documented in this study may also lack the metabolic pathways needed for self-sufficient energy generation. However, considering how recently this species was discovered nothing is known about its metabolic pathways or its impact on mosquito development. Future work should be aimed at isolating this spirochete and using it in gnotobiotic transformations of *A. albopictus* to assess its impact on early mosquito development and other aspects of mosquito physiology. It is also possible that the observed differences in time to pupation were due to delayed egg hatching times

in the C and HF mesocosms. Egg hatching in *Aedes* mosquitoes is affected by the concentration of dissolved oxygen (DO) in the aquatic environment (Judson, 1960; Judson & Gojrati, 1967). Bacteria have been shown to stimulate egg hatching in *Aedes* mosquitoes by directly reducing the DO concentration of the aquatic environment via aerobic respiration (Gjullin et al., 1941) or via the production of water soluble metabolites (Ponnusamy et al., 2011). It is possible that our highest filtration regimes impacted the bacterial community enough to impact hatch times in the C and HF mesocosms. We did not investigate egg hatching rates in this study; however, future studies on early mosquito development and the microbiome should account for the stimulation of egg hatching by bacteria.

Our results show adult survival was significantly impacted by having access to a carbohydrate source compared to those only given sterile water. There does not appear to be a clear advantage to the type of carbohydrate consumed as survival outcomes did not differ between the two carbohydrate-diet groups overall in our study. However, when comparing survival outcomes by mesocosm and diet there are interesting differences. Our MF and LF mesocosm adults fed sterile water died sooner than our control and HF mesocosm adults fed the same diet. However, when fed either 10% sucrose or 10% high-fructose, MF and LF adult survival times improved to those similar to HF and C. This outcome may potentially be affected by the presence of the *Entomospira sp.* The presence of this taxon may be metabolically intensive for the host; for example, this organism could be pathogenic and host immunity is upregulated to combat the infection or the taxon could have increased metabolic needs itself, increasing competition with the host for limited nutrients. Isolating this bacterium for future gnotobiotic studies is essential to distinguish among these hypotheses and assess its cumulative impact on *A. albopictus* biology.

However, unlike previous studies (Delatte et al., 2009; Puggioli et al., 2013; Xue et al., 2010), we saw a much shorter lifespan in our carbohydrate-fed control groups. This could be due to our housing containers, which were smaller than those used in previous studies—we housed mosquitoes individually in 50 ml centrifuge tubes instead of larger tents and this could have potentially impacted lifespan. Also, unlike previous studies we used a temperature regime that is more reflective of natural conditions. The shorter lifespans observed in this study are closer to those observed in semi-field conditions (Lacroix et al., 2009; Yang et al., 2020) where temperatures vary along a gradient coinciding with the photoperiod. It is possible that *A. albopictus* are more sensitive to field-like temperature gradients and this also may potentially explain the reduced lifespans observed in this study.

Our work demonstrates that simple filtration regimens of aquatic media can be utilized to alter *A. albopictus* microbiota and that these alterations have important impacts on mosquito development and adult survival. We demonstrated that microbial-rich environments increase the rate of mosquito development and adult emergence compared to environments with lower microbial richness such as a standard laboratory environment. These results emphasize the need to incorporate higher microbial diversity into studies of lab-colonized *A. albopictus* mosquitoes in order to better reflect the dynamic conditions wild populations would encounter and how that translates into success across natural landscapes.

Table 1.1. The model output for variables included in the full linear model to explain variation in the observed species richness. Observed species richness was used as the response variable in the model.

Full Model	Estimate	Standard Error	T value	P value
Intercept (Wild Adults)	-6.98	0.28	-24.74	<0.001
Control	-1.48	0.56	-2.62	0.009
HF	-1.81	0.50	-3.65	<0.001
LF	-2.24	0.46	-4.87	<0.001
MF	-2.05	0.45	-4.57	<0.001
Wild pupae	1.37	0.41	3.37	<0.001
Sex (M)	0.09	0.29	0.31	0.76

Table 1.2. The estimates and associated standard errors of the model’s fixed effects and the variance and standard deviation of the model’s random effects which interrogates the β -diversity of bacteriomes between mesocosm treatments and wild-captured *Aedes albopictus*.

Full Model	Estimate	Standard Error	P-value
Intercept	-11.09	0.19	<0.01
Sex	-0.52	0.11	0.01
MFM3-(MF-LF)	-6.20	0.28	<0.01
MFM3-(HF-C)	-4.61	0.30	<0.01
MFM3-(WP)	2.75	0.23	<0.01
Random Effects	Variance	Standard Deviation	
Variable	3.96	1.99	
Variable x Sex	0.96	0.98	
Variable x MFM3	8.16	2.86	

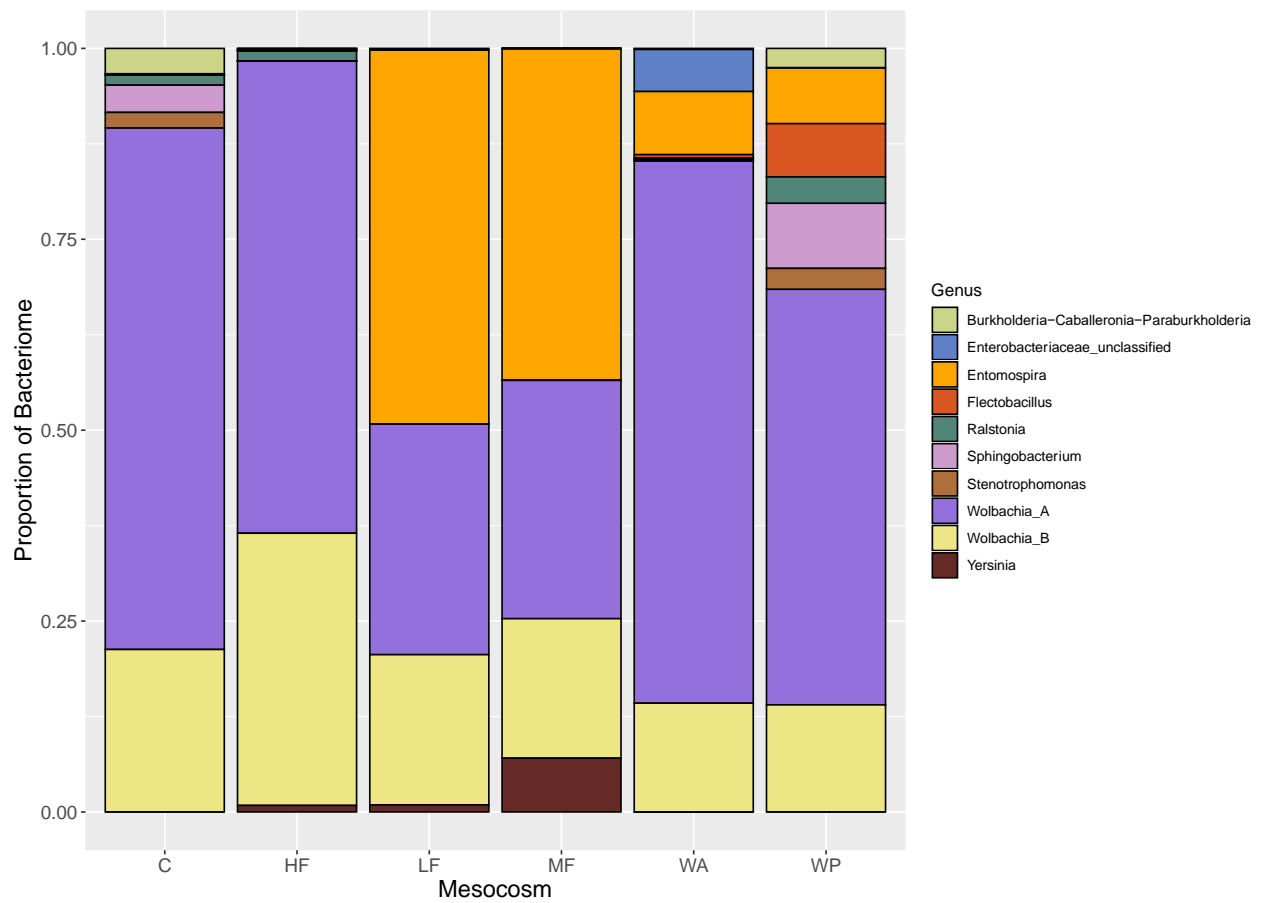


Figure 1.1. The composition of the bacteriome of *A. albopictus* among treatments. The top 9 OTUs are represented and comprise 96% of total reads. The wild pupae group were collected in the field during the pupal stage, but bacteriome sequencing was performed on adults after eclosion in the laboratory.

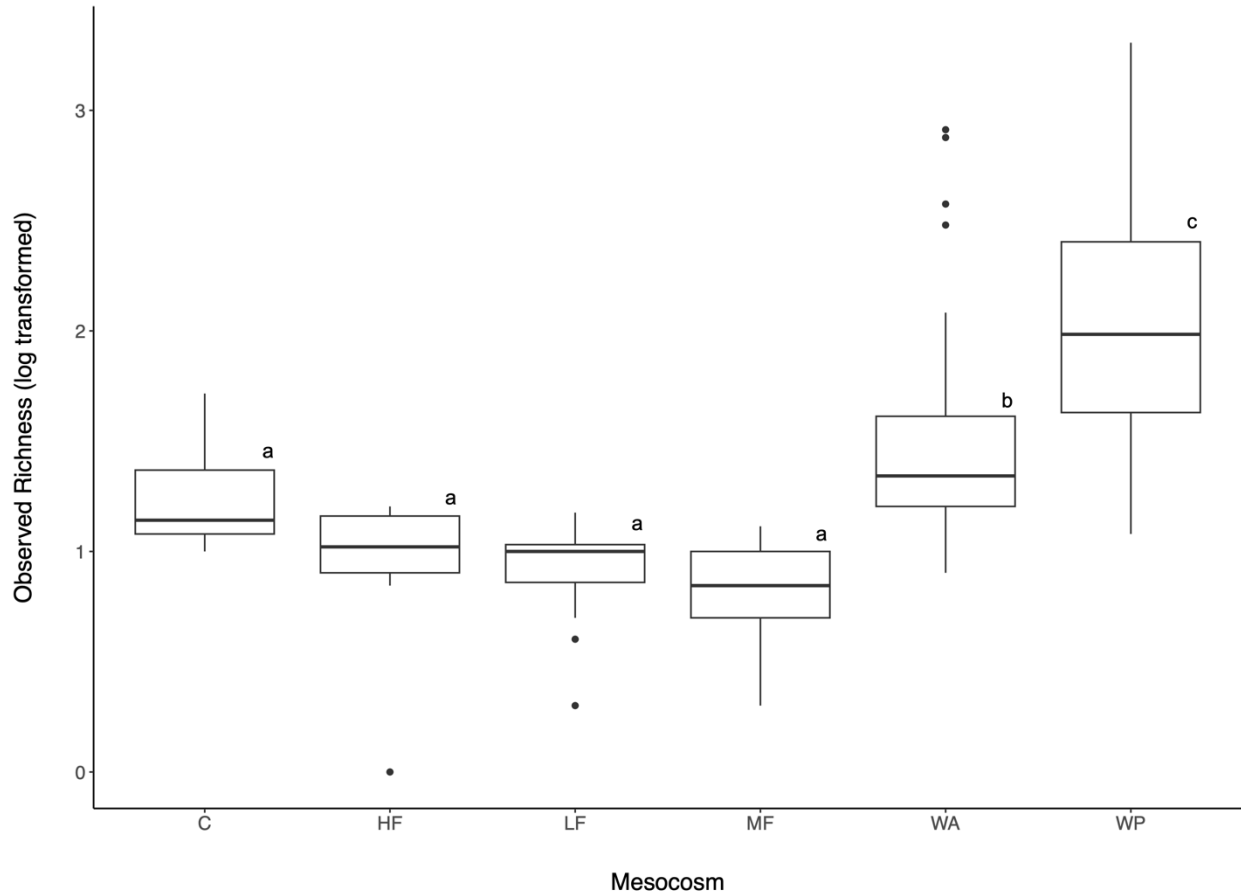


Figure 1.2. Box plots of observed alpha diversity measures and significant results from pairwise comparisons between the filtration treatments and wild-caught mosquito adults and pupae. Observed alpha diversity is presented on a log scale. Significant differences between mesocosms are indicated by letter. Box plots show the median as horizontal lines, and interquartile ranges as boxes with whiskers extending to 1.5 times the interquartile range.

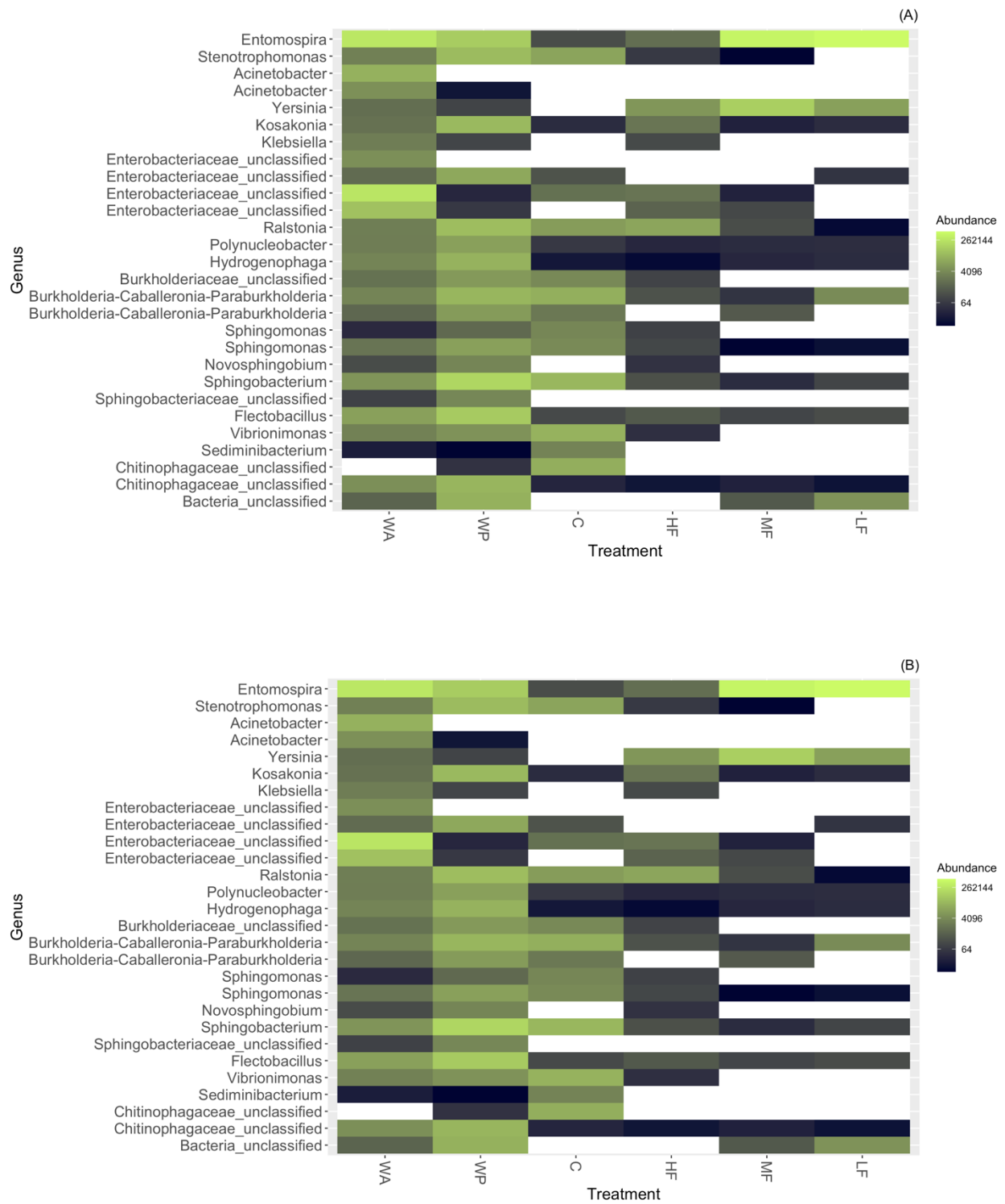


Figure 1.3. Heat maps demonstrating taxonomic abundance across mesocosms using (A) unweighted and (B) weighted unifracs distances.

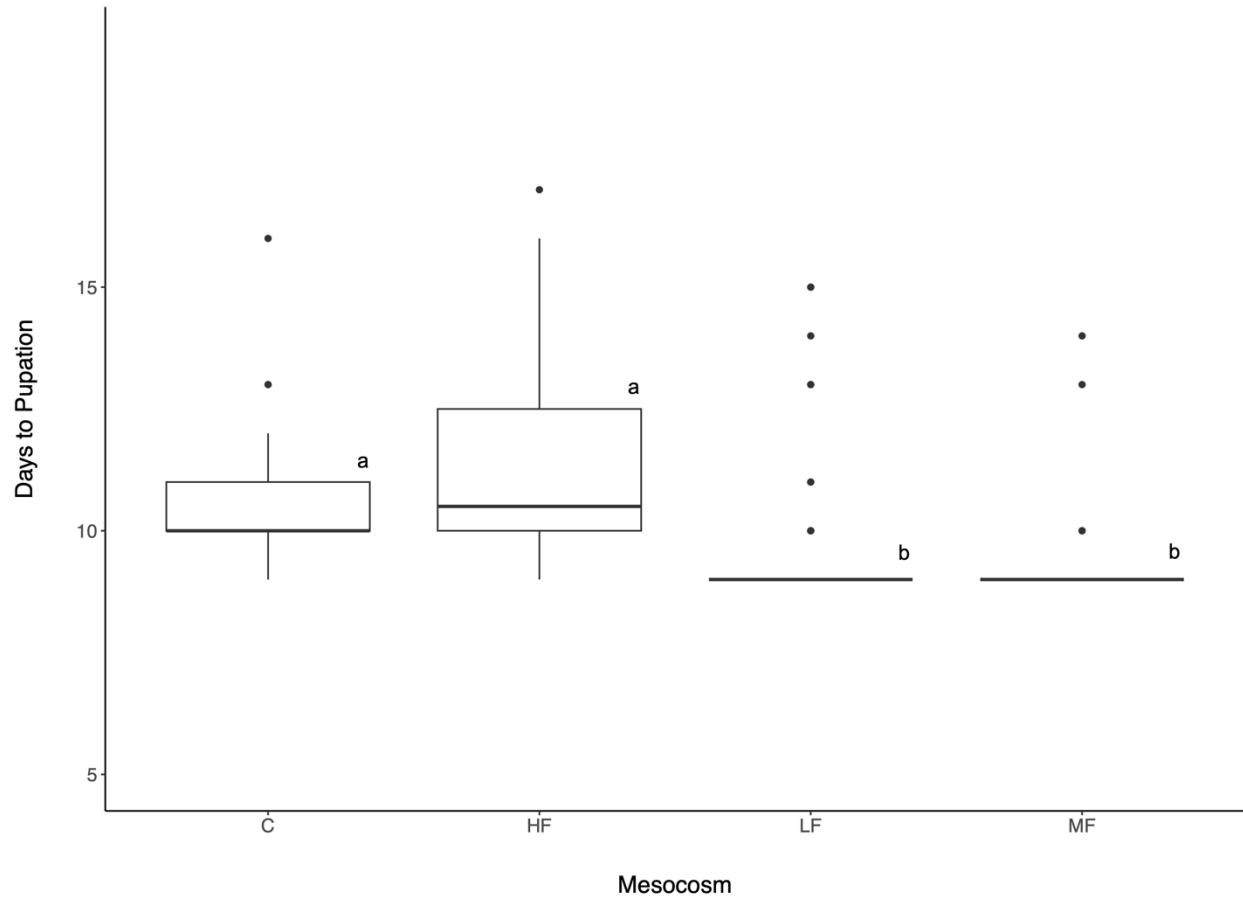


Figure 1.4. Box plots showing days to pupation by mesocosm. Mosquitoes in mesocosms LF (10 μm filter) and MF (2 μm filter) pupate on average 1.59 days faster than mosquitoes in mesocosms HF (0.2 μm filter) and C (Millipore water). Kruskal-Wallis test was used to identify statistically significant differences in time to pupation ($P < 0.05$). Significant differences between mesocosms are indicated by letter according to Dunn's post-hoc test. Box plots show the median as horizontal lines, and interquartile ranges as boxes with whiskers extending to 1.5 times the interquartile range.

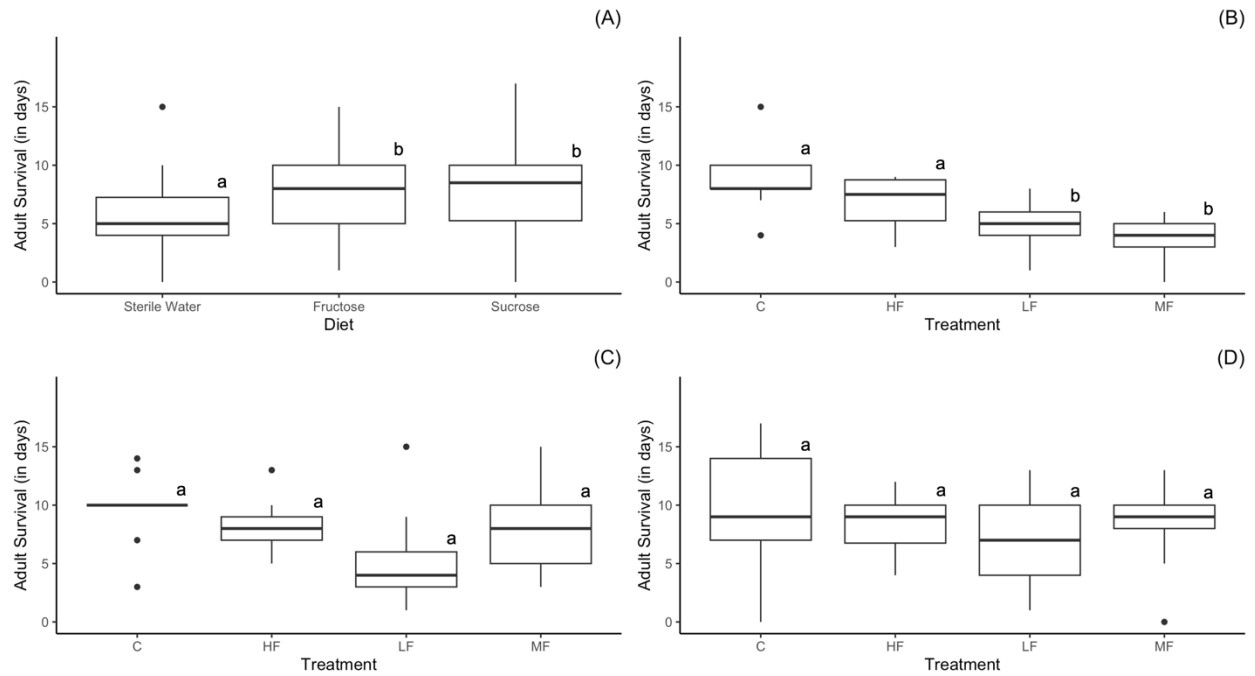


Figure 1.5. Adult survival in days by (a) diet, (b) by mesocosm on a sterile water diet, (c) by mesocosm on a 10% high-fructose diet, and (d) by mesocosm on a 10% sucrose diet. Cox Hazard regression was used to identify statistically different survival times ($P = <0.05$). Significant differences between mesocosms are indicated by letter. Boxplots show the median as horizontal lines, and interquartile ranges as boxes with whiskers extending to 1.5 times the interquartile range.

CHAPTER 2: FROM STRUCTURE TO ASSEMBLY: FUNGI ARE HIGHLY INFLUENTIAL IN THE *AEDEAS ALBOPICTUS* MICROBIOME

Introduction

Microorganisms routinely enter symbiosis with metazoans to form microbial communities, often referred to as microbiomes. These host-associated microbiomes modulate many physiological processes of the host including development, metabolism, immunity, nutrient provisioning, and behavior (McFall-Ngai et al., 2013; Gould et al., 2018). Despite their importance to host biology, microbiomes can exhibit substantial diversity among individuals within a population (Falony et al., 2016; Frankel-Bicker et al., 2020). The origin of this diversity is not fully understood, but it has been hypothesized that environmental variation may be a significant driver (Mushegian et al., 2019). A considerable portion of the microbiome is environmentally acquired (Seabourn et al., 2023); thus, environmental factors can influence the structure of microbial communities on the landscape (Medeiros et al., 2022), ultimately shaping the regional source pool from which a host will draw (Amend et al., 2022).

Tests of variance in composition such as PERMANOVA and principal coordinates analysis, have provided significant insight into the taxonomic diversity of host-associated microbiomes, but these techniques often fall short of explaining the mechanisms underlying that diversity. Techniques like network analysis may provide the first steps towards uncovering those ecological mechanisms. Network analyses are powerful approaches for inferring correlations among the microorganisms within complex microbial communities (Layeghifard et al., 2017), which might relate to direct associations and interactions. These analyses have been particularly insightful in revealing co-occurrence patterns among microorganisms across a range of habitats

(Faust et al., 2012, Williams et al., 2014). Such patterns of association can be positive or negative, related, for example, to mutualism, competition, and predatory interactions, and could provide evidence that certain microbe-microbe interactions shape microbiome composition (Wright et al., 2013, Hassani et al., 2018). Interactions of particular interest, though relatively poorly investigated in metazoan-associated microbiomes, are those between symbiotic bacteria and fungi. Bacterial-fungal interactions (BFI) play an important role in microbial communities (Frey-Klett et al., 2011; Sam et al., 2017), and these interactions could be potential drivers of diversity across host-associated microbiomes. For example, Tipton et al. (2018) demonstrated that microbiomes are more robust to stressors when bacteria and fungi co-occur, suggesting that cross-domain interactions help stabilize the microbial community and contribute to the overall assembly of the microbiome.

While computer-generated models and simulations of networks serve as a valuable tool to explore the complex dynamics of microbial communities, it is also necessary to test the predictions of network analyses in biological systems to validate model inferences. Some work has been done in this area using culturing techniques (Steinway et al., 2015; Das et al., 2018), but no work has been done manipulating entire microbiomes *in vivo* and *in situ* based on network predictions within a host organism. Insects are an excellent model for this purpose because they have a simpler microbiome that is more tractable than those of other host systems (Muturi et al., 2017; Bennet et al., 2019).

Here we use network analysis to inform *in vivo* host-level microbiome manipulations using a mosquito host, *Aedes albopictus*, as a model. We used a next generation sequencing dataset consisting of amplicon sequencing variants (ASVs) of the bacterial 16S rRNA gene and the fungal internal transcribed spacer (ITS) gene obtained from *A. albopictus* collected

throughout Mānoa Valley on O‘ahu, Hawai‘i. We generated three networks from the sequencing data: a 16S-only network, an ITS-only network, and a cross-domain network consisting of 16S and ITS. We analyzed each network’s attack robustness (Iyer et al., 2013), which is a measure of the network’s ability to remain connected when nodes are sequentially removed. We also performed a keystone species analysis using betweenness centrality (the total number of shortest paths from node to node) and node degree (a measure of how many connections one node makes to another node) (Tipton et al., 2018). From the predictions of the network analyses we hypothesized that the presence of fungi in the mosquito microbiome is an important driver of community assembly and structure of the microbiome. We tested the hypothesis by (i) sourcing microbial communities from three different environments, (ii) manipulating the composition of those communities using stratified filtration regimes that removed sequentially larger cells and particulates from aquatic substrate, (iii) exposing mosquitoes to the microbial communities in the filtered substrates, and (iv) characterizing the mosquito microbiome across manipulations.

Methods

Mosquito sample collection used for network analyses

Adult *A. albopictus* (n = 53) were collected throughout Makiki Valley, O‘ahu, Hawai‘i using hand nets and handheld aspirators. The mosquitoes were transported from the field to the lab at 4°C. Upon arrival in the lab, they were sterilized with 75% ethanol for 1 min and rinsed twice in sterile 1X PBS. Midguts were immediately dissected and placed individually into a 1.5 ml centrifuge tube containing sterile 1X PBS. Midgut samples were stored at – 80°C until DNA extraction. DNA was extracted and purified on a KingFisher Flex using a NucleoMag Tissue kit following the manufacturer’s protocol. SeqMatic (Fremont, California, USA) sequenced the 16S

library in a single run on an Illumina NovaSeq 6000 using a 250bp paired-end NovaSeq 6000 SP Reagent Kit v1.5 500 cycles. The ITS library was sequenced in a single run on an Illumina MiSeq PE300 platform using a 250 bp paired end with a MiSeq reagent kit v3.

Bioinformatics of mosquitoes used for network analyses

Bioinformatics analysis was performed using the MetaFlow|omics pipeline for microbiome marker data (Arisdakessian et al., 2020). Reads were truncated at position 220 (190 for the reverse read) and were discarded if they contained at least one base below quality 20 (minimum quality to assign nucleotide identity with <1% error) or a number of expected errors above 3. Two ASVs were merged if all the three following conditions were satisfied: *i*) they co-occur in every sample, *ii*) one of the two ASVs has a lower relative abundance than the other in every sample, and *iii*) they share a sequence similarity of at least 99%. All singletons (ASVs with reads in only one sample) and ASVs with no annotation at the kingdom level were removed. After quality control, sequencing resulted in 20.16 million 16S reads and 780,066 ITS reads. Further ASV processing was performed by merging the abundance data, taxonomic data, and sample data using the Phyloseq package (McMurdie and Holmes 2013) in R. 16S and ITS ASVs were included in the final analysis only if they appeared more than once in 2.5% of total samples.

Estimation of microbial association networks

We constructed our microbial association networks using the Sparse Inverse Covariance estimation for Ecological Association and Statistical Inference (SPIEC-EASI) framework (Kurtz et al., 2015). Nodes in each network corresponded to ASVs and edges corresponded to inferred associations between ASVs. We ran SPIEC-EASI in neighborhood selection mode and model

selection was performed based on the Stability Approach to Regularization Selection (StARS) (Liu et al., 2010) using a variability threshold of 0.05%.

Evaluating and comparing networks

Networks were analyzed using functions within the *igraph* R package version 1.3.5 (Csardi and Nepusz 2006). We evaluated node degree (the total edges a node has), betweenness centrality (the number of paths going through a node), modularity (the number of subgraphs or communities within the network). We also measured attack robustness (the network's ability to remain connected when nodes are removed) using the R package *brainGraph* version 3.0.0 (Watson 2020). We performed the robustness analyses by targeting nodes based on betweenness and node degree.

Habitat design for in vivo validation of network analyses

Two large plastic buckets were filled with one tablespoon of field topsoil and 1 teaspoon of crushed leaf detritus collected from the University of Hawai'i at Mānoa campus (UH-Mānoa), three liters of sterile water and one wooden shim (for oviposition). The buckets were placed outside, in a semi-shaded area, on the UH-Mānoa campus and were left exposed to natural conditions for 7 days. The buckets were checked every two days to ensure water levels never fell below two liters. The water level was restored to three liters with sterile water when necessary. After 7 days, the water from the buckets was collected and returned to the laboratory for processing. *Aedes albopictus* larvae were present in the habitat when the water was collected. Two liters of water were also collected from the tanks of bromeliads (genus *Neoregelia*), at Lyon

Arboretum in Mānoa Valley, Honolulu, Hawai‘i. The bromeliad water was collected on the day of processing; no *A. albopictus* were found in it.

For both water sources, three inocula were prepared: a 30-50 μm filtration inoculum, a 10 μm filtration inoculum, and a 0.1 μm filtration inoculum. The 30-50 μm inoculum was prepared by filtering the collected water through a 30-50 μm coffee filter once. The 10 μm inoculum was prepared by filtering the collected water through a 30-50 μm coffee filter once, then filtering the filtrate through a 10 μm syringe-filter once. The 0.1 μm inoculum was prepared in the same way as the 10 μm inoculum followed by a single filtration through a 0.1 μm vacuum filtration cup. We chose these filtration sizes to allow for the microbial composition of the inoculum to vary by cell size. The 30-50 μm filter would allow larger eukaryotic cells such as fungi and yeasts and bacterial cells to enter the filtrate. The 10 μm filter would prevent most eukaryotic cells from entering the filtrate but would allow some small yeasts and bacterial cells to pass. The 0.1 μm filter would prevent eukaryotic and bacterial cells from entering the filtrate, but would allow metabolites and other molecules to pass through. An approximate total of 300 ml was obtained from each filtration level for both water sources. A control inoculum, which consisted of pure water from a Millipore Milli-Q water filtration system (Massachusetts, USA), was included to represent the larval habitat conditions mosquitoes experience in a typical laboratory environment.

Mesocosm design

Experimental mesocosms were created by pipetting 100 ml of a single inoculum type into a 150 x 15 mm petri dish. There were seven treatment levels: Lyon Arboretum 0.1 μm , 10 μm , 30-50 μm , artificial container 0.1 μm , 10 μm , 30-50 μm , and laboratory environment control. All

treatments contained three replicates for a total of 21 mesocosm treatments. After pipetting each inoculum into the petri dish, 100 *A. albopictus* eggs were placed into each mesocosm. The eggs were obtained from our lab colony that originated from wild *A. albopictus* isolated from Mānoa, Oahu, Hawai‘i and raised in the lab for 21 generations prior to the start of the experiment.

Mosquito rearing and handling

We reared *A. albopictus* with a 12 L:12 D photoperiod. Temperature in the light period was 28°C, whereas temperature in the dark period was 22°C, which reflect average conditions found at sea level during the summer months on O‘ahu, Hawai‘i. Humidity was kept constant at 60% for the entire photoperiod. A custom food preparation was made that consisted of a 1:1 ratio of liver powder to dried yeast extract mixed with pure water to a concentration of 18 mg per ml. To kill viable microorganisms, the food preparation was autoclaved for 30 minutes prior to being introduced into each mesocosm. Larval food water was administered daily at a concentration of 0.2 mg per larva per mesocosm. On day 8 and day 10 of the experiment, L3-L4 larvae (n=5) were removed from each mesocosm, placed in a 1.5 ml centrifuge tube with 0.5 ml of water and stored at -20°C until processed for microbiome analysis. Remaining larvae were monitored daily for pupation. Pupae were removed using a pipette and transferred to a 50 ml sterile centrifuge tube. Pupae were housed individually after being collected from the mesocosm and were monitored daily for eclosion.

DNA extraction, amplification, and sequencing of mesocosm mosquitoes

Emerged adults were housed at 4°C for approximately 30 minutes for cold anaesthetization and transferred into 1.5 ml centrifuged tubes before being frozen at -20°C. Prior

to DNA extraction, all adults (n = 168; 84 males, 84 females, 4 per mesocosm replicate) and larvae (n = 84; 4 per mesocosm replicate) that were used for microbiome analysis were subjected to a surface-sterilization protocol adapted from Muturi et al., (2018) consisting of one wash in 70% ethanol followed by two rinses in sterile 1X PBS. DNA was extracted and purified on a KingFisher Flex using a Qiagen MagAttract PowerSoil DNA KF Kit following the manufacturer's protocol. The bacterial library preparation was done using a modified version of the Earth Microbiome Project 16S V4 protocol (Caporaso et al., 2011). PCR amplification targeted the V4 region of bacterial 16S rRNA using 515F and 806R primers from the Earth Microbiome Project. The ITS library preparation was also done using a modified version of the Earth Microbiome Project ITS Illumina Amplicon protocol (Caporoso et al., 2011). PCR amplification targeted the internal transcribed spacer region using ITS1f and ITS2 primers from the Earth Microbiome Project. Both libraries was checked for quality and quantity using a Bioanalyzer High Sensitivity chip (Agilent Technologies) and sequenced by the Advanced Studies in Genomics, Proteomics, and Bioinformatics (ASGBP) core facility at the University of Hawai'i at Mānoa using Illumina MiSeq PE300 with a MiSeq Reagent Kit v3 (Illumina). and sequenced by ASGBP at the University of Hawai'i at Mānoa using Illumina MiSeq PE300 with a MiSeq Reagent Kit v3 (Illumina).

Bioinformatics of mesocosm mosquitoes

Bioinformatics analysis was performed with the same method used for the network analyses mosquitoes. Further ASV processing was performed by merging the abundance data, taxonomic data, and sample data using the Phyloseq package (McMurdie and Holmes 2013) in R. 16S ASVs were included only if they appeared more than once in 15% of total samples.

Community assembly analyses

To compare bacteriomes, β -diversity was investigated among the mesocosms with different water filtration treatments. To assess β -diversity, changes in the composition of the bacteriome in response to the larval environment (control, 30-50 μm , 10 μm , and 0.1 μm) were tested statistically with a generalized linear mixed model (GLMM) using the R package `glmmTMB` (Brooks et al., 2017) assuming a negative binomial error distribution, similar to the approach detailed by Sweeny et al., (2023). All models also included a formula that allows the dispersion parameter to vary among levels of a specified fixed effect, which included the filtration level, mosquito stage, and individual ASV. All candidate models included an offset for sequencing reads per sample, fixed effects for mosquito type (larva, adult), filtration level, and a random intercept for ASV identity. Among specific models in the candidate set, the responses in relative abundance of every ASV to both mosquito type and filtration type were allowed to vary by specifying random interaction effects. The full set of candidate models are listed in Supplemental Table 1. We used the Akaike information criterion (AIC) to select the most suitable model among the models included in this candidate set.

Estimation of *Ascogregarina taiwanensis* load

Ascogregarina taiwanensis served as a marker to determine the presence of eukaryotes post-filtration since in the oocyst stage it is approximately 9 μm x 5 μm (Chen et al., 1997). *Ascogregarina taiwanensis* load was measured using the protocol described by Seabourn et al., (2020).

Results

Network analyses

The 16S single-domain network consisted of one main connected component (76 out of 84 ASVs (90.48%) and eight singleton 16S ASVs unconnected to the main network. The average node degree of the network was 3.69 ± 4.44 . The average betweenness centrality of the network was 122.06 ± 272.67 . Based on their connectivity pattern, we clustered the 16S ASVs using modularity optimization (Clauset *et al.*, 2004), resulting in 12 modules with a modularity score of 0.46. The fungal ITS single-domain network consisted of one main connected component (246 out of 276 ASVs (89.13%)), one dyad, and 28 singleton ASVs. The average node degree of the network was 2.96 ± 2.40 . The average betweenness centrality was 446.97 ± 766.31 . The fungal-only network consisted of 40 modules with a modularity score of 0.69. The 16S-ITS cross-domain network consisted of one main connected component (515 ASVs out of 518 ASVs (99.42%)) and three singleton fungal ASVs without connections to the main network (Supplemental figure 2). The average node degree of the network was 6.52 ± 3.14 . The average betweenness centrality was 702.03 ± 672.71 . The cross-domain network consisted of 12 modules with a modularity score of 0.48.

Attack robustness is a measure of the network's overall ability to withstand the failure of its constituent parts (Iyer *et al.*, 2013) and can be measured by sequentially removing nodes within the network and measuring the size of the largest remaining component after each removal (Ruiz *et al.*, 2015). We removed nodes in order of decreasing betweenness centrality (Figure 2.1A) and in order of decreasing node degree (Figure 2.1B). In each measure, the attack robustness of the cross-domain network was considerably increased compared to those of the 16S-only network and the ITS-only network.

The keystone species analysis of the cross-domain network revealed that fungal ASVs represent a higher proportion of important nodes with the greatest centrality values (Figure 2.2). High betweenness centrality indicates important connector taxa within the network and a high node degree indicates those taxa that are important hubs within the network. Together, both metrics highlight the importance of those taxa to the overall structure of the network.

Sequencing Data Summary of In Vivo Microbiome Manipulations

A total of 10,655,249 16S reads passed through quality filtering and were allocated among 1,959 ASVs. Of these 16S ASVs, 119 had a prevalence of greater than 15% across samples and were included in the subsequent analysis of the microbiome. Among the top 20 16S ASVs, there were three phyla (Proteobacteria, Actinobacteriota, and Bacteroidota) represented by 16 genera (Supplemental figure 2.1A). *Wolbachia*, a common symbiont of *A. albopictus*, was removed from the analysis because it is not environmentally acquired. A total of 960,796 ITS reads passed through quality filtering and were allocated among 234 ASVs. Of these 234 ASVs, the top 20 accounted for 98.99% of reads; there were two phyla (Ascomycota and Basidiomycota) represented by 13 genera (Supplemental figure 2.1B).

In Vivo Microbiome Analyses

Generalized linear mixed models were used to evaluate the response of the host-associated bacterial communities. For the treatments derived from Lyon Arboretum, the model that best fitted the data (AICc weight = 1; table 1) included fixed effects of *i*) mosquito type (larva, adult), *ii*) microbial source (natural or lab environment), *iii*) an interaction between mosquito type and microbial source, and random effects of *iv*) ASV identity, *v*) mesocosm

identity, *vi*) interaction between ASV identity and mosquito type, *vii*) interaction between ASV identity and mesocosm identity, *viii*) interaction between ASV identity and microbial source, and *ix*) three-way interaction between ASV identity, mosquito type, and microbial source. In this model, the microbial source variable was defined by grouping the filtration treatments into four distinct modules: lab (Millipore water), environmental water filtered at 0.1 μm , environmental water filtered at 10 μm , and environmental water filtered at 30-50 μm (Figure 2.3A). See Supplemental table 1 for the full set of candidate models and Supplemental table 2.2 for their AICc results. For the treatments derived from the UH-Mānoa campus, the model that best fitted the data (AICc weight = 1.0; table 2.2) was identical to the best fit model from the Lyon Arboretum treatments (Figure 2.3B). See Supplemental table 2.3 for the full set of candidate models and Supplemental table 2.4 for their AICc results.

Presence of *Ascogregarina taiwanensis*

None of all the 232 *A. albopictus* samples tested positive for the presence of *A. taiwanensis*.

Discussion

Network construction is a powerful computational tool for analyzing ecological associations. Networks provide a more integrated picture of ecological complexity and allow for a holistic analysis of the associations and interactions within communities (Fath et al., 2007). Based on sequences of bacterial 16S rRNA and fungal ITS genes, we inferred single-domain and cross-domain microbial-association networks of the *A. albopictus* microbiome. The inferred cross-domain network had higher connectivity than both single-domain networks. However, the

cross-domain network showed higher modularity than the 16S single-domain network, but lower modularity than the ITS single-domain network. The cross-domain network also showed higher attack robustness than both single-domain networks.

Several studies have shown that higher robustness has a stabilizing effect on the network when the network is under attack (Mahana et al., 2016, Ruiz et al., 2017, Lee et al., 2022). Since our cross-domain network showed the highest robustness, we then investigated which components of the network were driving the higher robustness. We performed a keystone species analysis by looking at the most important nodes (ASVs) in the network and found that six nodes were highly important to the overall connectivity of the network. Five of the six nodes were identified as ITS ASVs, indicating that fungi may have the most influence on the structure and assembly of the *A. albopictus* microbiome.

Based on the results of the network and keystone species analyses, we hypothesized that fungi have a prominent influence on the assembly of the *A. albopictus* microbiome. Therefore, we designed our filtration regimens to alter the compositionality of the microbial community in our mesocosm inocula based on microbial cell size. Our hypothesis was supported for the mesocosms derived from both Lyon Arboretum and UH-Mānoa. Our best-fit model for the Lyon Arboretum treatments (Table 2.1) suggested that the presence of large cells (i.e. fungi and other eukaryotes) is an important driver of bacteriome assembly in mosquitoes. However, it is likely that fungal identity is more important than fungal presence per se. We saw a unique fungal ASV (ASV_59) in our 30-50 μm filtration treatment from this environment that was not present in the other filtration treatments. ASV_59 was identified as belonging to Didymellaceae, a large family consisting of many species of plant pathogens (Chen et al., 2017). It is possible that this fungal

ASV could be influencing the bacterial community via BFIs or possibly via an indirect mechanism related to its plant pathogenicity.

For the UH-Mānoa treatments, our best-fit model suggested that bacterial community assembly was impacted when fungi are present in the environment. Both the 30-50 μm filtration and 10 μm filtration treatments included fungi, but each treatment contained unique fungal ASVs that potentially impacted the bacterial community. For example, one fungal ASV (ASV_16) was only found in the 30-50 μm filtration treatments, whereas the 10 μm treatments contained two unique fungal ASVs (ASV_7 and ASV_9) that were not present in the 30-50 μm treatments. It is possible that these ASVs were influential in the assembly process via BFI and that this could explain the observed differences in bacterial assembly between the two treatments. We were unable to identify ASVs 7, 9, and 16 beyond the kingdom level.

Another potential driver of microbiome assembly in *A. albopictus* is infection with the apicomplexan parasite *Ascogregarina taiwanensis*. This parasite is present in Hawaiian *A. albopictus* populations and infection with *A. taiwanensis* is associated with microbiome diversity in *A. albopictus* hosts (Seabourn et al., 2020). Since all of our mosquito samples were negative for *A. taiwanensis* infection, we conclude that the patterns of bacterial assembly we saw in our results were not caused by this eukaryotic parasite.

Both best-fit models also showed a significant effect on bacterial assembly of the interaction between mosquito type and filtration. *Aedes albopictus* larvae formed distinct groups in the Lyon Arboretum and UH-Mānoa 30-50 μm filtration, 10 μm filtration, 0.1 μm filtration and lab groupings. It is unlikely that the difference between the laboratory mesocosm and the 0.1 μm filtration is due to differences in bacterial source pools. Since the eggs used in this experiment were not sterilized, and the 0.1 μm filtration would have prevented viable cells in the

source pool from entering the filtrate used to inoculate the mesocosm, those two treatments probably had a similar source pool of viable bacteria at the onset of the experiment. The assembly of the mosquito bacteriome could have been influenced by any metabolites that passed through the 0.1 μm filter into the inoculum as secondary metabolite cross-feeding can promote taxonomic diversity within microbial communities (Embree et al., 2015, Douglas 2020). Alternatively, the distinctiveness of the 0.1 μm filtration group could be due to sequencing of 16S rRNA fragments present in the mesocosm post-filtration that were ingested by larvae during foraging. Lastly, both scenarios could also occur simultaneously; thus, a future experiment eliminating environmental DNA from the 0.1 μm inoculum while leaving secondary metabolites could clarify the role of secondary metabolites on bacteriome assembly in *A. albopictus*.

It is unsurprising that larvae and adults would have different bacteriomes because microorganisms were introduced during the larval stage only. Thus, larvae were exposed to a greater diversity of microbes than the adults. Mosquito larvae also evacuate their gut contents shortly before pupating, which eliminates a substantial proportion of the microbial community prior to becoming adults (Duguma et al., 2015). Furthermore, the larval midgut undergoes extensive remodeling during metamorphosis (Fernandes et al., 2014), which impacts bacteria present in the gut at eclosion (Moll et al., 2001). However, this is an area that needs research because no study has explored how the remodeling process mechanistically affects microbiome composition in mosquitoes.

Host-associated microbiomes exhibit considerable diversity within and among hosts. Yet, the origin of this diversity is not well understood. To the best of our knowledge, this is the first study to pair *in silico* modeling of microbial associations with *in vivo* community-level manipulations of whole environmental and host-associated microbiomes to describe how

microbial interactions contribute to microbiome diversity. The results from our *in vivo* experiments show that BFIs are an important mechanism shaping microbiome diversity in *A. albopictus*. These results demonstrate that the often overlooked fungal components of microbial communities can have substantial ecological roles in host-associated microbiomes. Thus, future microbiome studies should account for, and include, BFIs to the extent possible.

Table 2.1. Generalized linear mixed models demonstrating Δ AICc values of distinct models that partitioned variance in the composition of the bacteriome among different hypothetical groupings of the Lyon Arboretum filtration regimens.

Fixed effects	Random effects	Δ AICc	df	AICc weight	Hypothesis
offset(log(sum)), mosquito-stage, treatment2, mosquito- stage*treatment2	ASV, mesocosm, ASV*mosquito-stage, ASV*mesocosm, ASV*treatment2, ASV*mosquito- stage*treatment2	0	174	1	Mosquito bacteriome assembly is modulated by the inclusion of large microbial cells in the inoculate. Treatment2 groups filtrations into individual modules: lab (Millipore), 0.1 μ m, 10 μ m, and 30-50 μ m.
offset(log(sum)), mosquito-stage, BacSource3, mosquito- stage*BacSource3	ASV, mesocosm, ASV*BacSource3, ASV*mesocosm, ASV*BacSource3, ASV*mosquito- stage*BacSource3	85.5	171	<0.001	Mosquito bacteriome assembly is not modulated by the inclusion of large microbial cells in the environment but is modulated by bacteria source (natural environment vs. lab environment).
offset(log(sum)), mosquito-stage, treatment, mosquito- stage*treatment	ASV, mesocosm, ASV*mosquito-stage, ASV*mesocosm, ASV*treatment, ASV*mosquito- stage*treatment	312.7	180	<0.001	Mosquito bacteriome assembly is modulated by the inclusion of larger microbial cells in the inoculate. Treatment groups filtrations into individual modules: lab (Millipore), lab 2 (Millipore), lab 3 (Millipore), 0.1 μ m, 10 μ m, and 30-50 μ m.

Table 2.2. Generalized linear mixed models demonstrating ΔAICc values of distinct models that partitioned variance in the composition of the bacteriome among different hypothetical groupings of the UH-Mānoa filtration regimens.

Fixed effects	Random effects	ΔAICc	<i>df</i>	AICc weight	Hypothesis
offset(log(sum)), mosquito-stage, treatment2, mosquito- stage*treatment2	ASV, mesocosm, ASV*mosquito-stage, ASV*mesocosm, ASV*treatment2, ASV*mosquito- stage*treatment2	0	174	1	Mosquito bacteriome assembly is modulated by the inclusion of large microbial cells in the inoculate. Treatment2 groups filtrations into individual modules: lab (Millipore), 0.1 μm , 10 μm , and 30-50 μm .
offset(log(sum)), mosquito-stage, BacSource3, mosquito- stage*BacSource3	ASV, mesocosm, ASV*BacSource3, ASV*mesocosm, ASV*BacSource3, ASV*mosquito- stage*BacSource3	85.5	171	<0.001	Mosquito bacteriome assembly is not modulated by the inclusion of large microbial cells in the environment but is modulated by bacteria source (natural environment vs. lab environment).
offset(log(sum)), mosquito-stage, treatment, mosquito- stage*treatment	ASV, mesocosm, ASV*mosquito-stage, ASV*mesocosm, ASV*treatment, ASV*mosquito- stage*treatment	312.7	180	<0.001	Mosquito bacteriome assembly is modulated by the inclusion of larger microbial cells in the inoculate. Treatment groups filtrations into individual modules: lab (Millipore), lab 2 (Millipore), lab 3 (Millipore), 0.1 μm , 10 μm , and 30-50 μm .

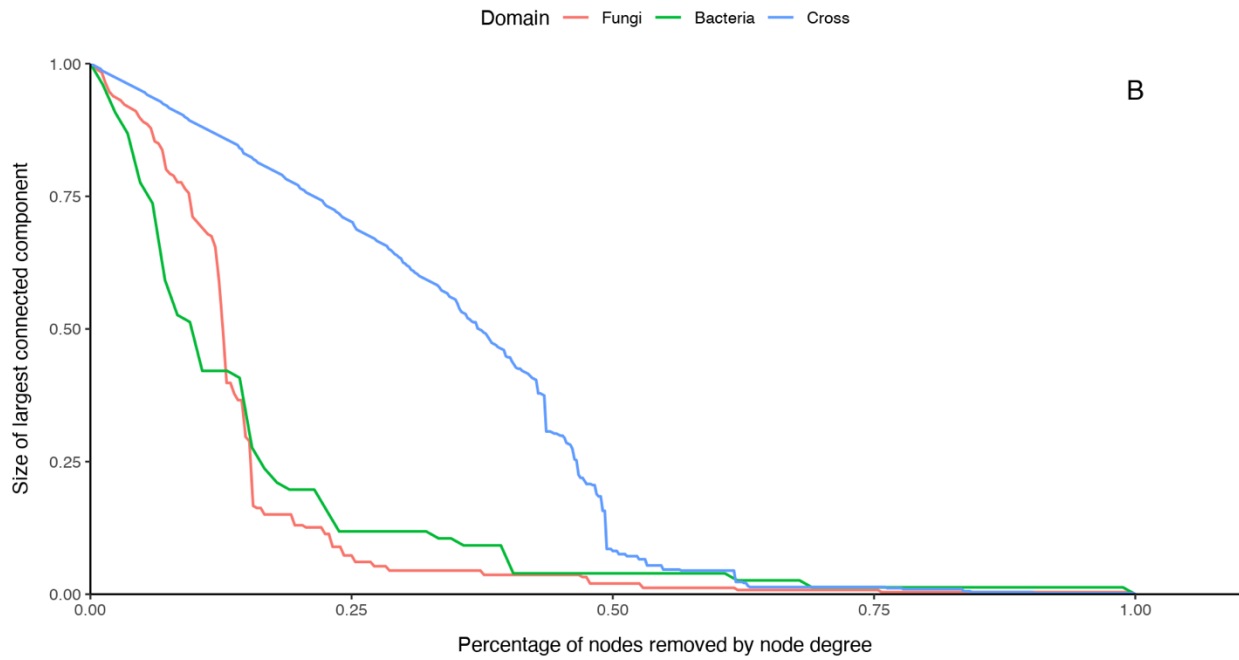
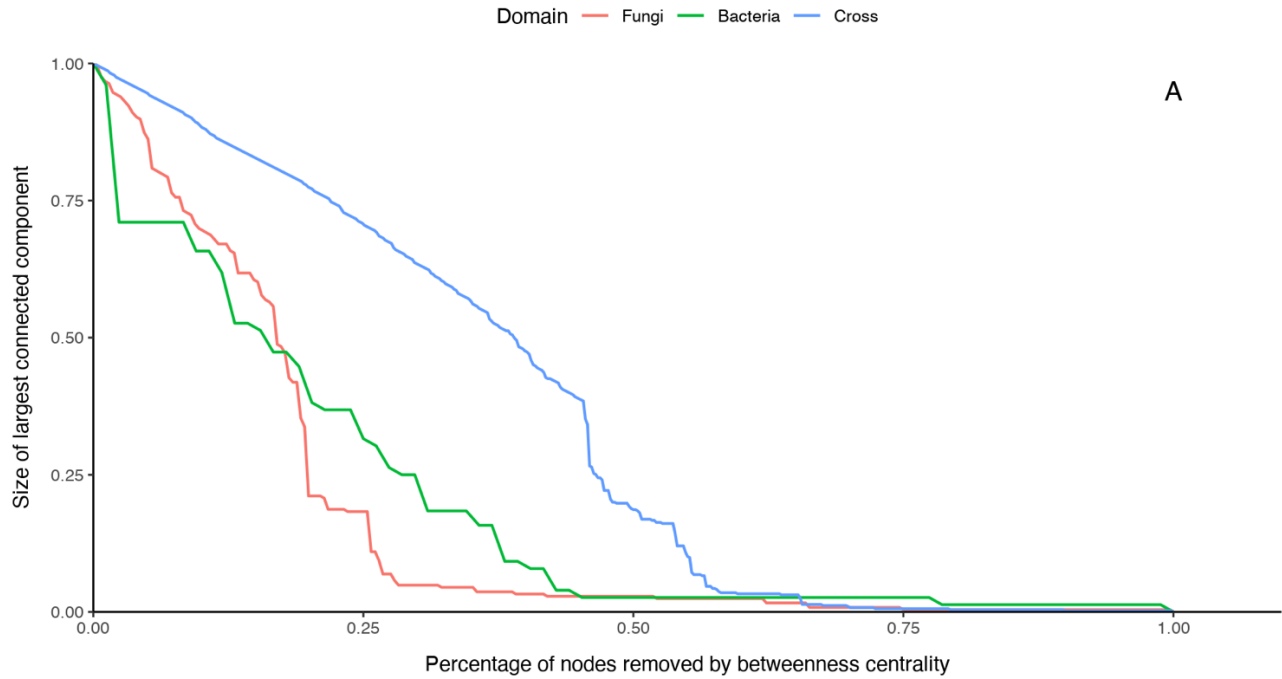


Figure 2.1. Robustness curves for all networks by A) betweenness centrality and B) node degree. Each network is expressed as a line on the graph. A more robust network is characterized by having a larger area under the curve.

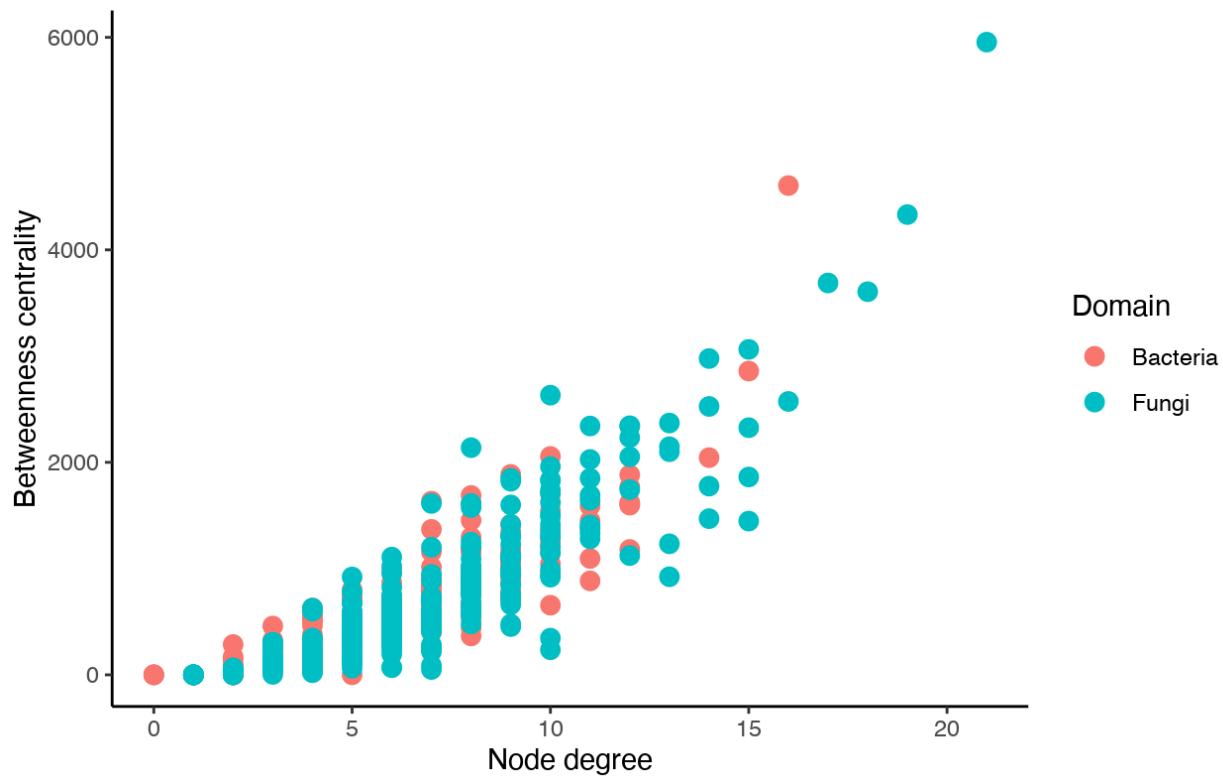


Figure 2.2. Keystone species analysis. Potential fungal and bacterial keystone ASVs were identified by comparing betweenness centrality and node degree. Nodes with high betweenness centrality represent taxa important to the connectivity of the network. Nodes with high degree represent taxa that are hubs in the network. Taxa are identified at the domain level. The vertical line delimits ASVs that have the highest node degree and betweenness centrality measures.

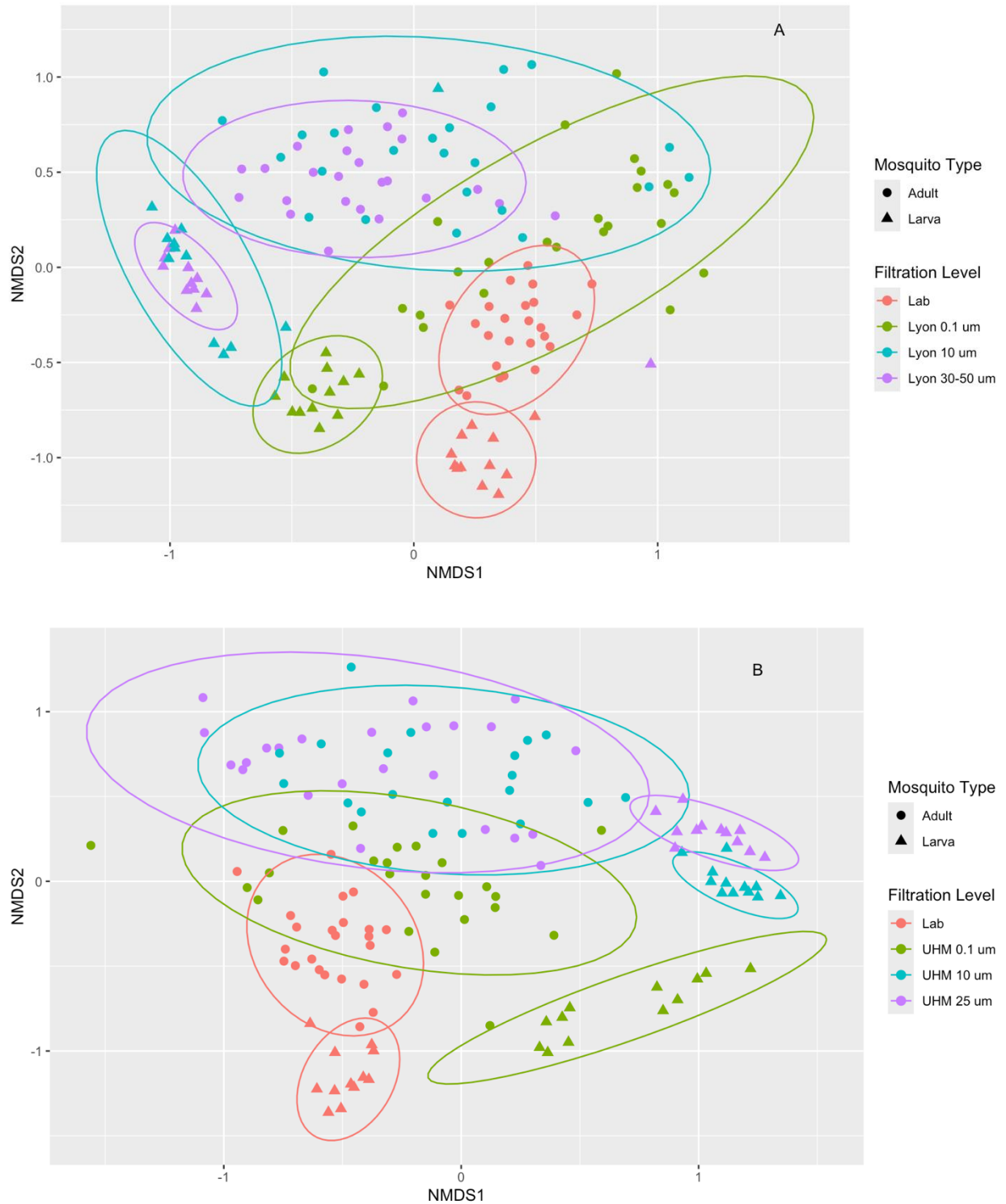


Figure 2.3. Non-metric multidimensional scaling plots demonstrating the composition of the bacteriome that assembled *Aedes albopictus* mosquitoes by filtration level and mosquito type in the A) Lyon Arboretum treatments and B) UH-Mãnoa treatments. Distances are based on the Morisita-Horn index.

APPENDIX A: CHAPTER 1 SUPPLEMENTAL TABLES

Supplementary table 1.1. Table contains the model names, model groupings and model specifications, and the model's name used in R. Model groupings were generated based on conditions of the mesocosm treatments and were arranged on how the mesocosm was manipulated.

Model Name	Model groupings and model structure	Model name in R
Full Group Model	LF; MF; HF; C; WP; WA FGM<-glmmTMB(value~offset(log(sum)) + Sex+FGM + (1 variable)+(1 variable:Sex)+(1 variable:FGM), ziformula=~0, family=nbinom2)	FGM
Environmental Microbes Models	LFMFWPWA; HF; C EMM1<-glmmTMB(value~offset(log(sum)) + Sex + EMM1 + (1 variable) + (1 variable:Sex)+(1 variable:EMM1), ziformula=~0, family=nbinom2)	EMM1
	LFMFWP; WA; HF; C EMM2<-glmmTMB(value~offset(log(sum)) + Sex + EMM2 + (1 variable) + (1 variable:Sex)+(1 variable:EMM2), ziformula=~0, family=nbinom2)	EMM2
Environmental Exposure Models	LFMFHFWAWP; C EEM1<-glmmTMB(value~offset(log(sum)) + Sex + EEM1 + (1 variable) + (1 variable:Sex)+(1 variable:EEM1), ziformula=~0, family=nbinom2)	EEM1
	LFMFHF; WPWA; C EEM2<-glmmTMB(value~offset(log(sum)) + Sex + EEM2 + (1 variable) + (1 variable:Sex)+(1 variable:EEM2), ziformula=~0, family=nbinom2)	EEM2

	LFMFHF, WP; WA; C EEM3<-glmmTMB(value~offset(log(sum)) + Sex + EEM3 + (1 variable) + (1 variable:Sex)+(1 variable:EEM3), ziformula=~0, family=nbinom2)	EEM3
Microbe Filter Models	LFMF; HFC; WPWA MFM1<-glmmTMB(value~offset(log(sum)) + Sex + MFM1 + (1 variable) + (1 variable:Sex)+(1 variable:MFM1), ziformula=~0, family=nbinom2)	MFM1
	LF; MF; HFC; WPWA MFM2<-glmmTMB(value~offset(log(sum)) + Sex + MFM2 + (1 variable) + (1 variable:Sex)+(1 variable:MFM2), ziformula=~0, family=nbinom2)	MFM2
	LFMF; HFC; WP; WA MFM3<-glmmTMB(value~offset(log(sum)) + Sex + MFM3 + (1 variable) + (1 variable:Sex)+(1 variable:MFM3), ziformula=~0, family=nbinom2)	MFM3
	LF; MF; HFC; WP; WA MFM4<-glmmTMB(value~offset(log(sum)) + Sex + MFM4 + (1 variable) + (1 variable:Sex)+(1 variable:MFM4), ziformula=~0, family=nbinom2)	MFM4
Lab Filter Models	LFMFHFC; WPWA LFM1<-glmmTMB(value~offset(log(sum)) + Sex + LFM1 + (1 variable) + (1 variable:Sex)+(1 variable:LFM1), ziformula=~0, family=nbinom2)	LFM1
	LFMFHFCWP; WA LFM2<-glmmTMB(value~offset(log(sum)) + Sex + LFM2 + (1 variable) + (1 variable:Sex)+(1 variable:LFM2), ziformula=~0, family=nbinom2)	LFM2
Combined Wild Pupae	LFMFWP; HFC; WA	cWP1

	cWP1<-glmmTMB(value~offset(log(sum)) + Sex + cWP1 + (1 variable) + (1 variable:Sex)+(1 variable:cWP1), ziformula=~0, family=nbinom2)	
	LFMF; HFCWP; WA cWP2<-glmmTMB(value~offset(log(sum)) + Sex + cWP2 + (1 variable) + (1 variable:Sex)+(1 variable:cWP2), ziformula=~0, family=nbinom2)	cWP2
Combined Wild Adult	LFMFWA; HFC; WP cWA1<-glmmTMB(value~offset(log(sum)) + Sex + cWA1 + (1 variable) + (1 variable:Sex)+(1 variable:cWA1), ziformula=~0, family=nbinom2)	cWA1
	LFMF; HFCWA; WP cWA2<-glmmTMB(value~offset(log(sum)) + Sex + cWA2 + (1 variable) + (1 variable:Sex)+(1 variable:cWA2), ziformula=~0, family=nbinom2)	cWA2
Null Models	null<-glmmTMB(value~offset(log(sum)) + Sex + (1 variable) + (1 variable:Sex), ziformula=~0, family=nbinom2)	Null1
	null2<-glmmTMB(value~offset(log(sum)) + Sex + FGM + (1 variable) + (1 variable:Sex), ziformula=~0, family=nbinom2)	Null2

Supplementary table 1.2. AICc table showing model comparisons and fits.

Model Structure	$\Delta AICc$	df	Weight
MFM3	0	9	1
EEM3	31.2	9	<0.001
MFM4	132.2	10	<0.001
FGM	140.8	11	<0.001
MFM1	817.1	8	<0.001
Null2	917.7	10	<0.001
MFM2	927.7	9	<0.001
LFM1	994.1	7	<0.001
cWP2	1724.8	8	<0.001
cWA1	1780.3	8	<0.001
EMM2	3055.1	8	<0.001
cWP1	3055.1	8	<0.001
EMM1	3226.2	7	<0.001
LFM2	3602.5	7	<0.001
EEM1	3632.8	7	<0.001
NULL	3696.3	5	<0.001

APPENDIX B: CHAPTER SUPPLEMENTAL TABLES

Supplemental table 2.1. Generalized linear mixed model candidate set and their model definitions* for the Lyon Arboretum treatments.

Three way random interaction-Response to treatments depends on type (male, female, larvae)	
lyonm1	glmmTMB(value~offset(log(sum)) + Type + Treatment + Type:Treatment + (1 ASV) + (1 ASV:Type) + (1 Mesocosm) + (1 ASV:Mesocosm) + (1 ASV:Treatment) + (1 ASV:Treatment:Type), dispformula=Type+Treatment+ASV, family=nbinom2)
lyonm2	glmmTMB(value~offset(log(sum)) + Type + Treatment2 + Type:Treatment2 + (1 ASV) + (1 ASV:Type) + (1 Mesocosm) + (1 ASV:Mesocosm) + (1 ASV:Treatment2) + (1 ASV:Treatment2:Type), dispformula=Type+Treatment2+ASV, family=nbinom2)
lyonm3	glmmTMB(value~offset(log(sum)) + Type + BacSource + Type:BacSource + (1 ASV) + (1 ASV:Type) + (1 Mesocosm) + (1 ASV:Mesocosm) + (1 ASV:BacSource) + (1 ASV:BacSource:Type), dispformula=Type+BacSource+ASV, family=nbinom2)
lyonm4	glmmTMB(value~offset(log(sum)) + Type + BacSource2 + Type:BacSource2 + (1 ASV) + (1 ASV:Type) + (1 Mesocosm) + (1 ASV:Mesocosm) + (1 ASV:BacSource2) + (1 ASV:BacSource2:Type), dispformula=Type+BacSource2+ASV, family=nbinom2)
lyonm5	glmmTMB(value~offset(log(sum)) + Type + BacSource3 + Type:BacSource3 + (1 ASV) + (1 ASV:Type) + (1 Mesocosm) + (1 ASV:Mesocosm) + (1 ASV:BacSource3) + (1 ASV:BacSource3:Type), dispformula=Type+BacSource3+ASV, family=nbinom2)
lyonm6	glmmTMB(value~offset(log(sum)) + Type + Substrate + Type:Substrate + (1 ASV) + (1 ASV:Type) + (1 Mesocosm) + (1 ASV:Mesocosm) + (1 ASV:Substrate) + (1 ASV:Substrate:Type), dispformula=Type+Substrate+ASV, family=nbinom2)
Two way random interaction-Response to treatments depends on type (male, female, larvae)	
lyonm7	glmmTMB(value~offset(log(sum)) + Type + Treatment + Type:Treatment + (1 ASV) + (1 ASV:Type) + (1 Mesocosm) + (1 ASV:Mesocosm) + (1 ASV:Treatment), dispformula=Type+Treatment+ASV, family=nbinom2)

lyonm8	glmmTMB(value~offset(log(sum)) + Type + Treatment2 + Type:Treatment2 + (1 ASV) + (1 ASV:Type) + (1 Mesocosm) + (1 ASV:Mesocosm) + (1 ASV:Treatment2), dispformula=Type+Treatment2+ASV, family=nbinom2)
lyonm9	glmmTMB(value~offset(log(sum)) + Type + BacSource + Type:BacSource + (1 ASV) + (1 ASV:Type) + (1 Mesocosm) + (1 ASV:Mesocosm) + (1 ASV:BacSource), dispformula=Type+BacSource+ASV, family=nbinom2)
lyonm10	glmmTMB(value~offset(log(sum)) + Type + BacSource2 + Type:BacSource2 + (1 ASV) + (1 ASV:Type) + (1 Mesocosm) + (1 ASV:Mesocosm) + (1 ASV:BacSource2), dispformula=Type+BacSource2+ASV, family=nbinom2)
lyonm11	glmmTMB(value~offset(log(sum)) + Type + BacSource3 + Type:BacSource3 + (1 ASV) + (1 ASV:Type) + (1 Mesocosm) + (1 ASV:Mesocosm) + (1 ASV:BacSource3), dispformula=Type+BacSource3+ASV, family=nbinom2)
lyonm12	glmmTMB(value~offset(log(sum)) + Type + Substrate + Type:Substrate + (1 ASV) + (1 ASV:Type) + (1 Mesocosm) + (1 ASV:Mesocosm) + (1 ASV:Substrate), dispformula=Type+Substrate+ASV, family=nbinom2)
Treatment does not influence microbiome assembly	
lyonm13	glmmTMB(value~offset(log(sum)) + Type + (1 ASV) + (1 ASV:Type) + (1 Mesocosm) + (1 ASV:Mesocosm), dispformula=Type+ASV, family=nbinom2)
Type and treatment does not influence microbiome assembly	
lyonm14	glmmTMB(value~offset(log(sum)) + 1 + (1 ASV) + (1 Mesocosm) + (1 ASV:Mesocosm), dispformula=ASV, family=nbinom2)

*Note model definitions are described in supplemental table 2.5.

Supplemental table 2.2. Δ AICc table showing weights of the Lyon Arboretum candidate models.

Model	dAIC	Df	Weight
Lyon model 2	0	174	1
Lyon model 5	85.48	171	<0.001
Lyon model 1	312.73	180	<0.001
Lyon model 6	824.85	168	<0.001
Lyon model 8	1092.07	170	<0.001
Lyon model 11	1129.20	168	<0.001
Lyon model 3	1179.64	171	<0.001
Lyon model 4	1208.67	168	<0.001
Lyon model 7	1381.19	174	<0.001
Lyon model 10	1659.64	166	0
Lyon model 9	1693.16	168	0
Lyon model 12	1735.22	166	0
Lyon model 13	2263.74	163	0
Lyon model 14	5846.47	160	0

	dAICc	df	Weight
lyonm2	0	174	1
lyonm5	85.48	171	<0.001
lyonm1	312.73	180	<0.001
lyonm6	824.85	168	<0.001
lyonm8	1092.07	170	<0.001
lyonm11	1129.20	168	<0.001
lyonm3	1179.64	171	<0.001
lyonm4	1208.67	168	<0.001
lyonm7	1381.19	174	<0.001
lyonm10	1659.64	166	0
lyonm9	1693.16	168	0
lyonm12	1735.22	166	0
lyonm13	2263.74	163	0
lyonm14	5846.47	160	0

	dAICc	df	Weight
lyonm2	0	174	1
lyonm5	85.48	171	<0.001
lyonm1	312.73	180	<0.001
lyonm6	824.85	168	<0.001
lyonm8	1092.07	170	<0.001
lyonm11	1129.20	168	<0.001
lyonm3	1179.64	171	<0.001
lyonm4	1208.67	168	<0.001
lyonm7	1381.19	174	<0.001
lyonm10	1659.64	166	0
lyonm9	1693.16	168	0
lyonm12	1735.22	166	0
lyonm13	2263.74	163	0
lyonm14	5846.47	160	0

Supplemental table 2.3. Generalized linear mixed model candidate set and their model definitions for the UH-Mānoa treatments.

Three way random interaction-Response to treatments depends on type (male, female, larvae)	
uhm1	glmmTMB(value~offset(log(sum)) + Type + Treatment + Type:Treatment + (1 ASV) + (1 ASV:Type) + (1 Mesocosm) + (1 ASV:Mesocosm) + (1 ASV:Treatment) + (1 ASV:Treatment:Type), dispformula=Type+Treatment+ASV, family=nbinom2)
uhm2	glmmTMB(value~offset(log(sum)) + Type + Treatment2 + Type:Treatment2 + (1 ASV) + (1 ASV:Type) + (1 Mesocosm) + (1 ASV:Mesocosm) + (1 ASV:Treatment2) + (1 ASV:Treatment2:Type), dispformula=Type+Treatment2+ASV, family=nbinom2)
uhm3	glmmTMB(value~offset(log(sum)) + Type + BacSource + Type:BacSource + (1 ASV) + (1 ASV:Type) + (1 Mesocosm) + (1 ASV:Mesocosm) + (1 ASV:BacSource) + (1 ASV:BacSource:Type), dispformula=Type+BacSource+ASV, family=nbinom2)
uhm4	glmmTMB(value~offset(log(sum)) + Type + BacSource2 + Type:BacSource2 + (1 ASV) + (1 ASV:Type) + (1 Mesocosm) + (1 ASV:Mesocosm) + (1 ASV:BacSource2) + (1 ASV:BacSource2:Type), dispformula=Type+BacSource2+ASV, family=nbinom2)
uhm5	glmmTMB(value~offset(log(sum)) + Type + BacSource3 + Type:BacSource3 + (1 ASV) + (1 ASV:Type) + (1 Mesocosm) + (1 ASV:Mesocosm) + (1 ASV:BacSource3) + (1 ASV:BacSource3:Type), dispformula=Type+BacSource3+ASV, family=nbinom2)
uhm6	glmmTMB(value~offset(log(sum)) + Type + Substrate + Type:Substrate + (1 ASV) + (1 ASV:Type) + (1 Mesocosm) + (1 ASV:Mesocosm) + (1 ASV:Substrate) + (1 ASV:Substrate:Type), dispformula=Type+Substrate+ASV, family=nbinom2)
Two way random interaction-Response to treatments depends on type (male, female, larvae)	
uhm7	glmmTMB(value~offset(log(sum)) + Type + Treatment + Type:Treatment + (1 ASV) + (1 ASV:Type) + (1 Mesocosm) + (1 ASV:Mesocosm) + (1 ASV:Treatment), dispformula=Type+Treatment+ASV, family=nbinom2)
uhm8	glmmTMB(value~offset(log(sum)) + Type + Treatment2 + Type:Treatment2 + (1 ASV) + (1 ASV:Type) + (1 Mesocosm) + (1 ASV:Mesocosm) + (1 ASV:Treatment2), dispformula=Type+Treatment2+ASV, family=nbinom2)

uhm9	glmmTMB(value~offset(log(sum)) + Type + BacSource + Type:BacSource + (1 ASV) + (1 ASV:Type) + (1 Mesocosm) + (1 ASV:Mesocosm) + (1 ASV:BacSource), dispformula=Type+BacSource+ASV, family=nbinom2)
uhm10	glmmTMB(value~offset(log(sum)) + Type + BacSource2 + Type:BacSource2 + (1 ASV) + (1 ASV:Type) + (1 Mesocosm) + (1 ASV:Mesocosm) + (1 ASV:BacSource2), dispformula=Type+BacSource2+ASV, family=nbinom2)
uhm11	glmmTMB(value~offset(log(sum)) + Type + BacSource3 + Type:BacSource3 + (1 ASV) + (1 ASV:Type) + (1 Mesocosm) + (1 ASV:Mesocosm) + (1 ASV:BacSource3), dispformula=Type+BacSource3+ASV, family=nbinom2)
uhm12	glmmTMB(value~offset(log(sum)) + Type + Substrate + Type:Substrate + (1 ASV) + (1 ASV:Type) + (1 Mesocosm) + (1 ASV:Mesocosm) + (1 ASV:Substrate), dispformula=Type+Substrate+ASV, family=nbinom2)
Treatment does not influence microbiome assembly	
uhm13	glmmTMB(value~offset(log(sum)) + Type + (1 ASV) + (1 ASV:Type) + (1 Mesocosm) + (1 ASV:Mesocosm), dispformula=Type+ASV, family=nbinom2)
Type and treatment does not influence microbiome assembly	
uhm14	glmmTMB(value~offset(log(sum)) + 1 + (1 ASV) + (1 Mesocosm) + (1 ASV:Mesocosm), dispformula=ASV, family=nbinom2)

Supplemental table2.4. Δ AICc table showing weights of the UH-Mānoa candidate models.

Model	dAIC	Df	Weight
-------	------	----	--------

UH model 2	0	147	1
UH model 5	55.31	144	<0.001
UH model 1	317.76	153	<0.001
UH model 4	733.95	141	<0.001
UH model 3	741.39	144	<0.001
UH model 6	1117.25	141	<0.001
UH model 8	11732.66	143	<0.001
UH model 11	1208.31	141	<0.001
UH model 7	1444.60	147	<0.001
UH model 9	1562.99	141	0
UH model 10	1564.51	139	0
UH model 12	1710.38	139	0
UH model 13	2150.92	136	0
UH model 14	4667.23	133	0

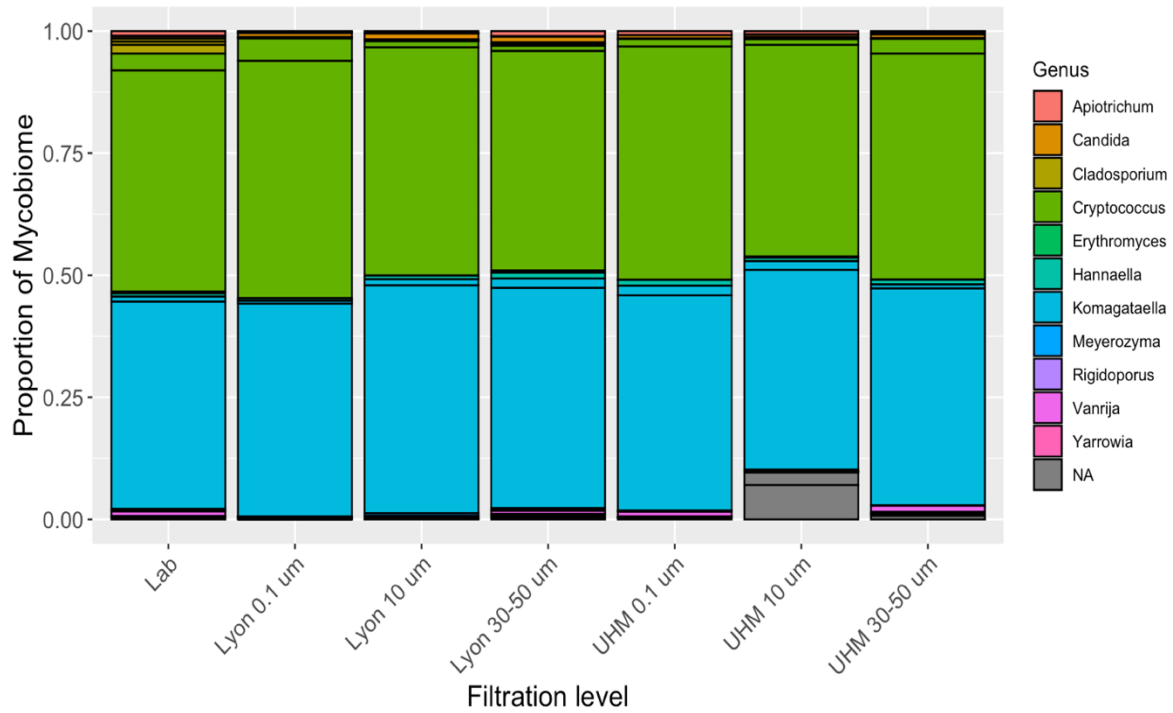
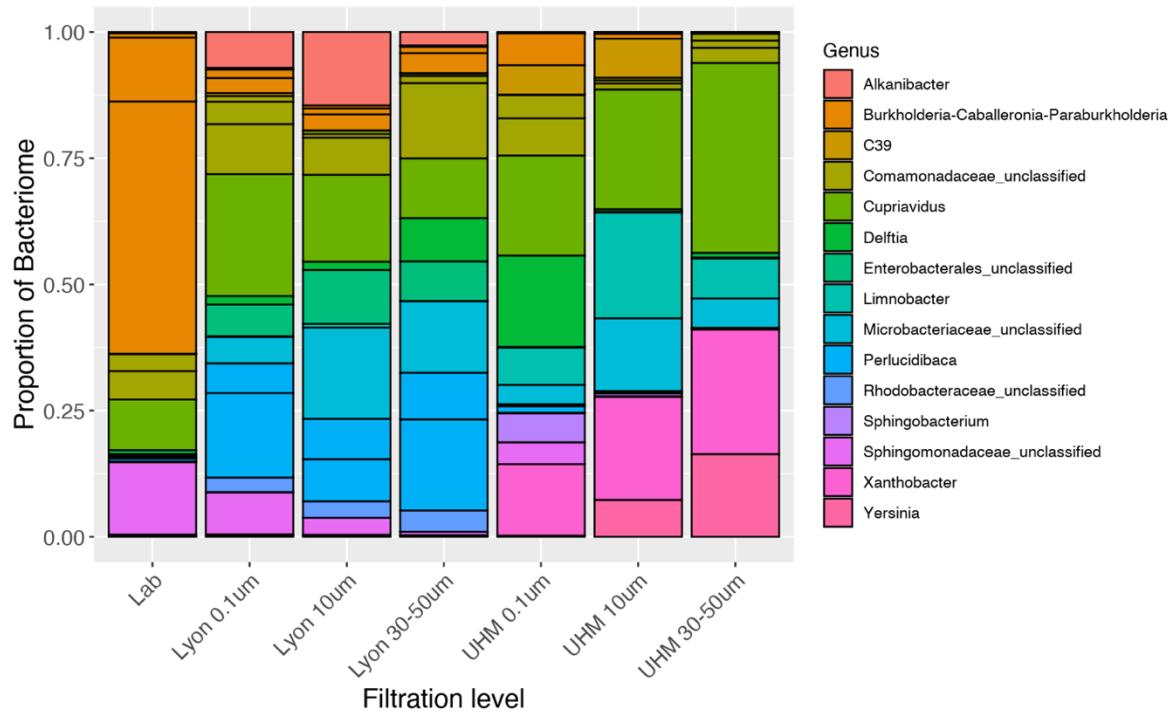
	dAICc	df	Weight
uhm2	0	147	1
uhm5	55.3089891	144	<0.001
uhm1	317.76472	153	<0.001
uhm4	733.953955	141	<0.001
uhm3	741.390406	144	<0.001
uhm6	1117.25066	141	<0.001
uhm8	1132.65561	143	<0.001
uhm11	1208.31758	141	<0.001
uhm7	1444.60484	147	<0.001
uhm9	1562.98953	141	0
uhm10	1564.5142	139	0
uhm12	1710.37942	139	0
uhm13	2150.91578	136	0
uhm14	4667.22751	133	0

	dAICc	df	Weight
uhm2	0	147	1
uhm5	55.3089891	144	<0.001
uhm1	317.76472	153	<0.001
uhm4	733.953955	141	<0.001
uhm3	741.390406	144	<0.001
uhm6	1117.25066	141	<0.001
uhm8	1132.65561	143	<0.001
uhm11	1208.31758	141	<0.001
uhm7	1444.60484	147	<0.001
uhm9	1562.98953	141	0
uhm10	1564.5142	139	0
uhm12	1710.37942	139	0
uhm13	2150.91578	136	0
uhm14	4667.22751	133	0

Supplemental table 2.5. Definitions of model parameter groupings.

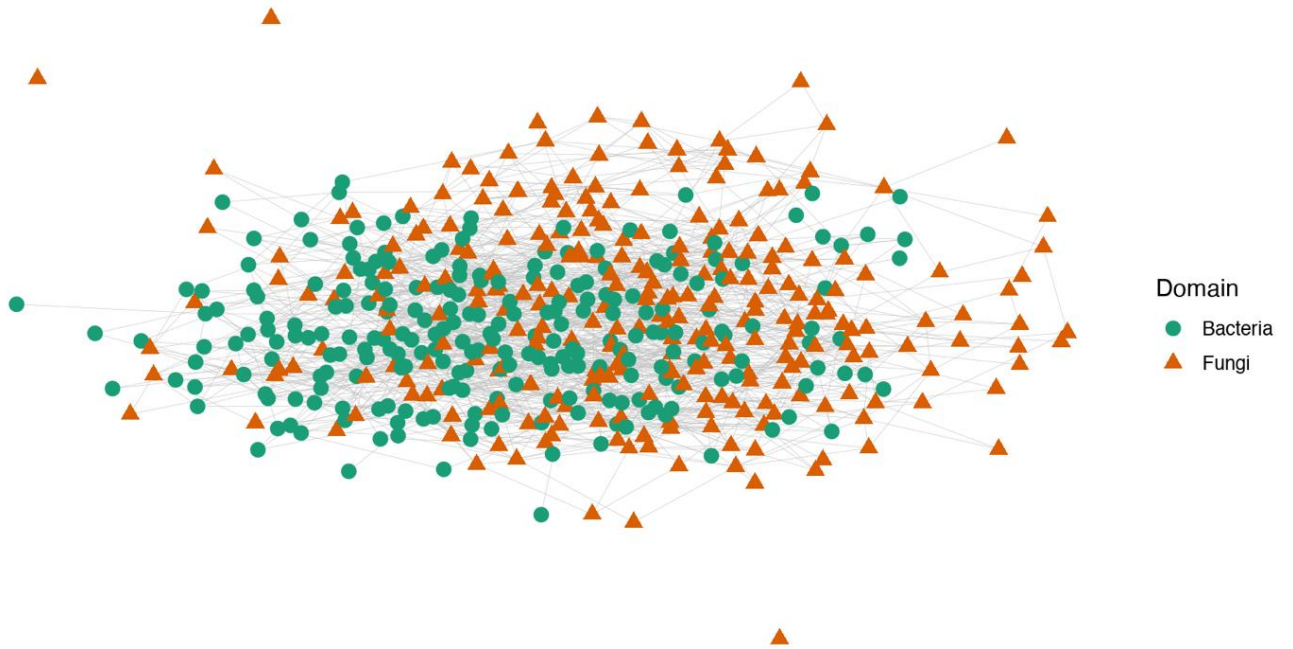
Model parameter	Description
Treatment	laboratory mesocosms were treated as individual replicates, replicates of the filtration mesocosms were grouped into a single group. Groupings included: Lab 1, Lab 2, Lab3, 0.1 µm filtration, 10 µm filtration, and 30-50 µm.
Treatment2	laboratory mesocosms replicates were treated as a single group, filtration mesocosms replicates were treated as a single group by filtration size. Groupings included: Lab, 0.1 µm filtration, 10 µm filtration, and 30-50 µm.
BacSource	laboratory and 0.1 um filtration mesocosms were grouped together, 30-50 um filtration mesocosms were treated as a single group, and 10 um filtration treatments were treated as a single group. This model accounted for egg-associated bacteria effects.
BacSource2	laboratory and 0.1 um filtration mesocosms were grouped together, 30-50 um and 10 um filtration mesocosms were grouped together. This model accounted for egg-associated bacteria effects.
BacSource3	laboratory mesocosms were grouped together, 0.1 um filtration mesocosms were an individual group, 10 um and 30-50 um filtration mesocosms were grouped together. This model assumes that egg-associated bacteria are not impacting the mesocosms.
Substrate	water is sourced from the laboratory or from the wild (bromeliads)

APPENDIX C: CHAPTER 2 SUPPLEMENTAL FIGURES



Supplemental figure 2.1. Relative abundance plot of the mosquito bacteriome (A) and mycobiome (B) by location and filtration level.

Full Cross-Domain Network



Supplemental figure 2.2. Full network generated using the Sparse Inverse Covariance estimation for Ecological Association and Statistical Inference (SPIEC-EASI) method. Bacterial ASVs are represented by green circles and fungal ASVs are represented by orange triangles. All ASVs are represented at the Domain level. Gray lines are edges which represent associations between ASVs.

CHAPTER 3: LARVAL INTERACTIONS WITH THE ENVIRONMENTAL MICROBIOME

IMPACT *Aedes albopictus* BIOLOGY ACROSS ITS LIFE CYCLE

Introduction

Globalization has interconnected the world, bringing with it the rapid movement of goods and people across the planet. That movement has also translocated many animal and plant species beyond their natural home ranges at unprecedented rates (Hulme, 2009). The introduction of invasive alien species (IAS) into non-native ranges can have profound negative consequences on native populations, native communities, food webs, and local ecosystem services (Charles & Dukes, 2007; Riley et al, 2008; Gallardo et al., 2016; Duenas et al., 2018; Duenas et al., 2021). IAS can harm native species by outcompeting natives for resources (Falaschi et al., 2020; Richter-Boix et al., 2013), through habitat alteration (Watling et al., 2011; Ransom, 2017), and by altering food web dynamics (David et al., 2017; Zhang et al., 2019)—ultimately threatening biodiversity in areas experiencing invasion.

Beyond threats to biodiversity, IAS also pose significant risks to human and wildlife health. From 1940 to 2004, the emergence of 335 infectious diseases were reported in the global human population (Jones et al., 2008). The majority of emerging infectious diseases (EIDs) have zoonotic origins, with a considerable proportion of EIDs are spread by arthropod vectors (Wolfe et al., 2007; Jones et al., 2008). Vector-borne diseases comprise 17% of annual global infections, resulting in hundreds of thousands of deaths (World Health Organization, 2020). The major vector-borne EIDs include chikungunya, dengue fever, Japanese encephalitis, West Nile fever,

and Zika (Huntington et al., 2016; Chala and Hamde, 2021)—all of which are vectored by mosquitoes.

One mosquito in particular, *Aedes albopictus*, is capable of vectoring all of the above diseases other than Japanese encephalitis (Gratz, 2004). *Aedes albopictus* is also considered one of the most invasive species on the planet (Global Invasive Species Database, 2011). It has been found on all continents except Antarctica (Benedict et al., 2007) and is expected to continue expanding its range across areas it has invaded (Kraemer et al., 2019), especially in future climate change scenarios (Cunze et al., 2016; Laporta et al., 2023; Liu et al., 2019). This presents opportunities for the spread of vector-borne EIDs into new areas which could challenge public health systems that are not prepared for these diseases. Furthermore, the emergence of arboviruses is linked to frequent switching of vertebrate hosts by vectors (Chevillon et al., 2008), which is likely to occur because *A. albopictus* shows plasticity in its feeding behavior (Delatte et al., 2010); thus, there is potential for novel vector-borne diseases to emerge because of *A. albopictus* invasions—especially if they act as a new link between two previously unlinked hosts.

Because of the combination of high invasiveness and capacity to vector pathogens, a deeper understanding of *A. albopictus* biology during invasion events is warranted. Understanding how the invasive mosquito responds to new environments could provide useful insight for vector control strategies and may also provide broader information about invasion biology in general. In recent years, substantial attention has been given to interactions between *A. albopictus* and its symbiotic microbiota. Those symbiotic microbiota, collectively known as the microbiome, have profound impacts on mosquito biology—affecting development time (Coon et al., 2014),

fecundity (Harrison et al., 2023), immunity (Gabrieli et al., 2021), and metabolism (Guégan et al., 2022). *Aedes albopictus*, like all mosquitoes, has a complex life cycle whereby larvae and adults occupy two distinct niches, aquatic and terrestrial respectively. As larvae, mosquitoes consume microbes as an essential part of their diet and the larval habitat is a major determinant of the microorganisms that a mosquito will encounter during development (Zouache et al., 2022). During periods of invasion, *A. albopictus* are likely to develop in habitats with substantial variation in microbial community composition and this could have significant implications not only for successful invasion, but also the capacity of those populations to sustain pathogen transmission (Cansado-Utrilla et al., 2021).

To investigate how *A. albopictus* populations respond to environments with compositionally distinct microbial communities, we reared mosquito larvae in water sourced from three distinctly different environmental locations: laboratory, bromeliad tanks, and artificial containers. The bromeliad tank sites and the artificial container sites were separated by 6.5 km, but were still in Mānoa Valley. Furthermore, the collected water was filtered using pore sizes selected for altering the microbial community based on cell size. We measured a suite of traits spanning the life cycle of *A. albopictus* that are impacted by the microbiome. In larvae, we assessed time to pupation, pupation success, and lipid concentrations. In adults, we assessed longevity under starvation conditions and immune responses to infection.

Materials and Methods

Mosquito habitat design and construction

UH-Mānoa plastic buckets

Two large plastic buckets were filled with 3 liters of sterile water, to which were added 1 tablespoon of field soil, and 1 teaspoon of crushed leaf detritus collected from the University of Hawai‘i at Mānoa campus (UH-Mānoa), one wooden shim (as an oviposition raft). The buckets were placed outside and at ground level on the UH-Mānoa campus and were left exposed to ambient conditions for 14 days. The buckets were checked every two days to ensure water levels never fell below two liters. The water level was restored to 3 liters with sterile water when necessary. After 14 days, the water from the buckets was collected and returned to the laboratory for processing. *Aedes albopictus* larvae were present in the container when the water was collected.

Lyon Arboretum bromeliads

Two liters of water were collected from the tanks of the bromeliad genus *Neoregelia*, at Lyon Arboretum in Mānoa Valley, Honolulu, Hawai‘i. The bromeliad water was collected on the day of processing and no *A. albopictus* larvae were found in the water at the time of collection, although the habitat was colonized by *Wyeomyia mitchellii* (Culicidae) and *Toxorhynchites amboinensis* (Culicidae).

Laboratory water

A third environment, which consisted of pure water from a Millipore Milli-Q water filtration system, was included to represent the larval habitat conditions mosquitoes experience in a typical laboratory setting.

Filtration regimen

For the UH-Mānoa plastic buckets and Lyon Arboretum bromeliads water sources, three separate inoculums were prepared using a differential filtration regimen that included a 30-50 μm coffee filter, a sterile syringe with a 10 μm filter, and a 0.1 μm vacuum-filter cup. An approximate total of 300 ml was obtained from each filtration level for both water sources.

Mesocosm construction

Mesocosms were created for the plastic buckets and bromeliad-water substrates by pipetting 100 ml of inoculum from either the 30-50 μm regimen, the 10 μm regimen, or the 0.1 μm regimen into individual 150 x 15 mm Petri dishes. The laboratory mesocosms contained 100 ml of pure water placed into individual 150 x 15 mm Petri dishes. Each mesocosm contained three replicates. One hundred *A. albopictus* eggs were placed into each mesocosm. The eggs were obtained from our laboratory colony that originated from wild *A. albopictus* isolated from Mānoa, Oahu, Hawai'i and was raised in the lab for 21 generations prior to the start of the experiment.

Mosquito rearing and handling

I reared *A. albopictus* with a 12 L:12 D photoperiod. Temperature in the light period was 28°C and in the dark period was 22°C, which reflect average conditions found at sea level during the summer months on O'ahu, Hawai'i. Humidity was kept constant at 60%. A custom food preparation was made that consisted of a 1:1 ratio of liver powder to dried yeast extract mixed with pure water to a concentration of 18 mg per ml. The food preparation was autoclaved for 30 minutes prior to introduction into the mesocosm to kill viable microorganisms. Larval food water was administered daily at a concentration of 0.2 mg per larva per mesocosm. On day 8 and day

10 of the experiment, late-instar (L3-L4) larvae (n=69) were removed from each mesocosm, placed in a 1.5 ml centrifuge tube with 0.5 ml of water and stored at -20°C until processed for lipid analysis. Upon pupation, pupae were removed from the mesocosm and placed individually into a 50 ml centrifuge tube and allowed to eclose into adults. The adults were randomly assigned into an immune challenge assay group (n=232) or a starvation assay group (n=472).

Developmental assays

Development was measured using two parameters: the number of successful pupations, and the time to reach pupation (measured in days). Mesocosms were monitored multiple times per day for 32 consecutive days.

Lipid extraction, esterification, and gas chromatography-mass spectrometry (GC-MS)

Lipid extraction

Larvae were thawed at room temperature then transferred to a new 1.5 ml centrifuge tube. Four small ceramic beads and 100 µl of water were added to each centrifuge tube. Larvae were homogenized for 30 seconds followed by two minutes of centrifugation. After centrifugation, 600 µl of a solution containing CHCl₃ and MeOH (2:1 ratio) spiked with pentadecanoic acid (10 µg/ml) was added to each tube. All tubes were continuously vortexed at 4°C for three hours. After three hours, 450 µl of diluted MeOH was added to each tube, tubes were briefly vortexed, and then centrifuged at 7,500 relative centrifugal force at 4°C for two minutes. The lower phase was collected and transferred to a 2 ml glass vial. After removal of the lower phase, the crude extract was transferred to a new 2 ml centrifuge tube and 400 µl of CHCl₃ was added, centrifuged, the lower phase was collected and added to the 2 ml glass vial; this step was

performed twice. The contents of the glass vial were concentrated by evaporating with N₂. The dried concentrate was stored at -20°C.

Esterification

To each lipid extract 200 µl of 0.5N methanolic HCl was added and the vial incubated at 65°C for 90 minutes and vortexed every 30 minutes. The solvent was evaporated with N₂ and stored at -20°C until further processing for gas chromatography-mass spectrometry (GC-MS) analysis.

Samples were thawed, reconstituted in 100 µL of hexane prior to GC-MS analysis.

Gas chromatography-mass spectrometry

GCMS analysis was performed on a 7820A GC system equipped with a 5975 Mass Selective Detector (Agilent Technologies, Inc.) and an HP-5 ms column ((5%-Phenyl)-methylpolysiloxane, 30 m length, 250 µm ID, 0.25 µm film thickness; Agilent Technologies, Inc.). Electron ionization (EI) energy was set at 70 eV. One microliter of the sample was injected in splitless mode and analyzed with helium flow at 1 ml/min. The oven was initially set at 50°C for 2 min, increased to 90°C at a rate of 20°C/min and held at 90°C for 1 min, increased to 280°C at a rate of 5°C/min and held at 280°C for 2 min. MS detection was set from m/z 33 to 500. Lipids were identified by retention times and ionization fragmentation pattern. To calculate total lipid levels, individual peaks areas were normalized to pentadecanoic acid and summed. To account for individual mosquito mass biasing total lipid concentrations, the normalized standard was further divided by the product of pentadecanoic acid and protein concentrations. Protein concentrations were quantified using a Pierce BCA Protein assay kit following the manufacturer's protocol.

Survival under starvation conditions

Adult mosquitoes were housed individually in 50 ml centrifuge tubes at the environmental conditions listed above. All adults were provided with 25 ml of fresh Millipore water in the tube and the tube caps were loosened to allow for oxygen flow. Mosquitoes were monitored every 24 hours until death and the date of death was recorded. No food was given at any point during the assay.

Immune challenge assay

Adults were provided with a sterile 10% sucrose solution upon emergence. The sucrose was refreshed every 24 hours for 72 hours prior to immune challenge. Approximately 72 hours post-emergence, adults were cold anesthetized on ice and *Escherichia coli* was administered via microinjection through a microcapillary glass needle using a Femtojet 4i microinjection system. *Escherichia coli* was grown and maintained in Luria Bertani (LB) broth at 28°C. Prior to injection, the bacterial culture was diluted with sterile LB broth to a concentration of approximately 5000 cells per milliliter. Adults were injected with 100 nl of the bacterial solution with approximately 500 live *E. coli* received by each mosquito. A sham injection consisting of sterile LB broth was used as an injury control and was also administered at approximately 100 nanoliters per mosquito. Mosquitoes were observed post-injection to ensure recovery; mosquitoes that did not survive the initial challenge were removed from the trial. Mosquitoes were sacrificed 24 hours post-injection, via cold anesthesia, placed in RNAlater RNA Stabilization Solution, and stored at 4°C for future molecular analysis.

Immune gene amplification

Immune gene amplifications were conducted on 232 individual mosquitoes across all replicates. RNA was extracted using the Qiagen RNeasy Mini Kit according to the manufacturer's protocols. The concentration of mRNA was quantified with a MultiSkan SkyHigh Microplate Spectrophotometer and samples were stored at -20°C. RNA samples were normalized to 1 µg prior to cDNA synthesis. cDNA synthesis was performed on the extracted RNA using a Qiagen Quantitect Reverse Transcription Kit with DNA wipeout according to the manufacturer's protocol. Gene amplification was performed by quantitative PCR with the PowerUp SYBR Green Master Mix (Applied Biosystems) and gene-specific primers adapted from Ramirez et al. (2021) which included the transcription factors relish 1 (REL1), relish 2 (REL2), and STAT, and the antimicrobial peptides (AMPs) cecropin-A (CEC-A), defensin-C (DEF-C), and lysozyme-E LYS-E (Supplemental table 3.1). One microliter of cDNA in 10 µl of SYBR Green Master Mix was used for each reaction. We used the RT-qPCR cycling conditions recommended for the master mix which consisted of holding for 10 minutes at 95.0°C, 40 cycles of 15 seconds at 95.0°C and 1 minute at 60°C. A melt curve analysis was included at the end of each qPCR run. Transcript abundance was evaluated using the $\Delta\Delta CT$ method (Livak & Schmittgen, 2001). Briefly, RpS7 was used as our housekeeping gene to establish ΔCT values (Ct of housekeeping gene – Ct of target gene). $\Delta\Delta CT$ values were obtained by using the mean of the sham injections (calculated for each treatment and by sex) as our calibrator. All reactions were performed in duplicates and the analyses were performed using the mean of the technical replicates.

Statistical analyses

Generalized linear mixed models (GLMMs) assuming a negative binomial error distribution were used to test the relationship between the amount of days mosquito larvae took to pupate and the fixed effect of water source and filtration level (hereafter referred to as treatment) and a random intercept of mesocosm identity (individual replicates). GLMMs assuming a negative binomial error distribution were used to test the relationship between the total number of remaining larvae and the fixed effect of treatment and a random intercept of mesocosm identity. GLMMs assuming a gamma error distribution were used to assess the relationship between total lipid concentrations and the fixed effect of treatment and a random intercept of mesocosm identity. All above analyses were performed on mosquito larvae. GLMMs assuming a Gaussian error distribution were used to test the relationship between survival under starvation conditions and the fixed effects of treatment and sex, random intercept of mesocosm identity.

GLMMs assuming a Gaussian error distribution were used to test the individual responses of each selected immune gene. Those models included the fixed effects of *i*) a three-way interaction of sex, treatment, and infection status, and *ii*) a random intercept for mesocosm identity. Each model was compared to a null model that dropped treatment as a predictor and the models were compared using likelihood ratio tests. All GLMMs were implemented in R using the package `glmmTMB` (Brooks et al., 2017). Likelihood ratio tests were performed in R with the `lrtest` function using the package `lmerTest` (Zeileis & Hothorn, 2002).

Results

Development-time to pupation

The model that best fitted the data (AIC weight = 1) assumed a negative binomial error distribution and included *i*) a fixed effect of the treatment (defined by grouping water source and filtration level), *ii*) a random effect of mesocosm, and *iii*) a formula that allowed the model's dispersion parameter to vary among the fixed effect of treatment. This model outperformed the null model that did not include treatment as a parameter ($\Delta\text{AIC} = 38.4$) while keeping all other parameters the same. Treatment had a significant effect on the time to pupation (Figure 3.1). The mesocosms with the shortest development times were the UH-Mānoa 0.1 μm filter treatments. The mean days to pupation in the UH-Mānoa 0.1 μm filter was 15.77 ± 5.88 (SD) days. That was 2.13 days faster than the laboratory mesocosms, which produced larvae the second fastest (17.91 ± 4.49 days). All other mesocosms had a mean development time of greater than 18 days (Table 3.1)

Development-remaining larvae

The model that best fitted the data (AIC weight = 1) assumed a negative binomial error distribution and included *i*) a fixed effect of the treatment (defined as water source and filtration level), and *ii*) a random effect of mesocosm. This model outperformed the null model that did not include treatment as a parameter ($\Delta\text{AIC} = 18.0$) while keeping all other parameters the same. Developmental success was highly influenced by treatment (Figure 3.2). The mesocosms with the fewest remaining larvae were the laboratory habitats and the UH-Mānoa 0.1 μm habitats with 1.33 ± 1.52 pupae remaining and 1.33 ± 0.58 pupae remaining at day 32 respectively. The number of remaining larvae was the highest in the UH-Mānoa 30-50 μm treatments with a mean of 28.33 ± 7.64 pupae remaining at day 32. That was approximately three times higher than its Lyon Arboretum counterpart with 9.33 ± 5.77 remaining pupae. The number of remaining larvae

was also high in the UH-Mānoa 10 μm treatments at 25.67 ± 9.23 pupae remaining compared to Lyon Arboretum 10 μm treatments with 10.00 ± 8.88 pupae remaining at day 32. The means for remaining larvae in all treatments are listed in table 3.1.

Lipid concentration

The model that best fitted the lipid data (AIC weight = 0.97) was the null model that dropped treatment as a parameter but included a random effect of mesocosm. The best-fit model outperformed the full model that kept treatment as a parameter ($\Delta\text{AIC} = 18.0$). According to the best-fitted model, treatment did not significantly affect total lipid concentrations in *A. albopictus* larvae.

Starvation assay

The model that best fitted the data (AIC weight = 0.96) included a fixed effect of the interaction between treatment and mosquito sex and a random effect of mesocosm. The best-fitted model outperformed a model that included treatment and sex as fixed effects without an interaction ($\Delta\text{AIC} = 7.3$) while keeping all other parameters the same. The best-fitted model also outperformed the null model that did not include treatment or sex as parameters ($\Delta\text{AIC} = 18.2$) while keeping all other parameters the same. Females survived the longest at 2.83 ± 0.71 days compared to males (2.56 ± 0.66 days). However, survival times differed across the treatments by sex (Figure 3.3). Female survival was highest in the Lyon Arboretum 0.1 μm (3.08 ± 0.64 days) and 10 μm treatments (3.03 ± 0.88 days). That was in contrast to UH-Mānoa 10 μm mesocosms where survival was the shortest at 2.14 ± 0.38 days. Male survival was highest in the laboratory

mesocosms at 3.06 ± 0.56 days and was lowest in the UH-Mānoa 30-50 μm mesocosms at 2.24 ± 0.50 days. The means for survival across all treatments are listed in table 3.2.

Immune expression

Treatment did not significantly affect the expression of REL1 ($\chi^2 = 30.9$; $p = 0.15$), REL2 ($\chi^2 = 24.1$; $p = 0.46$), or STAT ($\chi^2 = 22.9$; $p = 0.52$). For all three genes, the null model was not significantly different from the full model that included treatment. DEF-C was also not significantly affected by treatment ($\chi^2 = 24.4$; $p = 0.43$). For REL1, REL2, STAT, and DEF-C, differences in immune expression were driven sex. However, treatment did significantly affect the expression of CEC-A ($\chi^2 = 38.4$; $p = 0.03$; figure 3.4) and LYS-E ($\chi^2 = 45.4$; $p = 0.005$; figure 3.5) as indicated by a three-way interaction (sex x treatment x infection status). The means for CEC-A and LYS-E expression across all treatments are listed in table 3.3.

Discussion

Our study aimed to investigate the effects of distinct environmental microbial communities on the development, physiology, and immune responses of *A. albopictus*, a highly invasive mosquito species. Larvae reared in water with varying microbial community compositions exhibited significant differences in developmental time to pupation and pupation success. Specifically, larvae reared in water with a more diverse microbial community (i.e., 30- 50 μm coffee filter regimen) developed slower and had lower pupation success compared to those reared in water with a less diverse microbial community (i.e., 10 and 0.1 μm filter regimens).

The most probable cause for the differences observed between the filtration regimens is competition for food resources between mosquito larvae and the microbial community. Heterotrophic microorganisms need the same resources as mosquitoes to support their own growth and the needs of the community will likely depend on its species composition (Bauer et al., 2017), especially if there are a large number of competitive phenotypes in the community (Ghoul & Mitri, 2016). These dynamics may also be driven by cell size as metabolic needs scale with the size of the cell (Yoshiyama & Klausmeier, 2008; Serbanescu, Ojkic, & Banerjee, 2022) and would explain why the 30-50 μm filter treatment had the slowest developmental times and the least successful amount pupation as those treatments would have contained a microbial community consisting of large eukaryotic microorganisms. However, this effect is also likely to depend on how digestible the food sources in the environment are. In this experiment, we used an easily digestible food source for the mosquitoes and the microbes, and this type of food source is highly representative of a controlled laboratory environment. In nature, *A. albopictus* mosquitoes and microbes will inhabit environments that contain food sources that are not easily digestible, e.g, plant detritus. Thus, a more diverse environmental microbiome may contain members able to convert locked carbon sources, like cellulose, into usable carbohydrates for a mosquito. Follow-up experimentation would help elucidate the consequences of environmental microbiome diversity when food source is the limiting factor.

Mosquito larval development is also dependent on the availability of essential vitamins (Wang et al., 2021) and amino acids (Serrato-Salas & Gendrin (2023), which many bacteria readily synthesize and secrete into their environment. This often occurs in the mosquito after ingested microbes establish residence in the gut. However, in more diverse communities, there may also

be competition for limited space within the mosquito midgut; thus, leading to reduced benefit for the mosquito if non-symbionts comprise a higher proportion of the community and are not providing the necessary vitamins and amino acids usually supplied by symbionts. Furthermore, these essential vitamins are also used by other microorganisms in the community (Tyc et al., 2017), thus a larger and more diverse community might generate scarcity of these essential vitamins outside and inside of the mosquito. We saw the shortest development times and highest pupation success in our 0.1 μm treatments sourced from the UH-Mānoa campus. This treatment would have removed viable cells from the environmental water but allowed metabolites to enter the mesocosm, and the only microbes allowed to enter the experimental mesocosm were symbionts associated with lab-reared *A. albopictus* eggs. With reduced competition in the 0.1 μm treatments, the larvae would have had access to most of the available nutrients within the environment as compared to the mesocosms where a diverse community of microbes could outcompete the larvae for resources. It is also interesting that the mesocosms derived from the water sourced from artificial containers were originally colonized by *A. albopictus* prior to collection and filtration. It is possible that this initial colonization seeded the environment with *A. albopictus* symbionts prior to collection, leaving behind essential vitamins and metabolites in the 0.1 μm treatments specific to *A. albopictus* symbiosis.

Mosquito survival under starvation conditions was dependent on the sex of the mosquito and the treatment from which they emerged. Survival was highest for females in the Lyon Arboretum, i.e., bromeliad 0.1 μm and 10 μm treatments, and in the UH-Mānoa 0.1 μm treatment.

Interestingly, female survival was poor in the 10 μm and 30-50 μm treatments sourced from UH-Mānoa. The overall trend for male survival was that survival decreased with increasing diversity

of environmental microbes. Survival was highest in the laboratory mesocosms and the 0.1 μm filter treatments from both Lyon Arboretum and UH-Mānoa and lowest in the 30-50 μm filter treatments—a trend similar to that observed in females. It is not surprising that survival was poor from these environments considering that developmental success was also poor in the same environments, and the outcomes witnessed here are probably correlated to interactions with the environmental microbiome during development. However, the presence of pathogens may also be a cause for poor survival. I also tested for the presence of *A. taiwanensis*, a parasite commonly found in Hawai'i *A. albopictus* populations and found no evidence of infection with this parasite across all treatments. However, it is possible that some members of the microbial community were pathogenic to the mosquitoes, an alternate but not mutually exclusive hypothesis of energy reserves obtained during the larval phase determining adult survival.

We also tested the immune response of adult mosquitoes as a condition of the microbial composition within their larval habitat. Specifically, we quantified the genes REL1, REL2, and STAT, which are transcription factors in the Toll, Immune Deficiency (IMD), and Janus kinase-signal transducer and activator of transcription (JAK-STAT) pathways respectively. We also tested three antimicrobial peptides: CEC-A, DEF-C, and LYS-E. Combined, these target genes allowed us to broadly investigate the immune response, from the upstream activation of pathways to the downstream production of AMP transcripts. Mosquito immune function, although only consisting of innate immunity, is complex and varies with factors like temperature (Murdock et al., 2012, Murdock, Moller-Jacobs, & Thomas, 2013) and *Wolbachia* infection status (Ramirez et al., 2021). None of the three signaling genes were significantly impacted by the filtration treatment and infection status. It is not surprising that REL1 was not significantly

expressed. REL1 indicates upregulation of the Toll pathway which responds to Gram-positive bacteria (King, 2020). Interestingly, males showed higher REL1 expression levels in both infected and non-infected samples compared to females; however, there was no significant difference in REL1 expression between infected and non-infected males. Those results suggest that male *A. albopictus* have a higher basal expression of REL1 compared to females.

I hypothesized that expression of REL2 of the IMD pathway would be significantly higher than REL1 and STAT because the IMD pathway is induced by Gram-negative bacteria (Sim, Jupatanakul, & Dimopoulos, 2014) like *E. coli*. Although REL2 was not significantly affected by treatment, it was expressed in higher amounts compared to the mosquitoes that received a sham injection, but only in male mosquitoes. Female mosquitoes did not show any significant difference as a result of infection status. STAT expression did not vary across treatments, by sex, or infection status. The JAK-STAT pathway is the lesser described of the three major pathways in mosquito immunity, but it has primarily been implicated in anti-viral responses (Dong et al., 2012) although there is some evidence that the pathway responds to Gram-positive and Gram-negative bacteria (Gupta et al., 2009). If this pathway responded strongly to Gram-negative bacteria, I should have seen relative expression similar to REL2; however, I did not observe that in this study.

Expression of the AMPs CEC-A and LYS-E was dependent on mosquito sex and the treatment from which they emerged. For example, CEC-A expression in males was relatively uniform across all mesocosms, whereas CEC-A expression for females was highly expressed in the laboratory mesocosms, moderately expressed in the Lyon Arboretum mesocosms, and largely

unexpressed in the UH-Mānoa mesocosms. With LYS-E, expression primarily occurred in the laboratory environment and was expressed similarly in both sexes. In all of the other treatments, LYS-E was either not expressed or expressed at the same level as non-infected mosquitoes. Because AMP expression was not the same across the treatments, it suggests that compositional variation in the microbial community may have primed the AMP responses which led to the patterns observed in this study. Indeed, immune priming to bacterial exposure has been demonstrated previously in other mosquito taxa, like *Aedes aegypti* (Moreno-Garcia et al., 2015; Carlson et al., 2020). Unlike those studies, I exposed mosquitoes to diverse microbial communities rather than single bacterial taxon, which better reflect the ecology of wild mosquitoes and provides a more nuanced view of mosquito immune responses across different microbial environments. Ultimately, interactions with the environmental microbiome during the larval stages generate varied immune responses to infection in adult *A. albopictus* mosquitoes. However, the scale of the immune response is highly context-dependent, with the main conclusion being that exposure to compositionally diverse environmental microbiomes during the larval period differentially impacts adult female and male immune expression.

This study offers novel insights into the consequences of *A. albopictus* invading variable new habitats. We demonstrated that larval development times and pupation success vary when reared with different microbial communities. We saw that environments with less diverse microbial communities produce adult *A. albopictus* mosquitoes faster and in higher numbers, which has implications for how quickly and successfully a new population can establish and expand after an invasion event. Environments with less microbial diversity also produced mosquitoes that could survive starvation for longer periods of time, which also enhances the ability of adult *A.*

albopictus populations to persist in new environments if food resources are scarce upon eclosion. From a public health perspective, the variation in immune expression resulting from exposure to different microbial communities has potential consequences for mosquito-borne disease transmission. The mosquito immune system is active in combating pathogens of human relevance such as dengue virus (Mukherjee et al., 2019; Xi, Ramirez, & Dimopoulos, 2008), chikungunya virus (McFarlane et al., 2014), Zika virus (Angleró-Rodríguez et al., 2017), and West Nile virus (Arjona et al., 2022). Thus, immune priming from the microbial environment may predispose populations of adult females for higher vector competence which could manifest as localized mosquito-borne disease outbreaks under the right conditions. In conclusion, these findings underscore the intricate interplay between microbial communities and the developmental, physiological, and immune responses of *A. albopictus*, shedding light on the multifaceted dynamics shaping mosquito populations and their potential impact on public health.

Table 3.1. Means \pm standard errors of days to pupation and remaining larvae across all treatments.

Treatment	Days to pupation	Remaining larvae
Laboratory	17.91 \pm 0.32	1.33 \pm 0.76
Lyon Arboretum 0.1 μ m	19.70 \pm 0.42	3.67 \pm 0.76
Lyon Arboretum 10 μ m	19.82 \pm 0.50	10.00 \pm 1.62
Lyon Arboretum 30-50 μ m	18.55 \pm 0.48	9.33 \pm 1.09
UH-Mānoa 0.1 μ m	15.77 \pm 0.47	1.33 \pm 0.29
UH-Mānoa 10 μ m	18.13 \pm 0.71	25.67 \pm 1.05
UH-Mānoa 30-50 μ m	19.88 \pm 0.58	28.33 \pm 0.83

Table 3.2. Means \pm standard errors of survival times (in days) by sex across all treatments.

Treatment	Sex	Survival times in days
Laboratory	F	2.83 \pm 0.11
Lyon Arboretum 0.1 μm	F	3.08 \pm 0.13
Lyon Arboretum 10 μm	F	3.03 \pm 0.15
Lyon Arboretum 30-50 μm	F	2.56 \pm 0.09
UH-Mānoa 0.1 μm	F	3.05 \pm 0.11
UH-Mānoa 10 μm	F	2.14 \pm 0.14
UH-Mānoa 30-50 μm	F	2.43 \pm 0.20
Laboratory	M	3.06 \pm 0.08
Lyon Arboretum 0.1 μm	M	2.67 \pm 0.09
Lyon Arboretum 10 μm	M	2.44 \pm 0.10
Lyon Arboretum 30-50 μm	M	2.47 \pm 0.08
UH-Mānoa 0.1 μm	M	2.55 \pm 0.13
UH-Mānoa 10 μm	M	2.32 \pm 0.09
UH-Mānoa 30-50 μm	M	2.24 \pm 0.09

Table 3.3. Means \pm standard errors of the DDCt values of CEC-A and LYS-E by sex and treatment and infection status. Values shown are immune gene expression values in infected mosquitoes relative to non-infected mosquitoes. Positive values indicate higher expression of target gene.

Treatment	Sex	CEC-A	LYS-E
Laboratory	F	3.79 \pm 4.37	3.29 \pm 1.31
Lyon Arboretum 0.1 μ m	F	0.70 \pm 0.92	-5.36 \pm 1.00
Lyon Arboretum 10 μ m	F	1.61 \pm 0.68	-1.91 \pm 1.67
Lyon Arboretum 30-50 μ m	F	1.40 \pm 0.98	-3.66 \pm 1.20
UH-Mānoa 0.1 μ m	F	0.49 \pm 0.81	-2.30 \pm 1.56
UH-Mānoa 10 μ m	F	-1.45 \pm 0.66	-2.83 \pm 1.02
UH-Mānoa 30-50 μ m	F	-0.59 \pm 0.63	-5.74 \pm 0.97
Laboratory	M	2.40 \pm 0.49	3.04 \pm 1.73
Lyon Arboretum 0.1 μ m	M	1.55 \pm 0.34	-0.22 \pm 1.36
Lyon Arboretum 10 μ m	M	2.92 \pm 0.40	-2.94 \pm 1.76
Lyon Arboretum 30-50 μ m	M	1.46 \pm 1.11	-1.84 \pm 1.48
UH-Mānoa 0.1 μ m	M	2.53 \pm 0.99	-2.89 \pm 1.67
UH-Mānoa 10 μ m	M	4.81 \pm 1.03	1.00 \pm 1.55
UH-Mānoa 30-50 μ m	M	3.04 \pm 0.77	-2.06 \pm 1.59

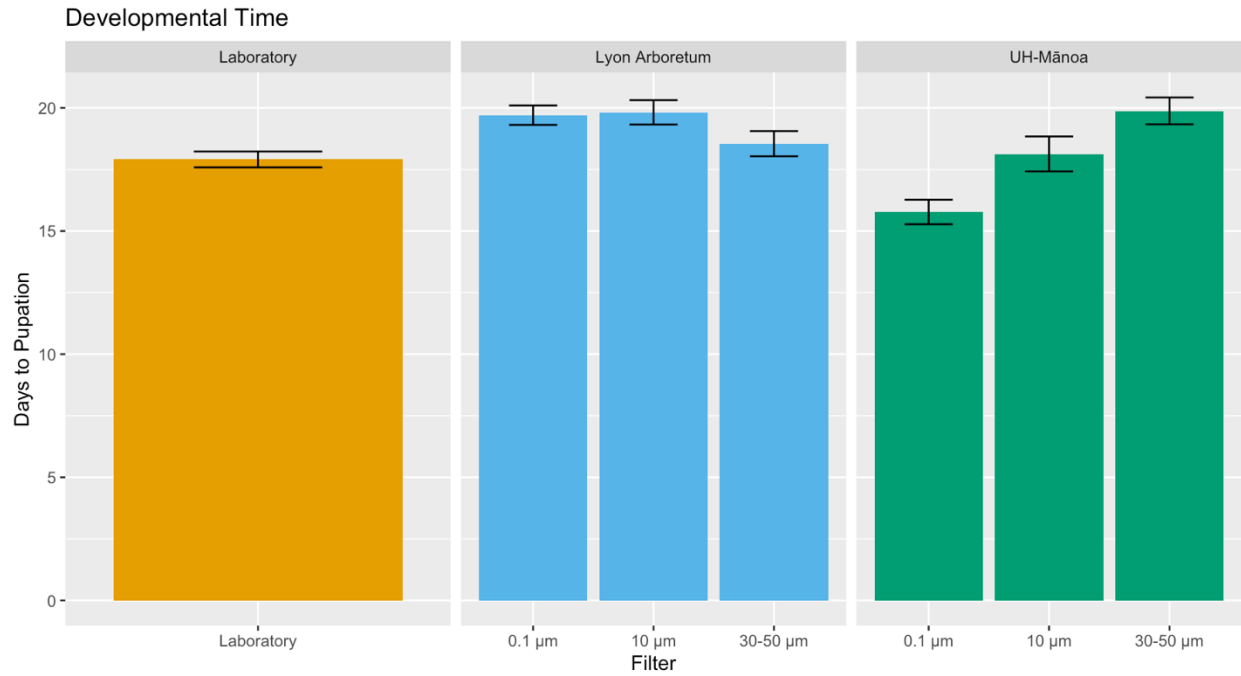


Figure 3.1. Bar plot showing the number of days (mean \pm SEM) to reach pupation by each water source and filtration level.

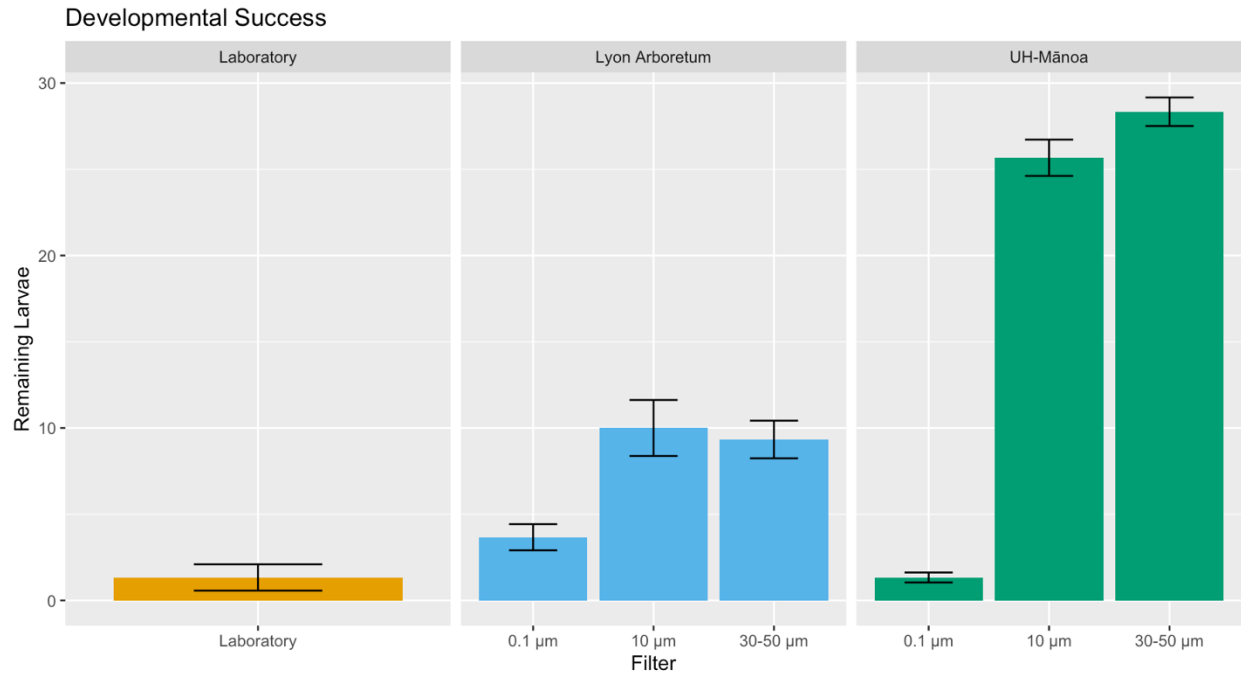


Figure 3.2. Bar plot showing the number of larvae remaining (mean \pm SEM) at day 32 of the experiment by each water source and filtration level.

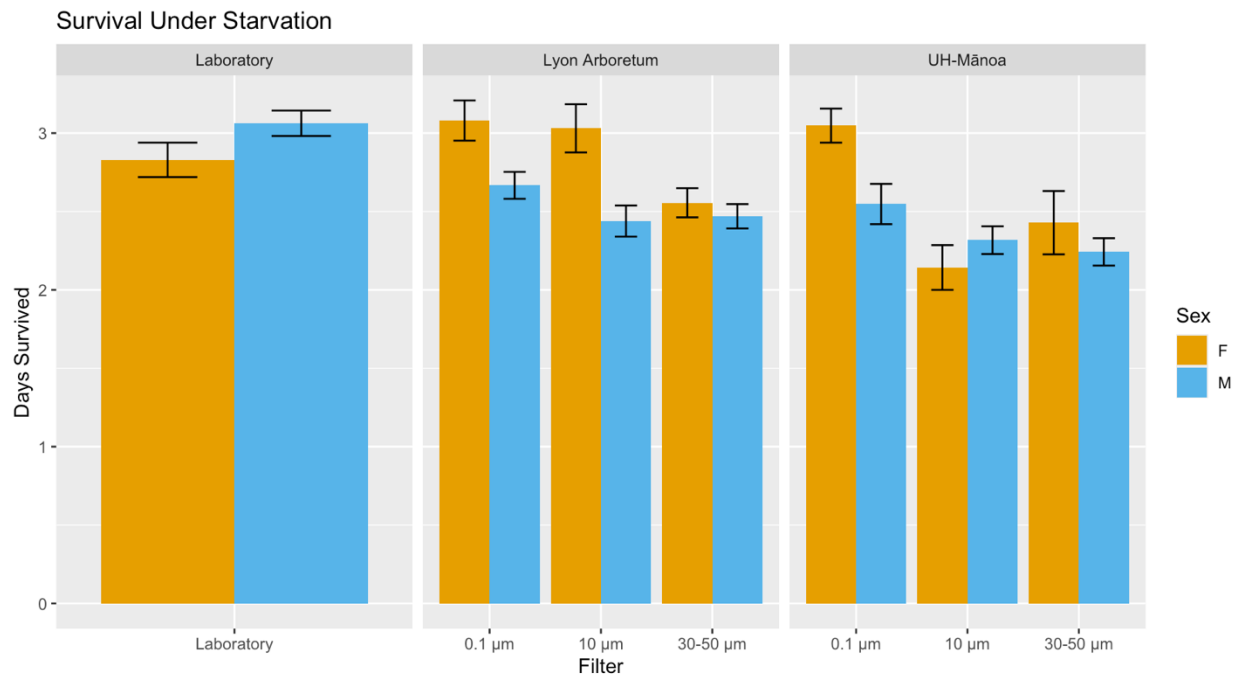


Figure 3.3. Bar plot showing the number of days (mean \pm SEM) adult female and male *Aedes albopictus* survived under starvation conditions by each water source and filtration level.

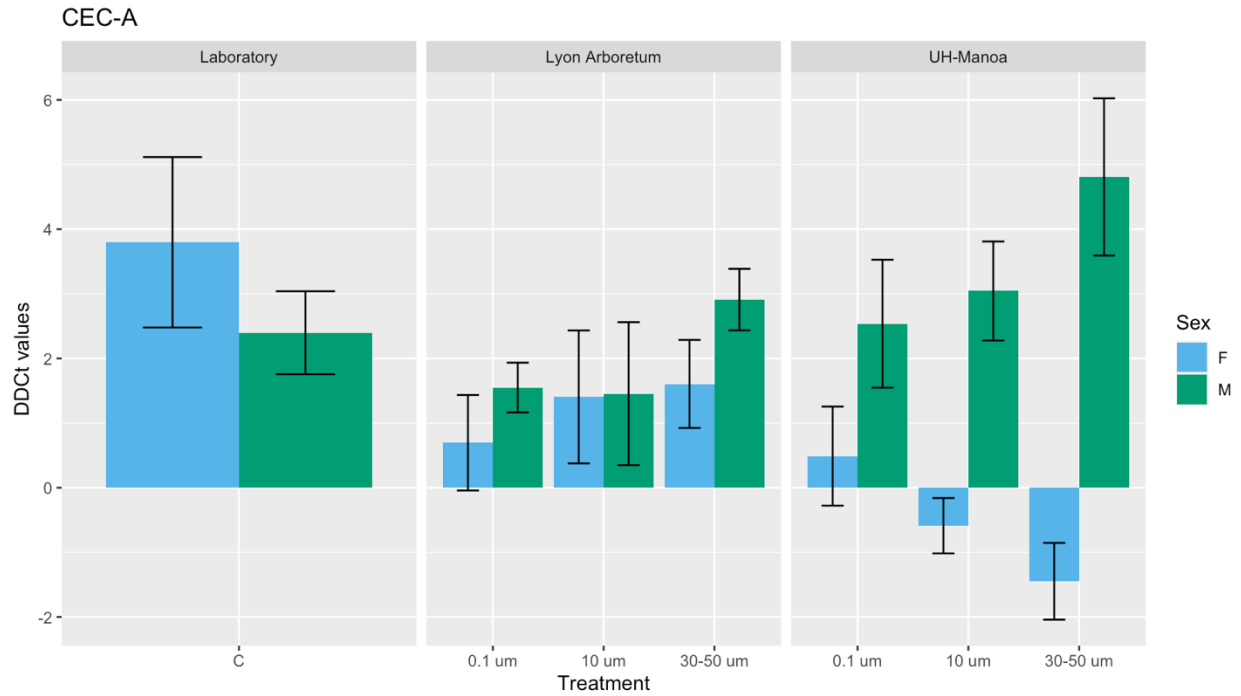


Figure 3.4. Bar plot showing the DDCt values (mean \pm SEM) of CEC-A in adult female and male *Aedes albopictus* by treatment. Values shown are immune gene expression values in infected mosquitoes relative to non-infected mosquitoes. Positive values indicate higher expression of target gene.

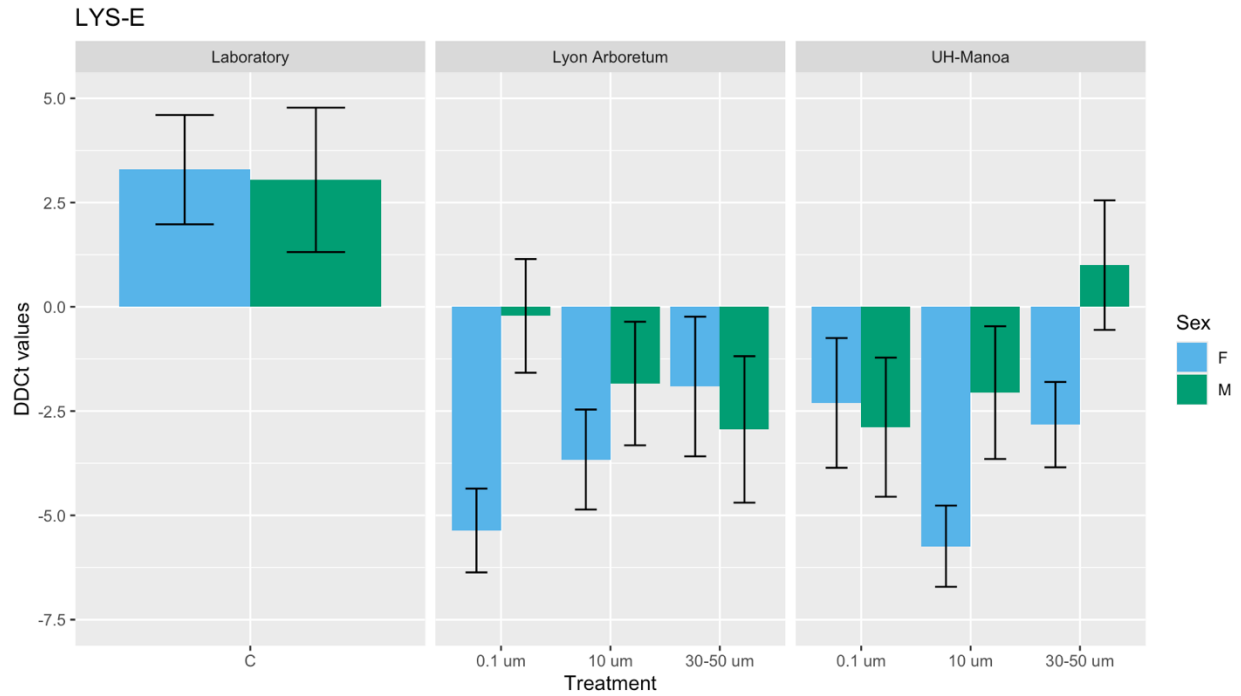


Figure 3.5. Bar plot showing the DDCt values (mean \pm SEM) of LYS-E in adult female and male *Aedes albopictus* by treatment. Values shown are immune gene expression values in infected mosquitoes relative to non-infected mosquitoes. Positive values indicate higher expression of target gene.

APPENDIX D: CHAPTER 3 SUPPLEMENTAL TABLE

Supplemental table 3.1. List of immune genes and primer sequences used for RT-qPCR analysis.

Gene Name	Forward Primer Sequence	Reverse Primer Sequence
Rps7	GTCCACGATCCCGCACTCT	GTGGTCTGCTGGTTCTTGTC
REL1	CTACCGGCAACCAAATGACT	GGGATTGTAGGGGGATGTCT
REL2	GCGATACGAGCTCCTTCAAC	GTGAGGGTGAGTTGGATCGT
STAT	CACCGGATCGTTAACCTG	AGCCATGGACACGTCGTC
CEC-A	CGGCGGTTTGAAGAAGTTCG	CGCAACGGGTAGAGCTTTCT
DEF-C	TCTCAGTGTCGTTTGCTTGG	GACAGCTCTTCAGGGAATGC
LYS-E	AACAATCGTAACGGGTCCAC	ATTCAGCAGCTCCGAACACT

LITERATURE CITED

- Angleró-Rodríguez, Y. I., MacLeod, H. J., Kang, S., Carlson, J. S., Jupatanakul, N., & Dimopoulos, G. (2017). *Aedes aegypti* molecular responses to Zika Virus: modulation of infection by the Toll and Jak/Stat immune pathways and virus host factors. *Frontiers in Microbiology*, 8, 2050. <https://doi.org/10.3389/fmicb.2017.02050>
- Arisdakessian, C, Cleveland, S. B., & Belcaid, M. (2020). MetaFlow|mics: scalable and reproducible nextflow pipelines for the analysis of microbiome marker data. PEARC '20: Practice and Experience in Advanced Research Computing, 120-124.
- Arjona, A., Wang, P., Montgomery, R. R., & Fikrig, E. (2011). Innate immune control of West Nile virus infection. *Cellular Microbiology*, 13(11), 1648–1658. <https://doi.org/10.1111/j.1462-5822.2011.01649.x>
- Bauer, M. A., Kainz, K., Carmona-Gutierrez, D., & Madeo, F. (2018). Microbial wars: Competition in ecological niches and within the microbiome. *Microbial Cell (Graz, Austria)*, 5(5), 215–219. <https://doi.org/10.15698/mic2018.05.628>
- Benedict, M.Q., Levine, R.S., Hawley, W.A., & Lounibos, L.P. (2007). Spread of the tiger: global risk of invasion by the mosquito *Aedes albopictus*. *Vector Borne and Zoonotic Diseases*, 7(1), 76–85.
- Bennett, K. L., Gómez-Martínez, C., Chin, Y., Saltonstall, K., McMillan, W. O., Rovira, J. R., & Loaiza, J. R. (2019). Dynamics and diversity of bacteria associated with the disease vectors *Aedes aegypti* and *Aedes albopictus*. *Scientific reports*, 9(1), 12160. <https://doi.org/10.1038/s41598-019-48414-8>

- Bonizzoni, M., Gasperi, G., Chen, X., & James, A. A. (2013). The invasive mosquito species *Aedes albopictus*: Current knowledge and future perspectives. *Trends in Parasitology*, 29(9), 460–468. <https://doi.org/10.1016/j.pt.2013.07.003>
- Boissière, A., Tchioffo, M. T., Bachar, D., Abate, L., Marie, A., Nsango, S. E., Shahbazkia, H. R., Awono-Ambene, P. H., Levashina, E. A., Christen, R., & Morlais, I. (2012). Midgut microbiota of the malaria mosquito vector *Anopheles gambiae* and interactions with *Plasmodium falciparum* infection. *PLoS Pathogens*, 8(5), e1002742. <https://doi.org/10.1371/journal.ppat.1002742>
- Briegel, H., & Timmermann, S. E. (2001). *Aedes albopictus* (Diptera: Culicidae): physiological aspects of development and reproduction. *Journal of Medical Entomology*, 38(4), 566–571. <https://doi.org/10.1603/0022-2585-38.4.566>
- Brooks, M. E., Kristensen, K., van Benthem, K. J., Magnusson, A., Berg, C. W., Nielsen, A., Skaug, H. J., Maechler, M., & Bolker, B. M. (2017). “glmmTMB balances speed and flexibility among packages for zero-inflated generalized linear mixed modeling.” *The R Journal*, 9(2), 378–400.
- Caimano, M. J., Drecktrah, D., Kung, F., & Samuels, D. S. (2016). Interaction of the Lyme disease spirochete with its tick vector. *Cellular Microbiology*, 18(7), 919–927. <https://doi.org/10.1111/cmi.12609>
- Cansado-Utrilla, C., Zhao, S. Y., McCall, P. J., Coon, K. L., & Hughes, G. L. (2021). The microbiome and mosquito vectorial capacity: rich potential for discovery and translation. *Microbiome*, 9(1), 111. <https://doi.org/10.1186/s40168-021-01073-2>
13. Caporaso, J. G., Lauber, C. L., Walters, W. A., Berg-Lyons, D., Lozupone, C. A., Turnbaugh, P. J., Fierer, N., & Knight, R. (2011). Global patterns of 16S rRNA diversity at a depth of

millions of sequences per sample. *Proceedings of the National Academy of Sciences of the United States of America*, *108 Suppl 1*(Suppl 1), 4516–4522.

<https://doi.org/10.1073/pnas.1000080107>

Carlson, J. S., Short, S. M., Angleró-Rodríguez, Y. I., & Dimopoulos, G. (2020). Larval exposure to bacteria modulates arbovirus infection and immune gene expression in adult *Aedes aegypti*. *Developmental and Comparative Immunology*, *104*, 103540.

<https://doi.org/10.1016/j.dci.2019.103540>

Chala, B., & Hamde, F. (2021). Emerging and re-emerging vector-borne infectious diseases and the challenges for control: a review. *Frontiers in Public Health*, *9*, 715759.

Charles, H., & Dukes, J.S. (2007). Impacts of invasive species on ecosystem services. In W. Nentwig (Ed.), *Biological invasions. Ecological Studies*, (193, pp. 293–310). Berlin: Springer.

Chen, Q., Hou, L.W., Duan, W.J., Crous, P.W., & Cai, L. (2017). *Didymellaceae* revisited. *Studies in mycology*, *87*, 105-159. <https://doi.org/10.1016/j.simyco.2017.06.002>

Chen, W. J., Wu, S. T., Chow, C. Y., & Yang, C. H. (1997). Sporogonic development of the Gregarine *Ascogregarina taiwanensis* (Lien and Levine) (Apicomplexa: Lecudinidae) in its natural host *Aedes albopictus* (Skuse) (Diptera: Culicidae). *Journal of Eukaryotic Microbiology*, *44*(4), 326-331.

Chevillon, C., Briant, L., Renaud, F., & Devaux, C. (2008). The Chikungunya threat: an ecological and evolutionary perspective. *Trends in Microbiology*, *16*(2), 80–88.

Clauset, A., Newman, M. E., & Moore, C. (2004). Finding community structure in very large networks. *Physical review. E, Statistical, nonlinear, and soft matter physics*, *70*(6 Pt 2), 066111. <https://doi.org/10.1103/PhysRevE.70.066111>

- Coon, K. L., Vogel, K. J., Brown, M. R., & Strand, M. R. (2014). Mosquitoes rely on their gut microbiota for development. *Molecular Ecology*, 23(11), 2727–2739.
- Coon, K. L., Brown, M. R., & Strand, M. R. (2016a). Gut bacteria differentially affect egg production in the anautogenous mosquito *Aedes aegypti* and facultatively autogenous mosquito *Aedes atropalpus* (Diptera: Culicidae). *Parasites & Vectors*, 9(1), 375.
<https://doi.org/10.1186/s13071-016-1660-9>
- Coon, K. L., Brown, M. R., & Strand, M. R. (2016b). Mosquitoes host communities of bacteria that are essential for development but vary greatly between local habitats. *Molecular Ecology*, 25(22), Article 22. <https://doi.org/10.1111/mec.13877>
- Csardi, G., & Nepusz, T. (2006). The igraph software package for complex network research. *Complex systems*, 1695.
- Cunze, S., Koch, L. K., Kochmann, J., & Klimpel, S. (2016). *Aedes albopictus* and *Aedes japonicus* - two invasive mosquito species with different temperature niches in Europe. *Parasites & Vectors*, 9(1), 573. <https://doi.org/10.1186/s13071-016-1853-2>
- Das, P., Ji, B., Kovatcheva-Datchary, P., Bäckhed, F., & Nielsen, J. (2018). In vitro co-cultures of human gut bacterial species as predicted from co-occurrence network analysis. *PloS one*, 13(3), e0195161. <https://doi.org/10.1371/journal.pone.0195161>
- David, P., Thébault, E., Anneville, O., Duyck, P.-F., Chapuis, E., & Loeuille, N. (2017). Impacts of invasive species on food webs. In: Bohan, D.A. , Dumbrell, A. J., Massol, F. (eds), *Advances in Ecological Research*, (56, pp. 1–60). Elsevier, Amsterdam.
- Delatte, H., Desvars, A., Bouétard, A., Bord, S., Gimonneau, G., Vourc'h, G., & Fontenille, D. (2010). Blood-feeding behavior of *Aedes albopictus*, a vector of Chikungunya on La Réunion. *Vector Borne and Zoonotic Diseases*, 10(3), 249–258.

- Dong, Y., Morton, J. C., Jr, Ramirez, J. L., Souza-Neto, J. A., & Dimopoulos, G. (2012). The entomopathogenic fungus *Beauveria bassiana* activate toll and JAK-STAT pathway-controlled effector genes and anti-dengue activity in *Aedes aegypti*. *Insect Biochemistry and Molecular Biology*, 42(2), 126–132. <https://doi.org/10.1016/j.ibmb.2011.11.005>
- Douglas A. E. (2020). The microbial exometabolome: ecological resource and architect of microbial communities. *Philosophical transactions of the Royal Society of London. Series B, Biological sciences*, 375(1798), 20190250. <https://doi.org/10.1098/rstb.2019.0250>
- Duguma, D., Hall, M. W., Rugman-Jones, P., Stouthamer, R., Terenius, O., Neufeld, J. D., & Walton, W. E. (2015). Developmental succession of the microbiome of *Culex* mosquitoes. *BMC microbiology*, 15, 140. <https://doi.org/10.1186/s12866-015-0475-8>
- Effler, P. V., Pang, L., Kitsutani, P., Vorndam, V., Nakata, M., Ayers, T., Elm, J., Tom, T., Reiter, P., Rigau-Perez, J. G., Hayes, J. M., Mills, K., Napier, M., Clark, G. G., Gubler, D. J., & Hawaii Dengue Outbreak Investigation Team. (2005). Dengue fever, Hawaii, 2001-2002.
- Embree, M., Liu, J. K., Al-Bassam, M. M., & Zengler, K. (2015). Networks of energetic and metabolic interactions define dynamics in microbial communities. *Proceedings of the National Academy of Sciences of the United States of America*, 112(50), 15450–15455. <https://doi.org/10.1073/pnas.1506034112>
- Falaschi, M., Melotto, A., Manenti, R., & Ficetola, G.F. (2020). Invasive species and amphibian conservation. *Herpetologica*, 76, 216–227.
- Falony, G., Joossens, M., Vieira-Silva, S., Wang, J., Darzi, Y., Faust, K., Kurilshikov, A., Bonder, M. J., Valles-Colomer, M., Vandeputte, D., Tito, R. Y., Chaffron, S., Rymenans, L., Verspecht, C., De Sutter, L., Lima-Mendez, G., D'hoë, K., Jonckheere, K., Homola, D.,

- Garcia, R., ... Raes, J. (2016). Population-level analysis of gut microbiome variation. *Science (New York, N.Y.)*, 352(6285), 560–564. <https://doi.org/10.1126/science.aad3503>
- Fath, B.D., Scharler, U.M., Ulanowicz, R.E., & Hannon, B. (2007). Ecological network analysis: network construction. *Ecological modelling*, 208(1), 49-55.
- Faust, K., Sathirapongsasuti, J. F., Izard, J., Segata, N., Gevers, D., Raes, J., & Huttenhower, C. (2012). Microbial co-occurrence relationships in the human microbiome. *PLoS computational biology*, 8(7), e1002606. <https://doi.org/10.1371/journal.pcbi.1002606>
- Fernandes, K. M., Neves, C. A., Serrão, J. E., & Martins, G. F. (2014). *Aedes aegypti* midgut remodeling during metamorphosis. *Parasitology international*, 63(3), 506–512. <https://doi.org/10.1016/j.parint.2014.01.004>
- Fikrig, K., Peck, S., Deckerman, P., Dang, S., St Fleur, K., Goldsmith, H., Qu, S., Rosenthal, H., & Harrington, L. C. (2020). Sugar feeding patterns of New York *Aedes albopictus* mosquitoes are affected by saturation deficit, flowers, and host seeking. *PLOS Neglected Tropical Diseases*, 14(10), e0008244. <https://doi.org/10.1371/journal.pntd.0008244>
- Frankel-Bricker, J., Song, M. J., Benner, M. J., & Schaack, S. (2020). Variation in the microbiota associated with *Daphnia magna* across genotypes, populations, and temperature. *Microbial ecology*, 79(3), 731–742. <https://doi.org/10.1007/s00248-019-01412-9>
- Frey-Klett, P., Burlinson, P., Deveau, A., Barret, M., Tarkka, M., & Sarniguet, A. (2011). Bacterial-fungal interactions: hyphens between agricultural, clinical, environmental, and food microbiologists. *Microbiology and molecular biology reviews : MMBR*, 75(4), 583–609. <https://doi.org/10.1128/MMBR.00020-11>

- Gabrieli, P., Caccia, S., Varotto-Bocazzi, I., Arnoldi, I., Barbieri, G., Comandatore, F., & Epis, S. (2021). Mosquito trilogy: microbiota, immunity and pathogens, and their implications for the control of disease transmission. *Frontiers in Microbiology*, *12*, 630438.
- Gallardo, B., Clavero, M., Sánchez, M. I., & Vilà, M. (2016). Global ecological impacts of invasive species in aquatic ecosystems. *Global Change Biology*, *22*(1), 151–163.
- Garcia-Rejon, J. E., Navarro, J.-C., Cigarroa-Toledo, N., & Baak-Baak, C. M. (2021). An Updated Review of the Invasive *Aedes albopictus* in the Americas; Geographical Distribution, Host Feeding Patterns, Arbovirus Infection, and the Potential for Vertical Transmission of Dengue Virus. *Insects*, *12*(11), 967. <https://doi.org/10.3390/insects12110967>
- Ghoul, M., & Mitri, S. (2016). The ecology and evolution of microbial competition. *Trends in Microbiology*, *24*(10), 833–845. <https://doi.org/10.1016/j.tim.2016.06.011>
- Gjullin, C. M., Hegarty, C. P., & Bollen, W. B. (1941). The necessity of a low oxygen concentration for the hatching of aedes mosquito eggs. *Journal of Cellular and Comparative Physiology*, *17*(2), 193–202. <https://doi.org/10.1002/jcp.1030170205>
- Global Invasive Species Database (2024). http://www.iucngisd.org/gisd/100_worst.php_on_10-02-2024. Accessed February 10, 2024.
- Gould, A. L., Zhang, V., Lamberti, L., Jones, E. W., Obadia, B., Korasidis, N., Gavryushkin, A., Carlson, J. M., Beerenwinkel, N., & Ludington, W. B. (2018). Microbiome interactions shape host fitness. *Proceedings of the National Academy of Sciences of the United States of America*, *115*(51), E11951–E11960. <https://doi.org/10.1073/pnas.1809349115>
- Graña-Miraglia, L., Sikutova, S., Vancová, M., Bílý, T., Fingerle, V., Sing, A., Castillo-Ramírez, S., Margos, G., & Rudolf, I. (2020). Spirochetes isolated from arthropods constitute a novel

- genus *Entomospira* genus novum within the order Spirochaetales. *Scientific Reports*, *10*(1), 17053. <https://doi.org/10.1038/s41598-020-74033-9>
- Gratz, N. G. (2004). Critical review of the vector status of *Aedes albopictus*. *Medical and Veterinary Entomology*, *18*(3), 215–227. <https://doi.org/10.1111/j.0269-283X.2004.00513.x>
- Gratz N. G. (2004). Critical review of the vector status of *Aedes albopictus*. *Medical and Veterinary Entomology*, *18*(3), 215–227.
- Griffin, C. D., Weber, D. E., Seabourn, P., Waiyanuhea, L. K., & Medeiros, M. C. I. (2023). Filtration of environmentally sourced aquatic media impacts laboratory-colonised *Aedes albopictus* early development and adult bacteriome composition. *Medical and Veterinary Entomology*, *37*(4), 693–704.
- Gubler, D. J. (2010). The global threat of emergent/re-emergent vector-borne diseases. *Vector Biology, Ecology and Control*, 39-62.
- Guégan, M., Martin, E., Tran Van, V., Fel, B., Hay, A. E., Simon, L., Butin, N., Bellvert, F., Haichar, F. E. Z., & Valiente Moro, C. (2022). Mosquito sex and mycobiota contribute to fructose metabolism in the Asian tiger mosquito *Aedes albopictus*. *Microbiome*, *10*(1), 138.
- Gupta, L., Molina-Cruz, A., Kumar, S., Rodrigues, J., Dixit, R., Zamora, R. E., & Barillas-Mury, C. (2009). The STAT pathway mediates late-phase immunity against *Plasmodium* in the mosquito *Anopheles gambiae*. *Cell Host & Microbe*, *5*(5), 498–507. <https://doi.org/10.1016/j.chom.2009.04.003>
- Harrison, R. E., Yang, X., Eum, J. H., Martinson, V. G., Dou, X., Valzania, L., Wang, Y., Boyd, B. M., Brown, M. R., & Strand, M. R. (2023). The mosquito *Aedes aegypti* requires a gut microbiota for normal fecundity, longevity and vector competence. *Communications Biology*, *6*(1), 1154.

- Hassani, M. A., Durán, P., & Hacquard, S. (2018). Microbial interactions within the plant holobiont. *Microbiome*, 6(1), 58. <https://doi.org/10.1186/s40168-018-0445-0>
- Hegde, S., Khanipov, K., Albayrak, L., Golovko, G., Pimenova, M., Saldaña, M. A., Rojas, M. M., Hornett, E. A., Motl, G. C., Fredregill, C. L., Dennett, J. A., Debboun, M., Fofanov, Y., & Hughes, G. L. (2018). Microbiome Interaction Networks and Community Structure from Laboratory-Reared and Field-Collected *Aedes aegypti*, *Aedes albopictus*, and *Culex quinquefasciatus* Mosquito Vectors. *Frontiers in Microbiology*, 9, 2160. <https://doi.org/10.3389/fmicb.2018.02160>
- Hegde, S., Rasgon, J. L., & Hughes, G. L. (2015). The microbiome modulates arbovirus transmission in mosquitoes. *Current Opinion in Virology*, 15, 97–102. <https://doi.org/10.1016/j.coviro.2015.08.011>
- Hillyer J. F. (2010). Mosquito immunity. *Advances in experimental medicine and biology*, 708, 218–238. https://doi.org/10.1007/978-1-4419-8059-5_12
- Hulme, P.E. (2009). Trade, transport and trouble: managing invasive species pathways in an era of globalization. *Journal of Applied Ecology*, 46(1), 10-18.
- Huntington, M.K., Allison, J., & Nair, D. (2016). Emerging vector-borne diseases. *American Family Physician*, 94(7), 551–557
- Iyer, S., Killingback, T., Sundaram, B., & Wang, Z. (2013). Attack robustness and centrality of complex networks. *PloS one*, 8(4), e59613. <https://doi.org/10.1371/journal.pone.0059613>
- Jackson, M. M., Turner, M. G., Pearson, S. M., & Ives, A. R. (2012). Seeing the forest and the trees: Multilevel models reveal both species and community patterns. *Ecosphere*, 3(9), art79. <https://doi.org/10.1890/ES12-00116.1>

- Johnston, D. I., Viray, M. A., Ushiroda, J. M., He, H., Whelen, A. C., Sciulli, R. H., Kunimoto, G. Y., & Y Park, S. (2020). Investigation and Response to an Outbreak of Dengue: Island of Hawaii, 2015-2016. *Public Health Reports (Washington, D.C.: 1974)*, *135*(2), 230–237.
<https://doi.org/10.1177/0033354920904068>
- Jones, K., Patel, N., Levy, M., Storeygard, A., Balk, D., Gittleman, J.L., & Daszak, P. (2008). Global trends in emerging infectious diseases. *Nature*, *451*, 990–993.
- Judson, C. L. (1960). The Physiology of Hatching of Aedine Mosquito Eggs: Hatching Stimulus. *Annals of the Entomological Society of America*, *53*(5), 688–691.
<https://doi.org/10.1093/aesa/53.5.688>
- Judson, C. L., & Gojrati, H. A. N. (1967). The effects of various oxygen tensions on embryogeny and larval responses of *Aedes aegypti*. *Entomologia Experimentalis et Applicata*, *10*(2), 181–188. <https://doi.org/10.1111/j.1570-7458.1967.tb00057.x>
- King J. G. (2020). Developmental and comparative perspectives on mosquito immunity. *Developmental and comparative immunology*, *103*, 103458.
<https://doi.org/10.1016/j.dci.2019.103458>
- Kern-Allely, S., Pobutsky, A., & Hancock, W. T. (2020). Notes from the Field: First Evidence of Locally Acquired Dengue Since 1944 - Guam, 2019. *MMWR. Morbidity and Mortality Weekly Report*, *69*(13), 387–388. <https://doi.org/10.15585/mmwr.mm6913a4>
- Kraemer, M.U.G., Reiner, R.C., Jr, Brady, O.J., Messina, J.P., Gilbert, M., Pigott, D.M., Yi, D., Johnson, K., Earl, L., Marczak, L.B., Shirude, S., Davis Weaver, N., Bisanzio, D., Perkins, T.A., Lai, S., Lu, X., Jones, P., Coelho, G.E., Carvalho, R.G., Van Bortel, W., ... Golding, N. (2019). Past and future spread of the arbovirus vectors *Aedes aegypti* and *Aedes albopictus*. *Nature Microbiology*, *4*(5), 854–863.

- Kurtz, Z. D., Müller, C. L., Miraldi, E. R., Littman, D. R., Blaser, M. J., & Bonneau, R. A. (2015). Sparse and compositionally robust inference of microbial ecological networks. *PLoS computational biology*, *11*(5), e1004226. <https://doi.org/10.1371/journal.pcbi.1004226>
- Lacroix, R., Delatte, H., Hue, T., & Reiter, P. (2009). Dispersal and survival of male and female *Aedes albopictus* (Diptera: Culicidae) on Réunion Island. *Journal of Medical Entomology*, *46*(5), 1117–1124. <https://doi.org/10.1603/033.046.0519>
- Laporta, G. Z., Potter, A. M., Oliveira, J. F. A., Bourke, B. P., Pecor, D. B., & Linton, Y. M. (2023). Global Distribution of *Aedes aegypti* and *Aedes albopictus* in a Climate Change Scenario of Regional Rivalry. *Insects*, *14*(1), 49. <https://doi.org/10.3390/insects14010049>
- Layeghifard, M., Hwang, D. M., & Guttman, D. S. (2017). Disentangling interactions in the microbiome: a network perspective. *Trends in microbiology*, *25*(3), 217–228. <https://doi.org/10.1016/j.tim.2016.11.008>
- Lee, K. K., Kim, H., & Lee, Y. H. (2022). Cross-kingdom co-occurrence networks in the plant microbiome: importance and ecological interpretations. *Frontiers in microbiology*, *13*, 953300. <https://doi.org/10.3389/fmicb.2022.953300>
- Liu, H., Roeder, K., & Wasserman, L. (2010). Stability approach to regularization selection (StARS) for high dimensional graphical models. *Advances in neural information processing systems*, *24*(2), 1432–1440.
- Liu, B., Gao, X., Ma, J., Jiao, Z., Xiao, J., Hayat, M. A., & Wang, H. (2019). Modeling the present and future distribution of arbovirus vectors *Aedes aegypti* and *Aedes albopictus* under climate change scenarios in Mainland China. *The Science of the total environment*, *664*, 203–214. <https://doi.org/10.1016/j.scitotenv.2019.01.301>

- Livak, K. J., & Schmittgen, T. D. (2001). Analysis of relative gene expression data using real-time quantitative PCR and the $2^{-(\Delta\Delta C(T))}$ Method. *Methods (San Diego, Calif.)*, 25(4), 402–408. <https://doi.org/10.1006/meth.2001.1262>
- Lounibos, L. P., Escher, R. L., & Lourenço-De-Oliveira, R. (2003). Asymmetric evolution of photoperiodic diapause in temperate and tropical invasive populations of *Aedes albopictus* (Diptera: Culicidae). *Annals of the Entomological Society of America*, 96(4), 512–518.
- Mahana, D., Trent, C. M., Kurtz, Z. D., Bokulich, N. A., Battaglia, T., Chung, J., Müller, C. L., Li, H., Bonneau, R. A., & Blaser, M. J. (2016). Antibiotic perturbation of the murine gut microbiome enhances the adiposity, insulin resistance, and liver disease associated with high-fat diet. *Genome medicine*, 8(1), 48. <https://doi.org/10.1186/s13073-016-0297-9>
- Martinson, V. G., & Strand, M. R. (2021). Diet-Microbiota Interactions Alter Mosquito Development. *Frontiers in Microbiology*, 12, 650743. <https://doi.org/10.3389/fmicb.2021.650743>
- McFall-Ngai, M., Hadfield, M. G., Bosch, T. C., Carey, H. V., Domazet-Lošo, T., Douglas, A. E., Dubilier, N., Eberl, G., Fukami, T., Gilbert, S. F., Hentschel, U., King, N., Kjelleberg, S., Knoll, A. H., Kremer, N., Mazmanian, S. K., Metcalf, J. L., Neelson, K., Pierce, N. E., Rawls, J. F., ... Wernegreen, J. J. (2013). Animals in a bacterial world, a new imperative for the life sciences. *Proceedings of the National Academy of Sciences of the United States of America*, 110(9), 3229–3236. <https://doi.org/10.1073/pnas.1218525110>
- McFarlane, M., Arias-Goeta, C., Martin, E., O'Hara, Z., Lulla, A., Mousson, L., Rainey, S. M., Misbah, S., Schnettler, E., Donald, C. L., Merits, A., Kohl, A., & Failloux, A. B. (2014). Characterization of *Aedes aegypti* innate-immune pathways that limit Chikungunya virus

replication. *PLoS Neglected Tropical Diseases*, 8(7), e2994.

<https://doi.org/10.1371/journal.pntd.0002994>

McMurdie, P. J., & Holmes, S. (2013). phyloseq: an R package for reproducible interactive analysis and graphics of microbiome census data. *PloS one*, 8(4), e61217.

<https://doi.org/10.1371/journal.pone.0061217>

McMurdie, P. J., & Holmes, S. (2014). Waste not, want not: why rarefying microbiome data is inadmissible. *PLoS Computational Biology*, 10(4), e1003531.

<https://doi.org/10.1371/journal.pcbi.1003531>

Medeiros, M. C. I., Seabourn, P. S., Rollins, R. L., & Yoneishi, N. M. (2022). Mosquito microbiome diversity varies along a landscape-scale moisture gradient. *Microbial ecology*, 84(3), 893–900. <https://doi.org/10.1007/s00248-021-01865-x>

Medlock, J. M., Hansford, K. M., Schaffner, F., Versteirt, V., Hendrickx, G., Zeller, H., & Van Bortel, W. (2012). A review of the invasive mosquitoes in Europe: Ecology, public health risks, and control options. *Vector Borne and Zoonotic Diseases (Larchmont, N.Y.)*, 12(6), 435–447. <https://doi.org/10.1089/vbz.2011.0814>

Messina, J. P., Brady, O. J., Pigott, D. M., Brownstein, J. S., Hoen, A. G., & Hay, S. I. (2014). A global compendium of human dengue virus occurrence. *Scientific Data*, 1, 140004.

<https://doi.org/10.1038/sdata.2014.4>

Mitraka, E., Stathopoulos, S., Siden-Kiamos, I., Christophides, G. K., & Louis, C. (2013). *Asaia* accelerates larval development of *Anopheles gambiae*. *Pathogens and Global Health*, 107(6), Article 6. <https://doi.org/10.1179/2047773213Y.0000000106>

Moll, R. M., Romoser, W. S., Modrzakowski, M. C., Moncayo, A. C., & Lerdthusnee, K. (2001). Meconial peritrophic membranes and the fate of midgut bacteria during mosquito (Diptera:

Culicidae) metamorphosis. *Journal of medical entomology*, 38(1), 29–32.

<https://doi.org/10.1603/0022-2585-38.1.29>

Moore, C. G., & Mitchell, C. J. (1997). *Aedes albopictus* in the United States: Ten-year presence and public health implications. *Emerging Infectious Diseases*, 3(3), 329–334.

<https://doi.org/10.3201/eid0303.970309>

Moreno-García, M., Vargas, V., Ramírez-Bello, I., Hernández-Martínez, G., & Lanz-Mendoza, H. (2015). Bacterial exposure at the larval stage induced sexual immune dimorphism and priming in adult *Aedes aegypti* mosquitoes. *PloS One*, 10(7), e0133240.

<https://doi.org/10.1371/journal.pone.0133240>

Mukherjee, D., Das, S., Begum, F., Mal, S., & Ray, U. (2019). The mosquito immune system and the life of dengue virus: what we know and do not know. *Pathogens (Basel, Switzerland)*, 8(2), 77. <https://doi.org/10.3390/pathogens8020077>

Murdock, C. C., Paaijmans, K. P., Bell, A. S., King, J. G., Hillyer, J. F., Read, A. F., & Thomas, M. B. (2012). Complex effects of temperature on mosquito immune function. *Proceedings. Biological sciences*, 279(1741), 3357–3366. <https://doi.org/10.1098/rspb.2012.0638>

Murdock, C. C., Moller-Jacobs, L. L., & Thomas, M. B. (2013). Complex environmental drivers of immunity and resistance in malaria mosquitoes. *Proceedings of the Royal Society B: Biological Sciences*, 280(1770), 20132030.

Mushegian, A. A., Arbore, R., Walser, J. C., & Ebert, D. (2019). Environmental Sources of Bacteria and Genetic Variation in Behavior Influence Host-Associated Microbiota. *Applied and environmental microbiology*, 85(8), e01547-18. <https://doi.org/10.1128/AEM.01547-18>

- Muturi, E. J., Ramirez, J. L., Rooney, A. P., & Kim, C. H. (2017). Comparative analysis of gut microbiota of mosquito communities in central Illinois. *PLoS Neglected Tropical Diseases*, *11*(2), e0005377. <https://doi.org/10.1371/journal.pntd.0005377>
- Osei-Poku, J., Mbogo, C. M., Palmer, W. J., & Jiggins, F. M. (2012). Deep sequencing reveals extensive variation in the gut microbiota of wild mosquitoes from Kenya. *Molecular Ecology*, *21*(20), Article 20. <https://doi.org/10.1111/j.1365-294X.2012.05759.x>
- Muturi, E. J., Lagos-Kutz, D., Dunlap, C., Ramirez, J. L., Rooney, A. P., Hartman, G. L., Fields, C. J., Rendon, G., & Kim, C. H. (2018). Mosquito microbiota cluster by host sampling location. *Parasites & vectors*, *11*(1), 468. <https://doi.org/10.1186/s13071-018-3036-9>
- Paupy, C., Delatte, H., Bagny, L., Corbel, V., & Fontenille, D. (2009). *Aedes albopictus*, an arbovirus vector: From the darkness to the light. *Microbes and Infection*, *11*(14–15), 1177–1185. <https://doi.org/10.1016/j.micinf.2009.05.005>
- Poff, K. E., Stever, H., Reil, J. B., Seabourn, P., Ching, A. J., Aoki, S., Logan, M., Michalski, J. R., Santamaria, J., Adams, J. W., Eiben, J. A., Yew, J. Y., Ewing, C. P., Magnacca, K. N., & Bennett, G. M. (2017). The Native Hawaiian Insect Microbiome Initiative: A Critical Perspective for Hawaiian Insect Evolution. *Insects*, *8*(4), E130. <https://doi.org/10.3390/insects8040130>
- Ponnusamy, L., Böröczky, K., Wesson, D. M., Schal, C., & Apperson, C. S. (2011). Bacteria Stimulate Hatching of Yellow Fever Mosquito Eggs. *PLoS ONE*, *6*(9), e24409. <https://doi.org/10.1371/journal.pone.0024409>
- Puggioli, A., Balestrino, F., Damiens, D., Lees, R. S., Soliban, S. M., Madakacherry, O., Dindo, M. L., Bellini, R., & Gilles, J. R. L. (2013). Efficiency of three diets for larval development

- in mass rearing *Aedes albopictus* (Diptera: Culicidae). *Journal of Medical Entomology*, 50(4), 819–825. <https://doi.org/10.1603/ME13011>
- R Core Team. (2021). *R: A language and environment for statistical computing*. R Foundation for Statistical Computing. URL <https://www.R-project.org/>.
- Rai, K. S. (1991). *Aedes albopictus* in the Americas. *Annual Review of Entomology*, 36, 459–484. <https://doi.org/10.1146/annurev.en.36.010191.002331>
- Ramirez, J. L., Schumacher, M. K., Ower, G., Palmquist, D. E., & Juliano, S. A. (2021). Impacts of fungal entomopathogens on survival and immune responses of *Aedes albopictus* and *Culex pipiens* mosquitoes in the context of native *Wolbachia* infections. *PLoS Neglected Tropical Diseases*, 15(11), e0009984.
- Ransom, T.S. (2017). Local distribution of native and invasive earthworms and effects on a native salamander. *Population Ecology*, 59, 189–204.
- Rezza, G. (2012). *Aedes albopictus* and the reemergence of Dengue. *BMC Public Health*, 12, 72. <https://doi.org/10.1186/1471-2458-12-72>
- Richter-Boix, A., Garriga, N., Montori, A., Franch, M., San Sebastian, O., Villero, D. & Llorente, G.A. (2013). Effects of the non-native amphibian species *Discoglossus pictus* on the recipient amphibian community: niche overlap, competition and community organization. *Biological Invasions*, 15, 799–815.
- Riley, L.A., Dybdahl, M.F., & Hall, R.O. (2008). Invasive species impact: asymmetric interactions between invasive and endemic freshwater snails. *Journal of the North American Benthological Society*, 27, 509-520.
- RStudio Team. (2021). *RStudio: Integrated Development Environment for R*. RStudio, PBC.

- Ruiz, V. E., Battaglia, T., Kurtz, Z. D., Bijmens, L., Ou, A., Engstrand, I., Zheng, X., Iizumi, T., Mullins, B. J., Müller, C. L., Cadwell, K., Bonneau, R., Perez-Perez, G. I., & Blaser, M. J. (2017). A single early-in-life macrolide course has lasting effects on murine microbial network topology and immunity. *Nature communications*, 8(1), 518.
<https://doi.org/10.1038/s41467-017-00531-6>
- Sam, Q. H., Chang, M. W., & Chai, L. Y. (2017). The fungal mycobiome and its interaction with gut bacteria in the host. *International journal of molecular sciences*, 18(2), 330.
<https://doi.org/10.3390/ijms18020330>
- Schrieke, H., Maignien, L., Constancias, F., Trigodet, F., Chakloute, S., Rakotoarivony, I., Marie, A., L'Ambert, G., Makoundou, P., Pages, N., Murat Eren, A., Weill, M., Sicard, M., & Reveillaud, J. (2022). The mosquito microbiome includes habitat-specific but rare symbionts. *Computational and Structural Biotechnology Journal*, 20, 410–420.
<https://doi.org/10.1016/j.csbj.2021.12.019>
- Seabourn, P., Spafford, H., Yoneishi, N., & Medeiros, M. (2020). The *Aedes albopictus* (Diptera: Culicidae) microbiome varies spatially and with Ascogregarine infection. *PLoS neglected tropical diseases*, 14(8), e0008615. <https://doi.org/10.1371/journal.pntd.0008615>
- Seabourn, P. S., Weber, D. E., Spafford, H., & Medeiros, M. C. I. (2023). *Aedes albopictus* microbiome derives from environmental sources and partitions across distinct host tissues. *MicrobiologyOpen*, 12(3), e1364. <https://doi.org/10.1002/mbo3.1364>
- Serbanescu, D., Ojkic, N., & Banerjee, S. (2022). Cellular resource allocation strategies for cell size and shape control in bacteria. *The FEBS journal*, 289(24), 7891–7906.
<https://doi.org/10.1111/febs.16234>

- Shepard, D. S., Undurraga, E. A., Halasa, Y. A., & Stanaway, J. D. (2016). The global economic burden of dengue: A systematic analysis. *The Lancet Infectious Diseases*, *16*(8), 935–941. [https://doi.org/10.1016/S1473-3099\(16\)00146-8](https://doi.org/10.1016/S1473-3099(16)00146-8)
- Sim, S., Jupatanakul, N., & Dimopoulos, G. (2014). Mosquito immunity against arboviruses. *Viruses*, *6*(11), 4479–4504. <https://doi.org/10.3390/v6114479>
- Steinway, S. N., Biggs, M. B., Loughran, T. P., Jr, Papin, J. A., & Albert, R. (2015). Inference of network dynamics and metabolic interactions in the gut microbiome. *PLoS computational biology*, *11*(5), e1004338. <https://doi.org/10.1371/journal.pcbi.1004338>
- Stump, E., Childs, L. M., & Walker, M. (2021). Parasitism of *Aedes albopictus* by *Ascogregarina taiwanensis* lowers its competitive ability against *Aedes triseriatus*. *Parasites & Vectors*, *14*(1), 79. <https://doi.org/10.1186/s13071-021-04581-0>
- Tawidian, P., Rhodes, V. L., & Michel, K. (2019). Mosquito-fungus interactions and antifungal immunity. *Insect Biochemistry and Molecular Biology*, *111*, 103182. <https://doi.org/10.1016/j.ibmb.2019.103182>
- Tipton, L., Müller, C. L., Kurtz, Z. D., Huang, L., Kleerup, E., Morris, A., Bonneau, R., & Ghedin, E. (2018). Fungi stabilize connectivity in the lung and skin microbial ecosystems. *Microbiome*, *6*(1), 12. <https://doi.org/10.1186/s40168-017-0393-0>
- Tuanudom, R., Yurayart, N., Rodkhum, C., & Tiawsirisup, S. (2021). Diversity of midgut microbiota in laboratory-colonized and field-collected *Aedes albopictus* (Diptera: Culicidae): A preliminary study. *Heliyon*, *7*(10), e08259. <https://doi.org/10.1016/j.heliyon.2021.e08259>
- Tyc, O., Song, C., Dickschat, J. S., Vos, M., & Garbeva, P. (2017). The ecological role of volatile and soluble secondary metabolites produced by soil bacteria. *Trends in Microbiology*, *25*(4), 280–292. <https://doi.org/10.1016/j.tim.2016.12.002>

- Van Dine, D.L. (1904). Mosquitoes in Hawaii. *Bulletin/Hawaii Agricultural Experiment Station*, no. 6.
- Vazeille, M., Moutailler, S., Coudrier, D., Rousseaux, C., Khun, H., Huerre, M., Thiria, J., Dehecq, J.-S., Fontenille, D., Schuffenecker, I., Despres, P., & Failloux, A.-B. (2007). Two Chikungunya Isolates from the Outbreak of La Reunion (Indian Ocean) Exhibit Different Patterns of Infection in the Mosquito, *Aedes albopictus*. *PLoS ONE*, 2(11), e1168. <https://doi.org/10.1371/journal.pone.0001168>
- Vezzani, D. (2007). Review: Artificial container-breeding mosquitoes and cemeteries: a perfect match: Mosquitoes and cemeteries. *Tropical Medicine & International Health*, 12(2), 299–313. <https://doi.org/10.1111/j.1365-3156.2006.01781.x>
- Wang, X., Liu, T., Wu, Y., Zhong, D., Zhou, G., Su, X., Xu, J., Sotero, C. F., Sadruddin, A. A., Wu, K., Chen, X.-G., & Yan, G. (2018). Bacterial microbiota assemblage in *Aedes albopictus* mosquitoes and its impacts on larval development. *Molecular Ecology*, 27(14), 2972–2985. <https://doi.org/10.1111/mec.14732>
- Wang, Y., Eum, J. H., Harrison, R. E., Valzania, L., Yang, X., Johnson, J. A., Huck, D. T., Brown, M. R., & Strand, M. R. (2021). Riboflavin instability is a key factor underlying the requirement of a gut microbiota for mosquito development. *Proceedings of the National Academy of Sciences of the United States of America*, 118(15), e2101080118.
- Watling, J.I., Hickman, C.R., & Orrock, J.L. (2011). Invasive shrub alters native forest amphibian communities. *Biological Conservation*, 144, 2597–2601.
- Watson, C.G. (2020) brainGraph: graph theory analysis of brain MRI data. R package version 3.0.0. <https://CRAN.R-project.org/package=brainGraph>

- Weaver, S. C. (2014). Arrival of chikungunya virus in the new world: Prospects for spread and impact on public health. *PLoS Neglected Tropical Diseases*, 8(6), e2921.
<https://doi.org/10.1371/journal.pntd.0002921>
- Williams, R. J., Howe, A., & Hofmockel, K. S. (2014). Demonstrating microbial co-occurrence pattern analyses within and between ecosystems. *Frontiers in microbiology*, 5, 358.
<https://doi.org/10.3389/fmicb.2014.00358>
- Winchester, J. C., & Kapan, D. D. (2013). *History of Aedes Mosquitoes in Hawaii*. *Journal of the American Mosquito Control Association*, 29(2), 154–163. doi:10.2987/12-6292r.1
- World Health Organization. (2020). Vector-borne diseases. March 2020.
<https://www.who.int/news-room/fact-sheets/detail/vector-borne-diseases>. Accessed February 9, 2024.
- Wolfe, N., Dunavan, C. & Diamond, J. (2007). Origins of major human infectious diseases. *Nature* 447, 279–283. <https://doi.org/10.1038/nature05775>
- Wright, C. J., Burns, L. H., Jack, A. A., Back, C. R., Dutton, L. C., Nobbs, A. H., Lamont, R. J., & Jenkinson, H. F. (2013). Microbial interactions in building of communities. *Molecular oral microbiology*, 28(2), 83–101. <https://doi.org/10.1111/omi.12012>
- Xi, Z., Ramirez, J. L., & Dimopoulos, G. (2008). The *Aedes aegypti* toll pathway controls dengue virus infection. *PLoS Pathogens*, 4(7), e1000098.
<https://doi.org/10.1371/journal.ppat.1000098>
- Xiao, X., Liang, Y., Zhou, S., Zhuang, S., & Sun, B. (2018). Fungal community reveals less dispersal limitation and potentially more connected network than that of bacteria in bamboo forest soils. *Molecular Ecology*, 27(2), 550–563. <https://doi.org/10.1111/mec.14428>

- Xue, R.-D., Barnard, D. R., & Muller, G. C. (2010). Effects of Body Size and Nutritional Regimen on Survival in Adult *Aedes albopictus* (Diptera: Culicidae). *Journal of Medical Entomology*, 47(5), 778–782. <https://doi.org/10.1093/jmedent/47.5.778>
- Yamada, R., Deshpande, S. A., Bruce, K. D., Mak, E. M., & Ja, W. W. (2015). Microbes Promote Amino Acid Harvest to Rescue Undernutrition in *Drosophila*. *Cell Reports*, 10(6), Article 6. <https://doi.org/10.1016/j.celrep.2015.01.018>
- Yang, D., He, Y., Ni, W., Lai, Q., Yang, Y., Xie, J., Zhu, T., Zhou, G., & Zheng, X. (2020). Semi-field life-table studies of *Aedes albopictus* (Diptera: Culicidae) in Guangzhou, China. *PLoS One*, 15(3), e0229829. <https://doi.org/10.1371/journal.pone.0229829>
- Ye, Y. H., Carrasco, A. M., Frentiu, F. D., Chenoweth, S. F., Beebe, N. W., van den Hurk, A. F., Simmons, C. P., O'Neill, S. L., & McGraw, E. A. (2015). *Wolbachia* Reduces the Transmission Potential of Dengue-Infected *Aedes aegypti*. *PLoS Neglected Tropical Diseases*, 9(6), e0003894. <https://doi.org/10.1371/journal.pntd.0003894>
- Yoshiyama, K., & Klausmeier, C. A. (2008). Optimal cell size for resource uptake in fluids: a new facet of resource competition. *The American naturalist*, 171(1), 59–70. <https://doi.org/10.1086/523950>
- Zhang, H., Rutherford, E.S., Mason, D.M., Whitman, M.E., Lodge, D.M., Zhu, X., Johnson, T.B., & Tucker, A. (2019) Modeling potential impacts of three benthic invasive species on the Lake Erie food web. *Biological Invasions* 21, 1697–1719.
- Zouache, K., Martin, E., Rahola, N., Gangué, M. F., Minard, G., Dubost, A., Van, V. T., Dickson, L., Ayala, D., Lambrechts, L., & Moro, C. V. (2022). Larval habitat determines the bacterial and fungal microbiota of the mosquito vector *Aedes aegypti*. *FEMS Microbiology Ecology*, 98(1), fiac016. <https://doi.org/10.1093/femsec/fiac016>